Mechanical Engineering Department

Doctor of Philosophy's Thesis

An Efficient Biomimetic Swimming Robot Capable of Multiple Gaits of Locomotion

Design, Modelling and Fabrication

Author:
Sayyed Farideddin Masoomi

Supervisors:
Dr. Stefanie Gutschmidt
Prof. XiaoQi Chen
Dr. Mathieu Sellier

May 26, 2014

This thesis is dedicated to Imam Mahdi (AJ).

Acknowledgements

First and foremost, I would never been able to finish my project without the guidance of Imam Mahdi (AJ) that helped me to surpass all trials that I encountered. I cordially appreciate him since he made this study possible for me and determined me to finish this project.

I would like to express my deep gratitude to my supervisor, Dr. Stefanie Gutschmidt, for her guidance, understanding, patience and continuous support of my PhD study and research. I would like to thank Prof. XiaoQi Chen who trusted me and let me work on this project. I would also like to thank Dr. Mathieu Sellier for his help in the hydrodynamic aspects of my research. My sincere thanks goes to Dr. Don Clucas and Dr. Nock Volker for their generous guidance and supports in the fabrication part of my research.

I would also like to thank all interns, Axel Haunholter, Dominic Merz, Nicolas Gaume, Connor Eatwell and Thomas Guillaume who significantly helped me to finish my project. I will never forget their helps.

My special thanks goes to Julian Murphy, Garry Cotton, David Read, Ian Shepard, Bruce Robertson and all other technician in the department of engineering who helped me in the fabrication process of my research.

I also thank my parents, Fatemeh and Sayyed Mohsen, for their faith in me and allowing me to experience new things. Their encouragement and spiritual support have always motivated me throughout my life.

Finally and importantly, I would like to thank my wife, Fatemeh, for her caring, quiet patience and support. Her pure love has strengthened me to tolerate the stress that I have had during past three years.

Abstract

Replacing humans with underwater robots for accomplishing marine tasks such as oceanic supervision and undersea operations have been an endeavour from long time ago. Hence, a number of underwater robots have been developed. Among those underwater robots, developing biomimetic swimming robots has been appealing for many researchers and institutes since these robots have shown superior performance.

Biomimetic swimming robots have higher swimming efficiency, manoeuvrability and noiseless performance. However, the existing biomimetic swimming robots are specialised for a single gait of locomotion like cruising, manoeuvrability and accelerating while for efficient accomplishment of marine tasks, an underwater robot needs to have multiple gaits of locomotion.

In order to develop multiple-gaited swimming robots, the optimal characteristics of each gait of swimming must be combined together, whereas the combination is not usually possible. The problem needs to be addressed during the design process.

Moreover, the optimality of the actuation mechanism of robots - that do not utilise any artificial muscle - could be assured using the mathematical model employed for simulation of their swimming behaviour. However, the existing models are incomplete and, accordingly, not reliable since their assumptions like the constant speed of flow around the fish robot could be used when the average speed of the flow is determined during experiment while before development of robots, the flow speed is not known.

In addition to that, the simulation results must be optimised using the experimental observations in nature and analytical results while the optimisation algorithms are based on one fitness function.

The aforementioned problems as well as the fabrication challenges of free-swimming biomimetic robots are addressed in a development process of multiple-gaited fish-mimetic robots introduced by the author in this thesis.

This development method engages the improvement of all development steps of fish robots including design, mathematical modelling, optimisation and fabrication steps. In this thesis, the aforementioned steps are discussed and the contributions of the method for each step are introduced. As an outcome of the project, two prototypes of fish robots called UC-Ika 1 & 2 are built.

Publications

1. S. F. Masoomi, S. Gutschmidt, X.Q. Chen, and M. Sellier. (2013) 'Engineering Creative Design in Robotics and Engineering', Chapter *Novel Swimming Mechanism for a Robotic Fish*, pp.41-58, IGI Global, Hershey, PA, USA.
2. S. F. Masoomi, S. Gutschmidt, X.Q. Chen, and M. Sellier. (2012) 'Mathematical modelling and parameter optimization of a 2-DOF fish robot' in *19th International Conference on Mechatronics and Machine Vision in Practice (M2VIP)*,pp.212-217.
3. S. F. Masoomi, S. Gutschmidt, X.Q. Chen, and M. Sellier. (2012) 'Efficiency-based optimisation of a 2-DOF robotic fish model', *International Journal of Biomechatronics and Biomedical Robotics*, Vol. 2, Nos 2/3/4, pp.93-101.
4. S. F. Masoomi, A. Haunholter, D. Merz, S. Gutschmidt, X.Q. Chen, and M. Sellier. (2014) 'Design, fabrication and swimming performance of a free-swimming tuna-mimetic robot', *Journal of Robotics*, Volume 2014, Hindawi Publishing Corporation (accepted).
5. S. F. Masoomi, S. Gutschmidt, X.Q. Chen, and M. Sellier. (2014) 'The kinematics and dynamics of undulatory motion of a tuna-mimetic robot', *International Journal of Advanced Robotic Systems* (under review).
6. S. F. Masoomi, S. Gutschmidt, X.Q. Chen, and M. Sellier. (2014) 'Handbook of Robotics and Mechatronics', Chapter *The Design Principles of a Tuna-Mimetic Robot Specialised in Cruising*, IGI Global, Hershey, PA, USA (Submitted).
7. S. F. Masoomi, S. Gutschmidt, X.Q. Chen, and M. Sellier. (2014) 'Optimal Design of robotic fishes: a review', *IEEE Journal of Oceanic Engineering* (prepared).
8. S. F. Masoomi, S. Gutschmidt, X.Q. Chen, and M. Sellier. (2014) 'Optimisation and simulation of the undulatory motion of a biomimetic swimming robot', *Robotics and Biomimetics* (prepared).

9. S. F. Masoomi, N. Gaume, T. Guillaume, C. Eatwell, S. Gutschmidt, X.Q. Chen, and M. Sellier. (2014) 'Design and construction of a specialised biomimetic robot in multiple swimming gaits', *International Journal of Advanced Robotic Systems* (prepared).

Contents

List of Tables

LIST OF TABLES

List of Figures

Chapter 1

Introduction

Undersea operation, oceanic supervision, aquatic life-form observation, pollution search and military detection are just a few examples that demand development of underwater robots to replace humans [Bingham et al., 2002; Inzartsev and Pavin, 2009; Yu et al., 2004]. Hence, many underwater vehicles such as remotely operated vehicles (ROVs), autonomous underwater vehicles (AUVs) and underwater biomimetic robots have been developed in the past decade [Aqu, 2013; HUG, 2013; MER, 2013; Aldehayyat et al., 2009; Griffiths and Edwards, 2003; Morgansen et al., 2007; Williams, 2004]. Three typical examples for the aforementioned types of underwater vehicles are shown in Fig. 1.1.

Among underwater robots, biomimetic swimming robots have shown superior performance in comparison to screw propeller underwater robots. This superiority roots in the efficient cruising, manoeuvrability and noiseless motion of biomimetic swimming robots[1] which are defined as fish-like aquatic vehicles which propel through undulatory or oscillatory motion of either body or fins [Hu et al., 2006]. For instance, the propulsion system for some types of fishes is up to 90 percent efficient, while a conventional screw propeller is around 40 to 50 percent efficient [Yu and Wang, 2005]. Due to the capabilities of biomimetic swimming robots, they have been employed for various applications [Hu et al., 2012; Marras and Porfiri, 2012; Polverino et al., 2012; Yu et al., 2012].

During last two decades, many researchers have focused on the design and construction of biomimetic swimming robots. The first biomimetic swimming robot was inspired by tuna called RoboTuna that was built at MIT [Triantafyllou and Triantafyl-

[1] Bear in mind that Bandyopadhyay [2005] believes that the efficiency of biomimetic swimming robot is not higher than screw propeller robots but animals do show superior manoeuvrability in swimming.

(a) AUV [HUG, 2013]

(b) ROV [MER, 2013]

(c) Fish robot [Aqu, 2013]

Figure 1.1: Three different types of underwater vehicles

lou, 1995]. Three years later, Vorticity Control Unmanned Undersea Vehicle (VCUUV) was developed based on RoboTuna with some improvement and more capabilities such as avoiding obstacles and having up-down motion [Anderson and Chhabra, 2002; Liu and Hu, 2004]. Afterwards, a number of institutes and universities developed their own fish robots with more functionalities such as cruising and turning by pectoral fins [Lachat et al., 2005], cruising by undulating anal fins [Low, 2009] and so on. Figure 1.2 shows two typical fish robots built in University of Washington and Essex University.

Nevertheless, the existing fish robots have deficiencies regarding their swimming behaviours. The fish robots have been developed to have a specific gait of swimming such as cruising, accelerating and manoeuvring. However, to accomplish marine tasks, underwater robots must be skilled for swimming in various gaits. For instance, VCUUV is a well known tuna-mimetic robot [Anderson and Chhabra, 2002]. Tuna-mimetic robots show proficiency in cruising gait of swimming while this kind of robots is notorious for not being manoeuvrable among narrow areas [Masoomi et al., 2013]. Accordingly, tuna-mimetic robots are suitable only for navigation-based tasks such as coastal monitoring,

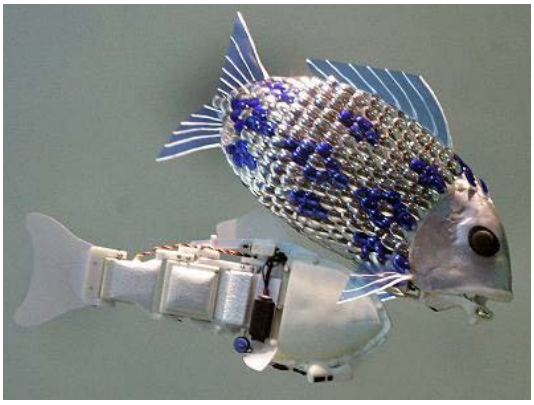

(a) Fish robot model G9 fabricated in Essex University [Beciri, 2009]

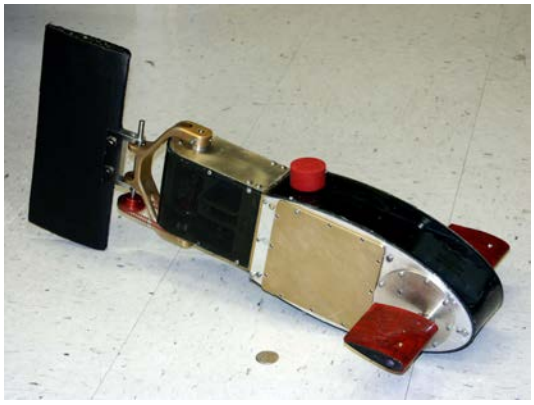

(b) RoboFish built in University of Washington [Morgansen et al., 2007]

Figure 1.2: Two typical fish robots

oil and gas exploration which need long distance of swimming. On the other hand, Boxybot series of robots are inspired from boxfishes and adapted for slow swimming and manoeuvring gaits [Fankhauser and Ijspeert, 2010; Lachat et al., 2005]. Boxybots are not sufficiently competent for cruising gait of swimming. Hence, this type of robots is talented for discovery tasks such as exploring ship wrecks or oil pipelines.

In order to address the single gaited motion of the existing fish robots, the author has presented a method for developing multiple-gaited fish robots. The accomplishment of this method engages the improvement of all development steps of fish robots including design, mathematical modelling, optimisation and fabrication. As an outcome of the project, two prototypes of fish robots called UC-Ika 1 & 2[1] are built[2].

UC-Ika 2 is designed for two gaits of swimming - cruising and manoeuvring - while it is capable of up-down motion. The cruising motion of the robot must be highly efficient to save energy of swimming. Prior to developing UC-Ika 2, UC-Ika 1 is also designed and fabricated adapted only for cruising gait of motion. The fabrication of this robot is to prove the functionality of the conceptual design for cruising gait of motion of UC-Ika 2.

[1]The name of the fish robots originates from the Maori name "ika" which means fish

[2]Usually using the term swimming gaits causes a confusion regarding the swimming behavior of the robot. In other words, claiming that a robot is single-gaited for instance in cruising, it does not mean that the robot is not able to manoeuvre or accelerate. But the swimming properties of the robot - explained in Chapter 2 - is optimised only for one gait of motion like cruising. Hence having a multiple gaits of locomotion delivers the idea of having swimming characteristics of different gaits. In terms of UC-Ika 2, the robot has swimming characteristics of two distinct gaits of motion including cruising and manoeuvring.

In the following sections, the challenges and open questions in the world as well as the contributions of the author to this field of robotics are presented.

1.1 Challenges

Chronologically speaking, design, mathematical modelling, optimisation, simulation and fabrication are five main steps of developing a new fish robot (see Fig. 1.3). The challenges and deficiencies of each step are described in this section.

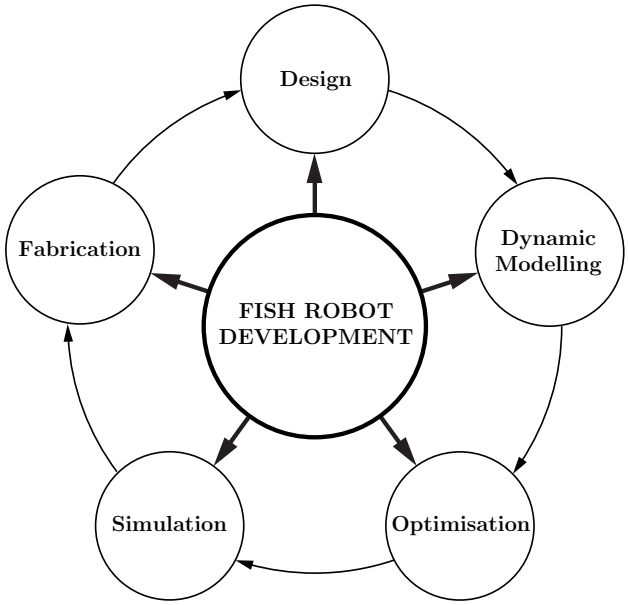

Figure 1.3: The steps of developing of fish robots

1.1.1 Design

The primary step of developing fish robots is the design of an optimal shape and swimming mechanism corresponding to their gait of locomotion. Accordingly, among fishes, the optimal shape for cruising gait of locomotion is found out and designed for UC-Ika 1, and the swimming mechanism of the corresponding fish is mimicked. The design is even more challenging for UC-Ika 2 that has two gaits of locomotion: cruising and manoeuvring. The optimal swimming characteristics for each aforementioned gaits are determined, and combined such a way that their characteristics do not deteriorate the overall swimming performance of the robot.

All aquatic species have finest swimming mechanism with respect to their swimming

specialities including cruising/sprinting, accelerating and manoeuvring [Webb, 1994]. These specialities depend on the swimming biology and hydrodynamics of fishes. Biology reveals how the propulsors and muscles of fishes are engaged for swimming, and what locomotion gaits the fishes are capable of. On the other hand, hydrodynamics reveals how fishes generate maximum and minimum propulsive and resistive forces, respectively. Hence, biology and hydrodynamics of fishes must be thoroughly investigated to figure out the most appropriate shape and swimming mechanism for different gaits of swimming.

The combination of the optimal characteristics of the gaits is also a challenging issue since the combination of the gaits is not possible in some cases or at least weakens the overall swimming performance of the robots. The former is often because of biological properties of the gaits and the latter is mainly due to the hydrodynamic force generation of each gait.

In some cases, different gaits like cruising and fast-start have quite opposite shape of propulsors like caudal fin. Based on hydrodynamic analysis, fishes in cruising gait have long and narrow shape of caudal fin while fast-start gait requires short and deep caudal fin. Accordingly, the biological combination of these two gaits of locomotion is impossible in terms of their caudal fin if the optimality of the individual gaits is targeted.

Sometimes the optimality of different swimming gaits like cruising and manoeuvring strongly depends on different propulsors like caudal fin for cruising and pectoral fins for manoeuvring. Thus biologically speaking the combination of these two gaits is possible; however, the overall performance of the robot is not as expected since they have distinct methods of thrust generation. For instance, angelfish is a manoeuvrable fish that its pectoral fins have rowing motion while swordfish is a fast fish with rather flapping motion of caudal fin [Videler, 1993]. The hydrodynamic principles behind rowing and flapping motion are quite opposite. This distinct hydrodynamic principles weakens the overall swimming performance of the robot.

1.1.2 Mathematical Modelling

Subsequent to the design, the swimming behaviour of the robot requires analytical modelling. Modelling of fish robots is necessary to analyse their swimming behaviour and improve their performance. Since the cruising efficiency of both aforementioned robots (UC-Ika 1 & 2) is targeted for analysis and optimisation, the deficiencies of the existing analytical models in cruising gait are described.

In total, the modelling field of fishes in cruising mode is rather founded by Wu [1961] and Lighthill [1960, 1970]. These models are categorized into two major groups: trajectory-based models and dynamic models. Regardless of dynamic behaviour of fish robots, trajectory-based models such as [Yan et al., 2008; Yu et al., 2004] use only the experimental observations of the body shape of real fishes during swimming and apply those observations for modelling of the body form of the swimming robots. These models are geometry-based models and cannot fully represent the robot motion since the role of propulsive and resistive forces are ignored.

On the other hand, others have modelled the fish swimming taking both kinematics and dynamics of the robots into account such as [Liu et al., 2008; Morgansen et al., 2007; Wang and Tan, 2013; Yu et al., 2006; Zhou et al., 2008]. These dynamic models are more reliable than trajectory-based models since the essential role of hydrodynamic forces are observed. However, the usage of current dynamic models are limited due to the following assumptions.

- The robots are assumed to be made of a chain of links in series while the swimming motion of fish robots can be done through diverse mechanisms.
- The models are built up with the assumption of steady or quasi-steady state condition. These two state conditions assume that the flow around the caudal fin has constant speed. Nevertheless, the speed of flow is variable and depends on the swimming behaviour of the fish robot.
- The existing models consider that the links are in contact with the surrounding fluid and the hydrodynamic forces are acting directly on them. This assumption is not reliable since most of the times the robot is covered by a skin layer.

Since these three assumptions attack the reliability of the existing dynamic models for cruising gait of fish robots, the main challenge in this step turns to be introducing a dynamic model without those previously mentioned assumptions.

1.1.3 Optimisation

Using dynamic model, the swimming performance of the robot should be simulated. To do so, the constant parameters of the equations including sizes of different parts of the robot, frequency and amplitude of fin stroking should be substituted into the equations. At this stage, those values of the constant parameters which are suitable for an optimal swimming must be determined.

In literature, two ways of determination of the constant parameters exist: experimentally testing different sizes for a particular part of the robotic fish (see [Kodati et al., 2008]), and mimicking all the features of the real fish even the tail beating frequency[1] (see [Anderson and Chhabra, 2002; Gao et al., 2009; Triantafyllou et al., 2000; Yu et al., 2007b]). The former method is not reliable since all parts of a robot must be optimised simultaneously. For instance, both long and short fins are optimal when they are optimised in separation from the fish. But a long fin cannot be optimal for fishes like boxfish due to the shape, size and their propulsion system. The short fins also cannot be optimal for fast fishes such as swordfishes.

The method of mimicking all the features of the real fish, although preferable in comparison to the previous method, ignores the task-based development of fish robots while fishes in nature need to survive and hence to perform various tasks. For instance, a bird-wrasse is a manoeuvrable fish with long knout which is essentially required for searching food and grasping prey [bir, 2013a]. Therefore, the presence of the long beak of bird-wrasses are not critical in their swimming motion. So, a manoeuvrable robot inspired by bird-wrasse does not need to have the shape of its knout.

In this optimisation step, the essential challenge is the simultaneous optimisation of all swimming parameters of fish robots in cruising mode with respect to the robot swimming character which is high efficiency in speedy cruising motion.

1.1.4 Fabrication

The last but not the least step of developing a fish robot is its fabrication. In this step, several issues are to be dealt with. Primarily, the fish-mimicking robots have intricate shapes to meet the optimal performance of fishes. This shape cannot be simply made by the conventional machining tools.

Besides, the swimming robots have rigid and flexible parts. The latter must be flexible enough to not demand additional motor torque during bending. Simultaneously, the flexible part has to be stiff enough to stand the pressure of water column.

Moreover, similar to the other underwater robots, the fish robots have waterproofing issues which is more challenging since the electronics and actuation mechanisms inside the body of the robot need to be accessible.

The last issue returns to the underwater communication problem. An underwater robot cannot be remotely controlled without an antenna that is come out of the aquatic

[1] There are many aquatic robot developers who have not explained explicitly why specific shape and values for, e.g., the sizes and tail beat of their fish robot are selected (see [Epstein et al., 2006; Kato et al., 2000; Liang et al., 2011; Low and Willy, 2005; Morgansen et al., 2007]).

environment whereas the antenna affects the hydrodynamic behaviour of the robot under water.

1.2 Contributions

In the process of developing UC-Ika 1 & 2, this project has contributed to the field of robotic fishes by addressing the aforementioned challenges in each step which is briefly mentioned in Fig. 1.4.

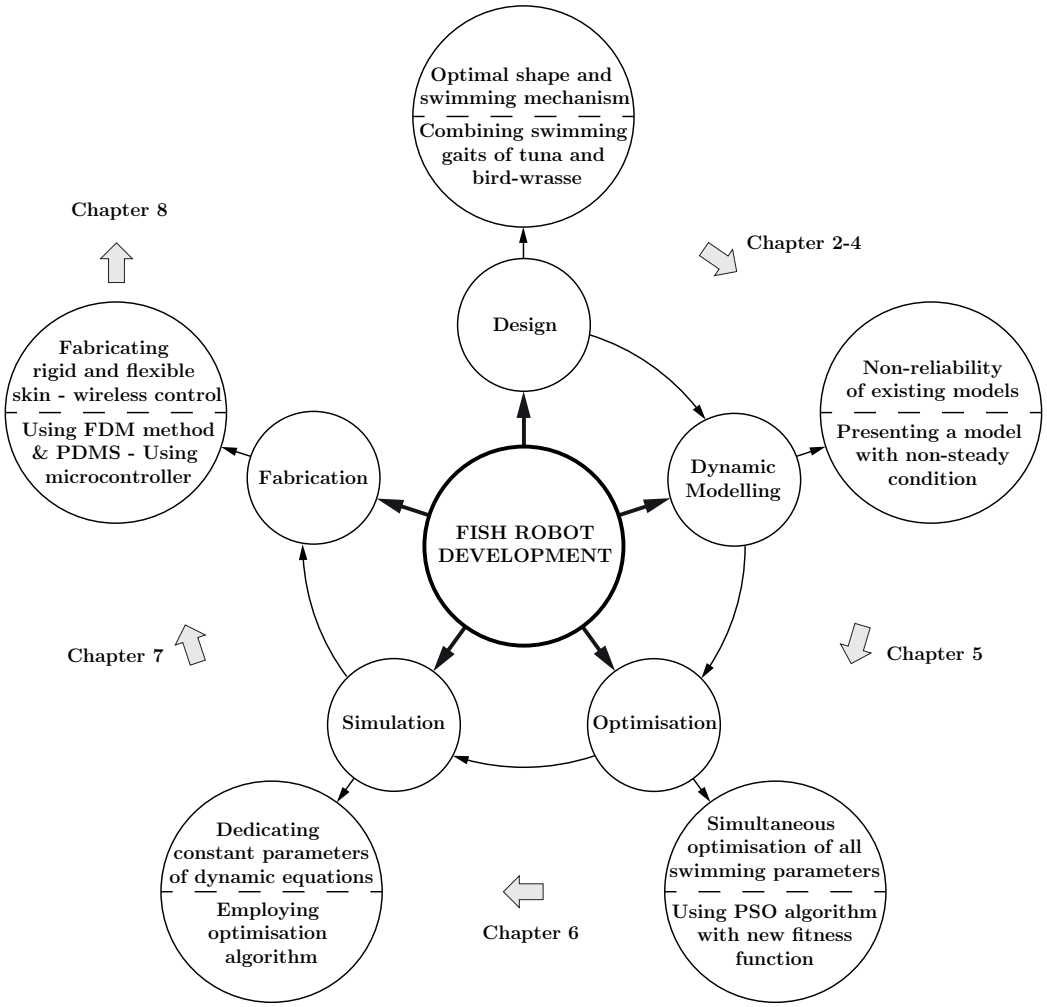

Figure 1.4: The steps of development of fish robot with the main challenges and contributions in each step.

In the design step, the optimal characteristics of swimming species are thoroughly investigated from both biology and hydrodynamics perspectives. Accordingly, the bi-

ological and hydrodynamic properties of fishes with respect to their swimming specialities are categorized. The existing biomimetic swimming robots are also introduced with respect to their swimming mode and discussed based on their shape and actuation mechanism.

The investigation of hydrodynamics and biology reveals that tuna is a competent candidate for cruising gait. Thus the design of shape and swimming mechanism of UC-Ika 1 which has purely cruising gait of swimming is motivated by tuna. Even for cruising gait of UC-Ika 2, tuna has been inspiring. For manoeuvrability mode of UC-Ika 2, among manoeuvrable fishes, bird-wrasse is selected since it has adaptable swimming features to combine with the swimming characteristics of a tuna. Tuna and bird-wrasse are shown in Fig. 1.5.

(a) Bird-Wrasse [bir, 2013b] (b) Tuna [Tun, 2013]

Figure 1.5: Typical tuna and bird-wrasse fishes.

The selection of swimming characteristics of tuna and bird-wrasse for combination is due to the fact that tuna has active tail and inactive pectoral fins during cruising mode, while bird-wrasse has active pectoral fins and somewhat inactive posterior part of body during manoeuvring [Lindsey, 1979]. Both tuna and bird-wrasse have also the same hydrodynamic principle of propulsion. Then the motion of pectoral fins and caudal fin do not affect the optimal nature of each other in thrust generation [Alexander, 2002]. Two actuation mechanisms for cruising and manoeuvring modes are designed. These mechanisms mimic the body forms of tuna and bird-wrasse during locomotion. For further information the reader is referred to Chapter 2-4.

To address the challenges in the modelling step, a comprehensive, distinct mathematical model for fish robots in cruising mode is presented. The model is made up of the kinematic analysis of the actuation mechanism of the fish and the consideration of hydrodynamic forces that are acting on the caudal fin of fish robot.

Initially, the actuation mechanism (see Fig. 1.6) designed for cruising mode in the previous step is geometrically analysed and the relationship between the rotational

motion of the motor and the end effector of the actuation mechanism, point F, is derived.

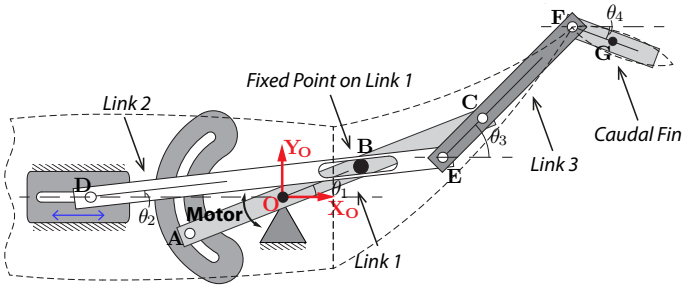

Figure 1.6: Link Mechanism of Tail Peduncle

Next, hydrodynamic forces are taken into account. Using the kinematic relationships, the robots in cruising mode are represented by the sketch shown in Fig. 1.7 where the hydrodynamic forces acting on the fish in cruising mode is illustrated. The hydrodynamic forces (F_{Cx} and F_{Cy}) are propulsive forces made by lift and fluid inertial forces[1]. These two forces are obtained considering that the flow around the fish has variable speed. This variability submits a more representative model, although it is vulnerable by the constant parameters of the equations including frequency and amplitude of undulation wave. F_{Dx} and F_{Dy} are drag forces of the fish body along X and Y directions. M_{Dp} is the momentum of force around the centre of mass and made by F_{Cx} and F_{Cy}. T is the motor torque that is inserted on link 1, $\overline{OC}$ in Fig. 1.7 .

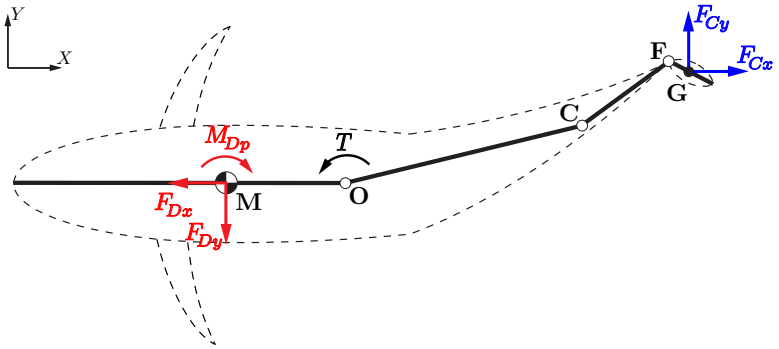

Figure 1.7: The free-body diagram of the forces acting on UC-Ika 1 & 2 in cruising gait.

Finally, the dynamic equation of motion with 4 degrees of freedom (DOF) is devel-

[1]Most of the existing mathematical models, e.g. [Mason, 2003], have considered the fluid inertia as an added mass to the mass of the fish which is in the left-hand side of the dynamic equations of motions. In this model, the fluid inertia force is directly employed as a force in the right-hand side of the equation. This simplifies the derivation of the equations.

oped. DOFs of the model are the displacements of the robot in X and Y directions, swinging motion of the robot about its centre of mass, Point M, and the oscillatory motion of the caudal fin about its pivot point, point F. The freedom of the caudal fin is caused by a spring placed at point F. The detailed mathematical model is provided in Chapter 5.

Following previous steps, several issues in the optimisation process need to be addressed. These issues are mainly due to the simultaneous optimisation of all swimming parameters of the robot with respect to its swimming character which is its high efficiency in speedy cruising. Accordingly, the author has presented a novel method which relies on optimisation through the dynamic equations of motion of the robot. In this method, the constant parameters of the mathematical model are optimised using a recent evolutionary algorithm for global optimisation called Particle Swarm Optimisation (PSO).

PSO is inspired by the social behaviour of birds within a flock. In other words, each bird in the swarm modifies its motion with the information obtained from other members of the swarm, its own experience and its current direction of motion. This makes the basic intuitive ideology of PSO algorithm. The birds are defined as particles in the algorithm.

In PSO, each particle has a position, $x_i(t)$, which represents a solution to the fitness function. In each iteration, the particles' positions are updated with the particles' velocities of that iteration, $v_i(t)$, which show the directions of motion of the particles. The velocities of the particles are computed considering three factors: velocities of the particles toward the best experienced position of the swarm called *gbest*, velocities of the particles toward the best experienced position of each particle called *pbest* and the previous particles' velocities. Note that the position and the velocity in the algorithm do not have their physical properties.

PSO algorithm has two inherent components (particles and fitness function) which must be defined for every optimisation problem. In the case of UC-Ika, particles are the solutions for the fitness function which is identified as a criterion for optimal cruising motion of the robot. Each particle is a set of constant parameters of dynamic equations of the robot. Each parameter is a dimension of the particle.

In order to define the fitness function to represent the optimal swimming characteristic of the robot, Froude efficiency and Strouhal number are exploited. Froude efficiency shows the efficiency of the robot during cruising; however, Froude efficiency cannot fully represent the efficiency of a fish swimming since it is derived upon simplified assumptions. Accordingly, Strouhal number is used to fulfil the deficiency of the

Froude efficiency. Strouhal number is a dimensionless parameter that illustrates the optimal thrust generation for fishes. The best value of this number obtained from experimental observation is employed in this application. Optimisation step is described in Chapter 6. The simulation result using the optimised and non-optimised parameters are also presented in Chapter 7.

For fabrication of both UC-Ika 1 & 2, a rapid prototyping method called Fused Deposition Modelling (FDM) is applied, which is a 3D-printing technology directly using the CAD model. By 3D-priting, intricate shape could be made whose material is Acrylnitril-Butadien-Styrol-Copolymerisat (ABS) which is used for fabrication of rigid parts. Accordingly, the main body of both fish robots are fabricated using this method [Chua et al., 2010].

Flexible part like tail peduncle and pectoral fins are produced from Polydimethylsiloxane (PDMS) silicone Sylgard 184 which is durable, tensile and resistant against water and most solvents [syl, 2013]. In order to build the moulds of flexible parts, FDM method is applied.

For waterproofing UC-Ika 1 and 2, different methods need to be applied since UC-Ika 1 is accessible from its tail and UC-Ika 2 from its head. For UC-Ika 1, the connection between the tail and the head of fish needs to be water proofed. On the other hand, the tail and the head of UC-Ika 2 are fixed together, and the connection between the head and its lid is waterproofed. Since the fabricated parts with FDM are slightly porous, they are painted with epoxy resin to avoid passing of water through the head over time.

To address the communication problem, the robot is designed to be free-swimming without any online controlling. The robot makes benefit of a microcontroller which are coded with various predefined paths of motion. Before each run of swimming motion, the specific path is introduced to the robot through a Bluetooth device. Further information regarding fabrication process of fish robots are available in Chapter 8.

As it has been introduced, in the process of developing a novel fish robot several challenges exist which have been addressed in this project. The challenges and contributions of this project is listed in Table 1.1.

1.3 Outline

This thesis has nine chapters. Chapter 2 describes the optimal swimming characteristics of fishes in terms of biology and hydrodynamics. Chapter 3 presents the state of the art in the field of biomimetic swimming robots. In this chapter, the robots are categorized based on their swimming mode while the corresponding fishes in each mode

are described. Chapter 4 describes the design process of both fish robots. In this chapter, the CAD design of both robots are presented. In Chapter 5, the mathematical model for fish robots in cruising mode of swimming is derived. The constant parameters of the model in this chapter is then obtained using the algorithm explained in Chapter 6. Using the model in Chapter 5 and the optimised parameters obtained in Chapter 6, the cruising gait of fish robots are simulated. The results of the simulation is presented in Chapter 7. Chapter 8 describes the fabrication process of fish robots. The experimental test result showing the swimming performance of the robot is also presented in Chapter 8. And finally, the development process of the fish robots are concluded in Chapter 9. In this section, the future work in biomimetic swimming robots are informed.

Table 1.1: Challenges in the development of biomimetic swimming robots and contribution of this project to this field.

Challenges	**Contribution**
Design	
1. Optimal shape of each gait	1. Investigation of swimming characteristics
2. Combination of gaits	2. Presenting state of the art in robotic fish
	3. Describing optimal shape of tuna in cruising
	4. Combining optimal shape of bird-wrasse in manoeuvring with tuna in cruising
Mathematical Modelling	
1. Complicated tail mechanism	1. Presenting state of the art in this field
2. Variable speed of flow	2. Presenting a model in cruising mode that: - apply kinematic analysis result of tail - shows all planar motions of fish robots - takes variable speed of flow into account
Optimisation	
1. Simultaneous optimisation of all swimming parameters	1. Presenting state of the art in this field
	2. Applying PSO algorithm
2. Defining fitness function	3. Defining a fitness function using Froude Efficiency and Strouhal Number
Fabrication	
1. Intricate shape	1. Applying FDM method for fabrication of rigid parts
2. Flexible part	2. Using PDMS material for fabrication of flexible parts
3. Underwater communication	3. Employing microcontroller with Bluetooth connection
4. Waterproofing while accessible	4. Painting the rigid parts with epoxy resin and employing sealing connector

Chapter 2

Optimal Swimming

Eels live among coral reefs. Hence, they need to have thin and flexible body that enables them to swim through those narrow areas. This shape and type of locomotion is optimal for an eel that is one sample out of countless number of swimming species. All of these species have optimal shape and swimming performance compromised by their nature and their habitats. In order to design an optimal shape and locomotion type for a swimming robot, the nature and habitats of swimming animals are thoroughly investigated.

The optimal nature of fishes is strongly determined by their swimming speciality. Webb [1994] has categorized the swimming speciality into three types: cruising/sprinting, accelerating and manoeuvring. Initially, all of these specialities depend on the swimming gaits of fishes such as slow swimming and fast-starting gaits. But further investigation clarifies that each swimming gait corresponds to specific swimming forces. For example, lift-based swimmers are more suitable for cruising while drag-based swimmers are preferred for fast-start. Eventually, the optimality of fish swimming owes to the optimal shape which is appropriate for its swimming gait and force.

In this chapter, swimming speciality of fishes is investigated through studying the swimming gaits (Sec. 2.1), the swimming forces (Sec. 2.2) and the body/fin shape of swimming animals (Sec. 2.3).

2.1 Swimming Gaits

Gaits in general are initially defined by Alexander [1989] as "a pattern of locomotion characteristic of a limited range of speeds described by quantities of which one or more

change discontinuously at transitions to the other gaits". Although general, Alexander's definition of locomotion gaits could be employed for fish swimming with one condition: it is not only the speed range which differentiates gaits but ranges of linear acceleration and turning must be taken into account. This is due to the fact that the speed of a fish could be determined using initial speed added to the linear and angular acceleration of the fish [Webb and Gerstner, 2000].

In order to define the aforementioned definition of gait for fishes, Webb [1994] has proposed taking four elements into account which are swimming propulsors, swimming kinematics, swimming muscles and swimming timed-based features.

2.1.1 Swimming Propulsors

Fishes propel through either undulatory or oscillatory motion of different parts of the body or fins which is called propulsors, presented in Fig. 2.1. In oscillation case, a fish oscillates a certain part of its body about its base like the motion of a simple pendulum. On the other hand, in undulation case, a fish generates travelling waves using their bodies or fins at a speed faster than total swimming speed of the fish [Sfakiotakis et al., 1999].

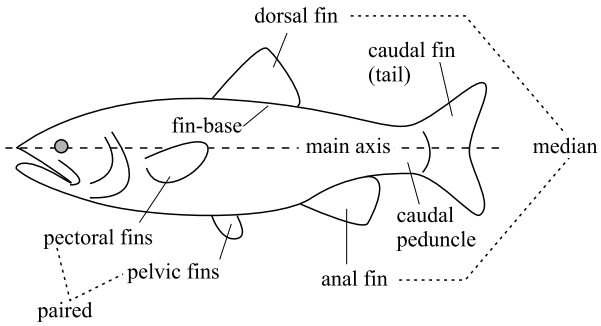

Figure 2.1: Fish terminologies used in this paper [Sfakiotakis et al., 1999].

Taking propulsors into account, fishes could be categorized into two main swimming modes. If a fish employs its body and/or caudal fin (BCF) for propulsion, its swimming mode is referred to as BCF. On the other hand, some fishes use their median and/or paired fins (MPF) like dorsal and pectoral fins for swimming. Accordingly, they are categorized in MPF swimming mode. Figure 2.2 demonstrates the aforementioned swimming modes.

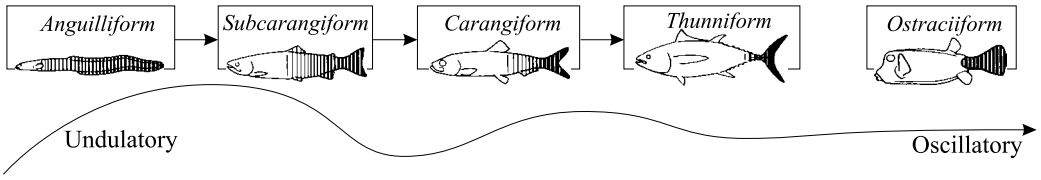

(a) BCF mode

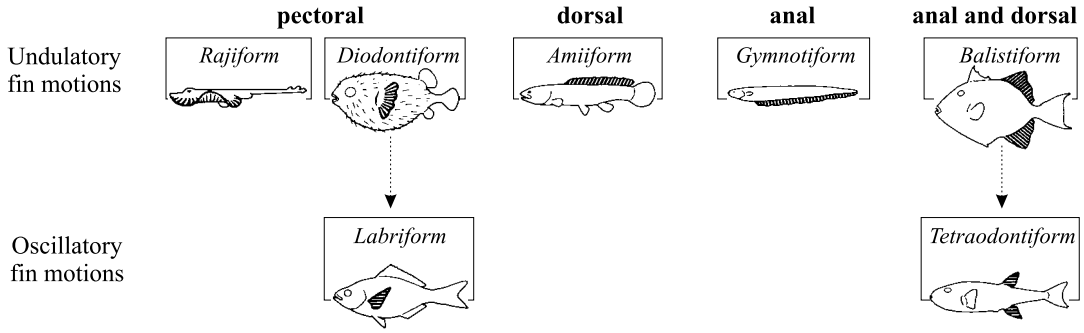

(b) MPF mode

Figure 2.2: Swimming modes [Sfakiotakis et al., 1999]

2.1.1.1 BCF Swimming Mode

As Fig. 2.2(a) shows, BCF mode could be further distinguished by undulatory and oscillatory swimming to five subcategories: 1. *anguilliform* like eel and lamprey, 2. *subcarangiform* like trout, 3. *carangiform* like mackerel, 4. *thunniform* like tuna and 5. *ostraciiform* like boxfish.

Anguilliforms are the most undulatory fishes among BCF swimmers. Whole anguilliforms' body participates in undulatory motion with large amplitude. Similarly, whole body of *subcarangiforms* participates in undulatory motion; however, the amplitude of the undulation is larger at the posterior half or one-third of the body. *Carangiforms* swim through undulation of the last third of their body whereas the thrust is mainly produced by the caudal fin. The undulation wavelength is never completed in a body length of carangiforms. *Thunniforms* generate undulatory wave significantly by the very last part of their tail peduncle and their caudal fin. Eventually, *ostraciiforms* are the only purely oscillatory BCF mode. In ostraciiform swimming mode, the caudal fin is the only propulsor for this mode which has pendulum-like oscillation about the connection point between the caudal fin and the tail peduncle.

2.1.1.2 MPF Swimming Mode

MPF mode, illustrated in Fig. 2.2(b), is also categorized further based on the type of fins like pectoral, dorsal and anal fins, and types of motion, undulation and oscillation, into seven subcategories: 1. *rajiform* like rays and mantas, 2. *diodontiform* like porcupine fishes, 3. *labriform* like bird-wrasse and angelfish, 4. *amiiform* like bowfin, 5. *gymnotiform* like south American electric fish, 6. *balistiform* like triggerfish and 7. *tetraodontiform* like puffer fish.

Rajiforms, *diodontiforms* and *labriforms* all use their pectoral fins to swim; however, rajiforms have enlarged pectoral fins that mostly have undulatory motion. Diodontiforms employ their vertical undulatory pectoral fins. And eventually labriforms use their narrow oscillatory pectoral fins.

Amiiforms and *gymnotiforms* propel through their undulatory dorsal and anal fins, respectively. *Balistiforms* and *tetraodontiforms* propel through both dorsal and anal fins, while in the former the fins are undulatory and in the latter the fins are oscillatory [Lindsey, 1979].

2.1.2 Swimming Kinematics

Considering ranges of speed, linear acceleration and turning, six swimming kinematics among swimming animals are recognized. These kinematics are station holding, hovering, slow swimming, cruising, sprinting and fast start [Webb, 1994] (see Fig. 2.3).

Station holding refers to the gait of swimming that the fish tries to keep its ground speed at zero while the water speed is greater than zero. Hovering and slow swimming gaits are similar except in the speed of water. In hovering gait, the speed of water is zero while in slow swimming the water is flowing.

Cruising gait distinguishes a part of swimming that a fish has a sustainable speed for more than 200 minutes without fatigue. While in sprinting, a fish has its maximum speed for at most 15 s. The speed greater than the cruising speed and less than the sprinting speed is called prolonged speed which last between 15 s to 200 min. The last swimming gaits is called fast-start gait. This gait is obtained by sudden change of body shape[1] to achieve high rates of acceleration in less than 1 s, approximately [Domenici and Blake, 1997].

[1]Two main types of body shapes are employed by fishes during fast-start gaits. It could be either 'C'-shape for predators or 'S'-shape for preys [Domenici and Blake, 1997].

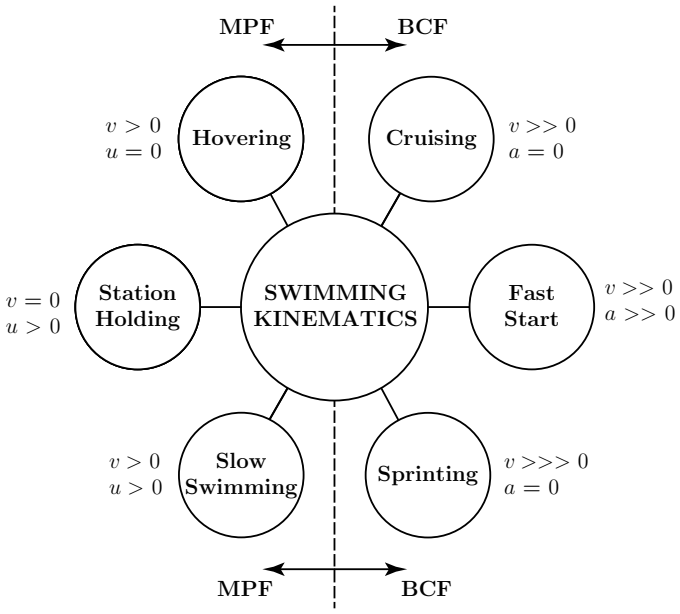

Figure 2.3: Swimming kinematics. u, v and a are water speed, ground speed and acceleration of swimming animal, respectively.

2.1.3 Swimming Muscles

Three types of muscles are responsible to convert the energy of fish into propulsion which are red, pink and white muscles. Red muscles or slow oxidative muscles have low power output and are, thus, non-fatiguing. The non-fatiguing nature of red muscles suits them for sustainable swimming. On the other hand, white or fast glycolyctic muscles produce high power output. This type of muscles are employed for swimming with high speed and/or high acceleration. However, white muscles fatigue very soon. This does not allow them to be used for sustainable swimming. Pink or fast oxidative muscles are intermediate muscles. They provide more power output for propulsion than red muscles and late fatigue in comparison to white muscles. Therefore, pink muscles are more appropriate for intermediate speeds like prolonged speed [Webb, 1994].

The distributions of the aforementioned muscles in various fishes are different. However, 80-100% of body bulk of the fish cross sections is consisted of white muscles. Depending on the habitat nature of a fish, red muscles have different proportion. For instance, the body of pelagic fishes has higher proportion of red muscles in comparison to benthic fishes [Altringham and Ellerby, 1999]. Despite the abundance of white muscles in the body of fish, the red fibres are more abundant in the fish fins. The white muscles seem to be in the fins only for adducting the fins to reduce the drag during

fast swimming [Webb, 1994].

Figure 2.4 illustrates the usage of different muscles in each swimming kinematics.

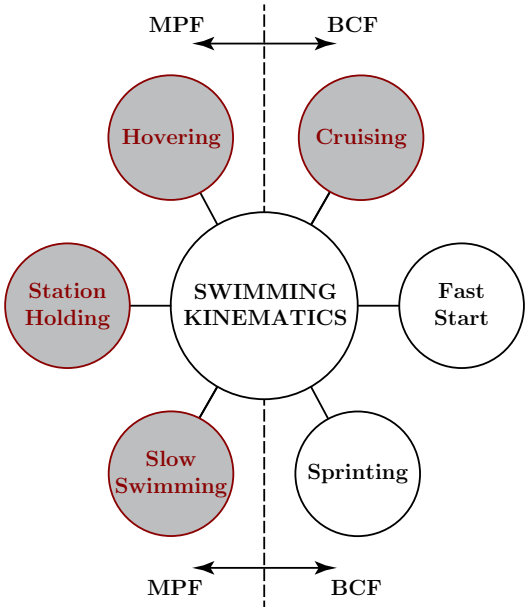

Figure 2.4: Fish swimming muscles: grey circles show the usage of red muscles and white circles show the usage of white muscle in the corresponding swimming kinematics. For simplicity's sake, the pink muscles are omitted.

2.1.4 Time-Based Behaviour

In order to classify the fish swimming motions with respect to time, two groups of swimming motion including periodic and transient motion could be mentioned. Periodic or steady motion like cruising continues in a long period of time to navigate long distances. The transient or unsteady motion like fast start and sharp turn takes a short period of time to escape from predators, to catch preys or manoeuvring among coral reefs [Sfakiotakis et al., 1999].

While speaking about transient motion, there is a distinguishable swimming performance of fish called burst-and-coast. It has been pointed out that MPF swimming mode is principally employed for slow swimming performance and BCF swimmers are efficient for cruising and sprinting. Accordingly, if a fish in BCF swimming mode swims slowly, its performance will not be efficient and fish needs to spend higher amount of energy. To save up to 50% of this energy, fish swims a short period of time with high speed and coasts downward or at a constant depth for another period of time.

Besides the high efficiency of BCF swimmers during bursting, the less drag imposed to the fish during coasting is another important reason of saving energy. Stretched-straight body of fish during coasting has 3 to 5 times lower drag than that of bursting. Burst-and-coast can be used to attain a speed slower than sustainable speed. It could also be used to achieve prolonged speeds [Webb, 1994].

Figure 2.5 shows where fishes use periodic and transient motions with respect to their swimming kinematics.

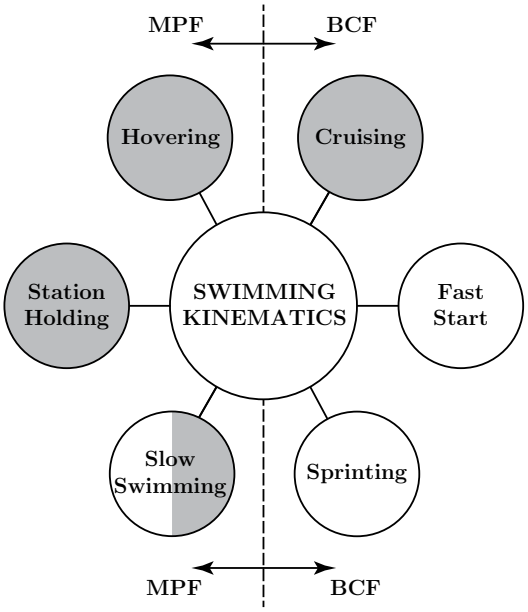

Figure 2.5: Periodic and transient motions of different swimming kinematics. Slow swimming can be periodic if the fish goes forward in a long period of time. Slow swimming can be transient if the fish manoeuvres. Grey and white circles show periodic and transient motions in the corresponding swimming kinematics.

Considering the propulsors, kinematics, muscles and time-based features of fish swimming, the swimming animals have six gaits of locomotion named after swimming kinematics. The first gait is *station holding* employed by some types of rajiforms, balistiforms and anguilliforms. Station holding is a periodic motion that generated mostly by slow oxidative muscles.

The next gaits are *hovering* and *slow swimming* gaits. These two gaits are employed by most of MPF swimmers whose actuating muscles are slow oxidative muscles. Both hovering and slow swimming motions are periodic motion except those slow motions that are used in turning.

Cruising is the next gait of swimming appropriate for all BCF swimmers except

ostraciiforms. As a periodic motion, cruising gait also requires slow oxidative muscles for swimming.

Sprinting is the fastest gait of swimming gait. This gait of swimming is applied by BCF swimmers except anguilliforms and ostraciiforms. Sprinting is a transient motion and is performed through fast glycolytic muscles.

The last gait is *fast-start* gait which is a transient motion similar to sprinting gait. The best swimming mode for fast-start gait is the carangiform mode which propels through the last third of their body. In this gait, fast glycolytic muscles are chiefly activated.

2.2 Swimming Forces

While underwater, a fish is dealing with two types of forces, hydrostatic and hydrodynamic forces. Hydrostatic forces such as weight and buoyancy are acting on the fish even if the fish is not moving underwater. On the other hand, hydrodynamic forces such as propulsive and resistive forces are generated during swimming motion. Although independent, hydrostatic and hydrodynamic forces affect each other during fish locomotion. Therefore, in order to analyse the swimming behaviour of the fish both hydrostatic and hydrodynamic forces - including weight, buoyancy, propulsive and resistive forces - are investigated.

2.2.1 Weight and Buoyancy

The balance of hydrostatic forces, weight and buoyancy, determine the stability of a fish. Weight, W, is defined as the mass of the animal multiplied by the gravity constant while the buoyancy, B, is defined by Archimedes' law as the displaced mass of water

$$W = M_{\mathrm{f}}\, g, \tag{2.1}$$

$$B = \rho_{\mathrm{w}}\, V_{\mathrm{f}}\, g, \tag{2.2}$$

where M_{f} is the mass of the fish, g is the gravity acceleration, V_{f} is the fish volume and ρ_{w} is the density of water. Weight and buoyancy act in the opposite directions. These two forces determine the position and attitude stability of a fish.

The position of the fish depends on its apparent weight, W_{apr}.

$$W_{\mathrm{apr}} = W - B \tag{2.3}$$

If W_{apr} is positive (negative), then the fish sinks (floats). If W_{apr} is zero, then the fish stays at its current depth. In this situation, the fish is neutrally buoyant. The approximate neutral buoyancy is a common feature among many pelagic fishes[1] since those fishes do not need to dive and surf often, and hence invest energy to compensate their non-zero W_{apr}.

The attitude stability of the fish depends on the positions of the centre of mass, C_{m}, and the centre of buoyancy, C_{b}, of the fish. For C_{m} and C_{b} being vertically aligned and equal, the fish attitude is in the equilibrium point. While in the equilibrium point, if C_{b} is positioned closer to the dorsal part of the fish than C_{m}, then the fish is in the stable attitude. On the contrary, if C_{b} is positioned closer to the ventral part of the fish than C_{m}, the fish is in the unstable attitude. In the former, the degree of stability depends on the distance between C_{m} and C_{b}. In the latter, the fish reaches its stable equilibrium attitude in the belly-up configuration.

The stable equilibrium is not usually the case for manoeuvrable fishes. For manoeuvrability, C_{m} and C_{b} of fishes are not vertically aligned to provide easy changes of body attitude. For instance, sharks could easily change their directions downward since their C_{m} is frontier and lower than C_{b} (see Fig. 2.6). This generates a momentum towards the shark head. Then for cruising forward, the animal needs to compensate this instability by dynamic forces [Videler, 1993].

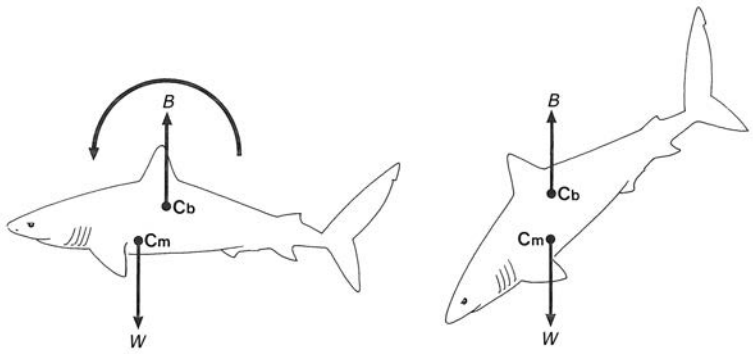

Figure 2.6: Buoyancy and weight acting on a shark [Videler, 1993].

[1] In other words, as cruising/sprinting experts, the pelagic fishes are negative buoyant [Webb, 1994]; however, the difference between their weight and buoyancy is very small and is compensated by hydrodynamic lift generated by their caudal fin, see Sec. 2.3.

Table 2.1: Reynolds number of several swimming organisms [Biewener, 2003]

Swimming Organism	Reynolds Number
Tuna swimming at 3 ms^{-1}	10,000,000.0
Trout fry swimming at 0.2 ms^{-1}	3,000.0
Copepod burst swimming at 0.2 ms^{-1}	300.0
Sperm swimming to advance the species at 0.2 mms^{-1}	0.03
Bacterium swimming at 0.01 mms^{-1}	0.00001

2.2.2 Resistive Forces

The generation of the fish swimming motion is through transferring momentum to the fluid. But not all of this momentum is converted into thrust. A part of this momentum is lost due to resistive forces. Hence an optimal swim requires primarily a motion with the least energy loss as a result of resistive forces.

Resistive forces are mainly created by fluid viscosity and pressure gradient along the animal body. The former is called the skin friction drag and the latter pressure drag or form drag. Depending on the shape and propulsion mechanism of the fish, the importance of these two forces is not the same for all swimming animals, but can be clarified by Reynolds number, Re.

$$Re = \frac{\rho l v}{\mu} \tag{2.4}$$

where ρ is the density of the fluid, l is the characteristic length, v is the velocity of the animal or its fins relative to the fluid and μ represents the viscosity of the fluid that shows the deformation resistance of a fluid.

Reynolds number is a dimensionless parameter that indicates the relative importance of the inertial force to the viscous force. For Reynolds numbers greater than 100, only the inertial forces should be taken into account while for Re less than 1 the viscous force is significantly essential [Biewener, 2003]. The Re values of some swimming organisms are shown in Table 2.1.

As (2.4) confirms, since large and fast fishes that are cruising/sprinting specialists such as tuna have large Re, shown in Table 2.1, pressure drag is the main concern for their optimal swimming not viscous drags. On the other hand, small and slow swimmers such as the majority of MPF swimmers have small Re. Accordingly, MPF swimmers need to minimize the viscous drag during swimming.

Drag forces and their effects on the optimal swimming of fishes are more discussed

in the body/fin shape section, Sec. 2.3.

2.2.3 Propulsive Forces

Several types of propulsion methods are found among fishes. These types of motion generation are classified into two main groups of motion characteristics of the fish body or fins to be either oscillatory or undulatory.

2.2.3.1 Oscillatory Motion

In the oscillation case, a fish generates propulsive waves by oscillating a certain part of its body about its base like the motion of a simple pendulum. This motion could be done like either rowing or flapping. The former is called *drag-based* method while the latter one is called *lift-based* method.

In the *drag-based* mechanism, the swimming motion includes two strokes per cycle: propulsive stroke and recovery stroke, see Fig. 2.7(a). In the propulsive stroke, the fin moves backward approximately perpendicular to the flow in order to increase the drag and acceleration reaction force of water on the fish. Whereas in the recovery stroke, the fin moves forward parallel to the water flow to keep the drag low. Hence, in this method, the forward motion is generated only during propulsive stroke. Figure 2.8(a) illustrates the path that a drag-based pectoral fin undergoes.

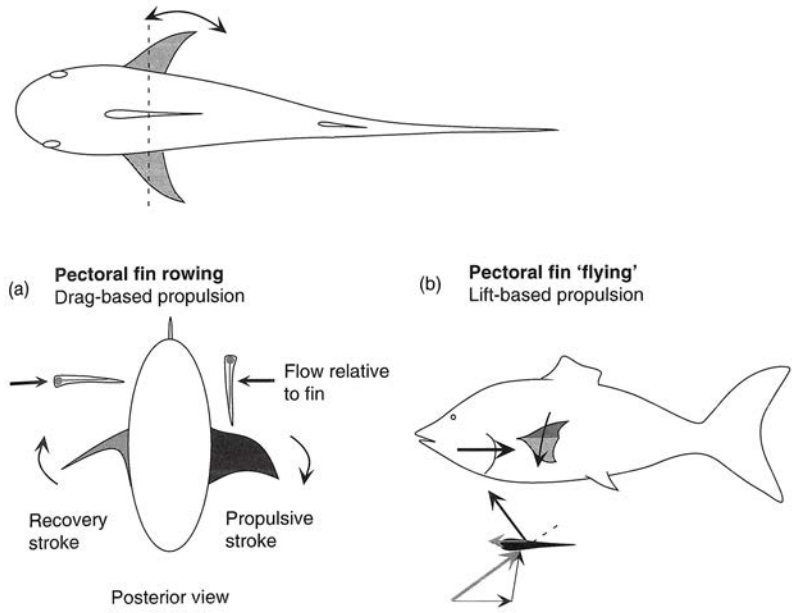

Figure 2.7: (a) Drag-based and (b) lift-based propulsion of pectoral fins [Biewener, 2003].

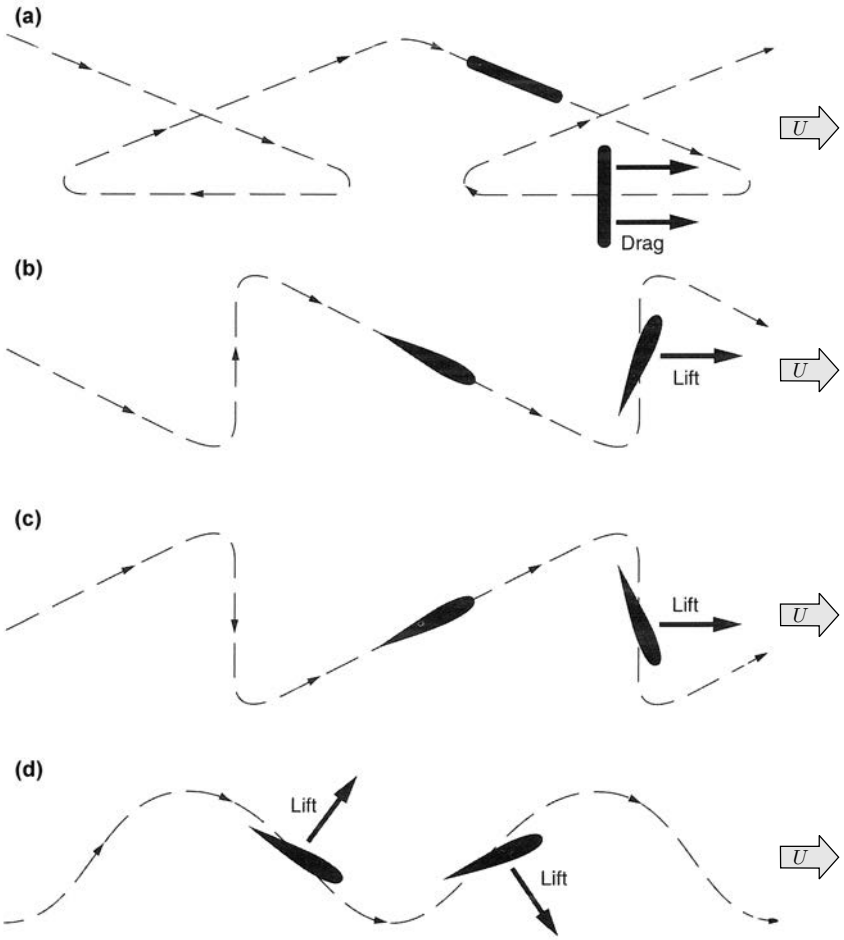

Figure 2.8: The pathway of fins while (a) drag-based swimming and (b-d) lift-based swimming (U is the overall swimming speed) [Alexander, 2002].

Note that, when considering drag-based swimming, another important force, called acceleration reaction force, is taken into account. This force has an important role for accelerating and decelerating the water around the fins. Acceleration reaction force will be discussed in the undulatory swimming section, Sec. 2.2.3.2.

Unlike the drag-based method that needs fins to be perpendicular to the flow, in the *lift-based* method, the fins are approximately parallel to the flow with small angle of attack as shown in Fig. 2.7(b). In the lift-based swimming, the fins are flapping like bird wings in air. In the upstroke, two projected components of lift force are made in horizontal and vertical plane of the flow. The vertical one takes the animal upward and the other one propels it forward. In the down-stroke the horizontal lift component remains constant but the vertical one changes its direction and is oriented downward.

Hence, in both up- and down-strokes, the animal produces thrust [Biewener, 2003].

The path that a flapping fin goes through could be similar to the diagrams illustrated in Fig. 2.8(b-d). For example, bird-wrasses use oscillation like what is shown in Fig. 2.8(b) while pectoral flippers of sea lions use the method used in Fig. 2.8(c). But those two types of fish swimming have limited speed with respect to the method shown in Fig. 2.8(d). This has been tested on Humboldt penguins which generally has the motion illustrated in Fig. 2.8(d) [Alexander, 2002].

Note that, the flapping wings and hydrofoils generate lift through shedding vortex rings, shown in Fig. 2.9. However, how the vortices are made will be discussed in the undulatory motion, Sec. 2.2.3.2.

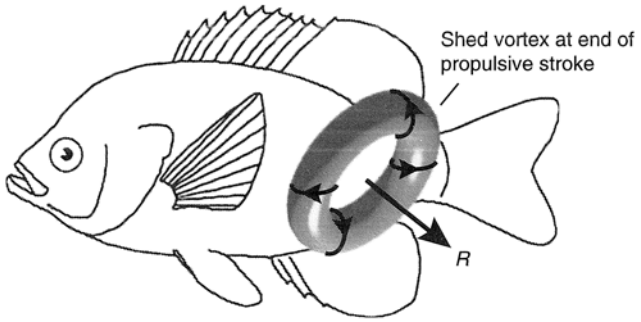

Figure 2.9: Votex rings generated by pectoral fins [Biewener, 2003].

2.2.3.2 Undulatory Motion

In addition to the oscillatory motion, a number of fishes generate propulsive waves by making traveling waves using their bodies or fins at a speed greater than the overall swimming speed of the fish. The tail and the fin of the fish, shown in Fig. 2.10, are generating an undulatory motion. In some types of fish like lamprey, the whole body participates in generation of motion. If this traveling wave has a speed greater than swimming speed of the fish, the fish goes forward, and if this traveling wave has a slower speed than swimming speed of the fish, the fish goes backward.

Similar to the oscillation mode, two distinctive methods of generating forward motion are realized, *acceleration reaction force* and *vorticity method*.

The *accelerating reaction force* is an unsteady flow force which is generated to accelerate and/or decelerate an amount of water that is in contact with its body and fins. To do so, the fish itself needs to be accelerated too. Hence, the acceleration of both the mass of fish and the additional amount of water called added-mass determines

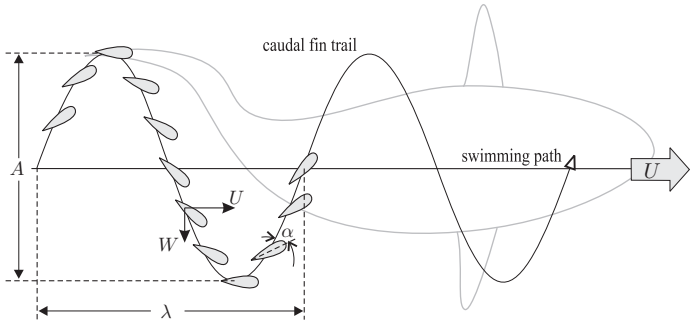

Figure 2.10: Traveling wave generated by undulatory motion of fish with the overall fish swimming speed, U, the lateral speed of the caudal fin, W, the instantaneous angle of attack of the caudal fin, α, the undulation amplitude, A, and the undulation wave length, λ [Sfakiotakis et al., 1999].

the fish swimming performance.

Alongside the undulating wave, the acceleration reaction force, $F_{R,i}$, is generated normal to the wave. This force has two projected components parallel, $F_{T,i}$, and perpendicular, $F_{L,i}$, to the direction of fish motion, see Fig. 2.11. Parallel components are added together and make a net forward force to propel the fish. And over a complete cycle the perpendicular components cancel out each other assuming that the amplitude of the wave stays the same. Nevertheless, most of the times, the wave amplitude enlarges towards the tail, and also the body makes more than one wave per body length. For instance, an eel forms 1.7 waves per body length at each instant [Alexander, 2002].

$$F_T = \sum_{i=1}^{n} F_{T,i} > 0$$
$$F_L = \sum_{i=1}^{n} F_{L,i} = 0$$

In addition to the acceleration reaction force, the undulatory motion could be generated by *vorticity method* which is similar to the oscillatory lift-based mechanism since fish swims using the lift force to shed vortices around the tips of the fin. In this method, the undulation wave is confined to the very last part of the body and the propulsive force is created mainly around the hydrofoil-like fin.

When the hydrofoil is placed in the current of flow with a small angle of attack, the flow around the fin will not stay symmetric anymore. This causes a velocity different at the sides of the hydrofoil. As Fig. 2.12(a) shows, the hydrofoil-like horizontal section of a

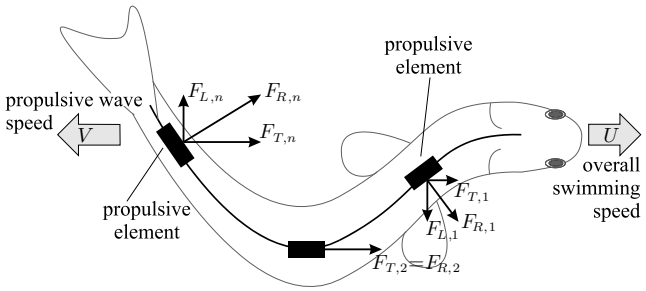

Figure 2.11: Acceleration reaction force method applied by an undulatory fish [Sfakiotakis et al., 1999].

fin when beating to the left, the velocity difference makes two circular and translational motion of flow around the hydrofoil. This could be explained clearly by considering Bernoulli's principle that pressure has inverse proportional relationship with velocity of the flow [Biewener, 2003].

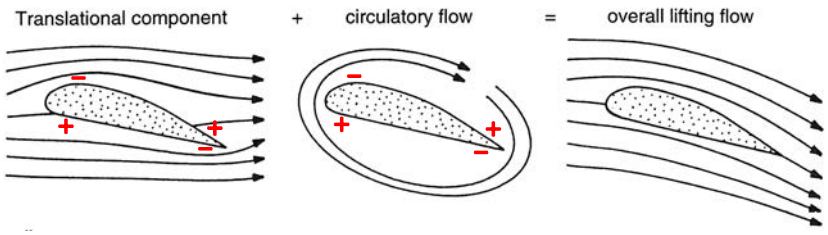

Figure 2.12: The flow around a hydrofoil [Biewener, 2003].

Assume the hydrofoil is beating left with a small angle of attack, α, the flow velocity at the left point of the fin just near to the leading edge and the right point of the fin just near to the trailing edge increases since the streamlines gets nearer together at those points Fig. 2.12-2.13. On the other hand, at the right and left points of the fin near to the leading edge and the trailing edge, the speed of the flow declines. Considering Bernoulli's principle and the fact that the flow moves toward higher pressure points, the flow around the fin moves clockwise. This flow circulation, called bound vortex, is counter-clockwise during right stroke of the fin, see Fig. 2.13(a). The direction of the bound vortex changes whenever the tail changes its direction. What has been seen in the nature indicates that the tail changes its direction at the end of each stroke.

In addition to bound vortices, there is another type of vortices called tail-tip vortex. As its name indicates, the tail-tip vortex are created at the tips of the fins to compensate the pressure difference between different sides of the fin. When the fin is in its left stroke

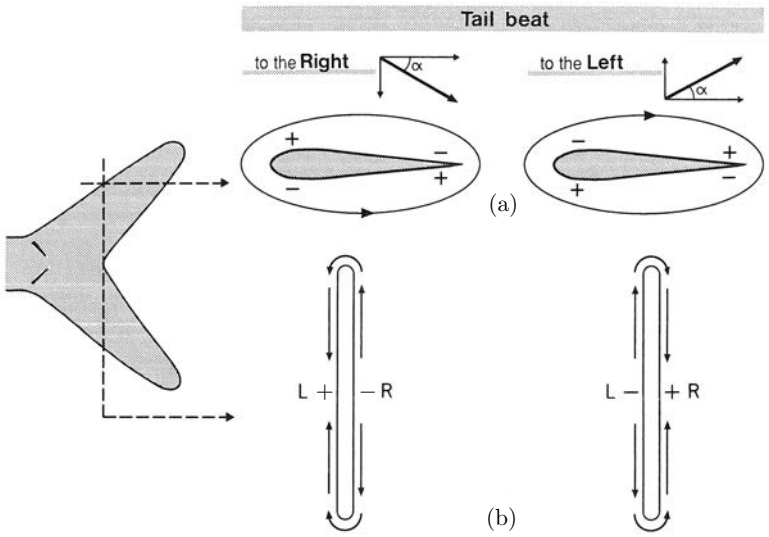

Figure 2.13: (a) The bound vortex around the horizontal section of a beating fin and (b) the tail-tip vortex around the vertical section of a beating fin [Videler, 1993].

the flow pressure at the left hand side of the upper tip of the fin is negative while that is positive in the right hand side. Then the pressure difference makes the flow to circulate over the edge of the tip. The direction of flow motion is opposite at the lower part of the fin, see Fig. 2.13(b).

The combination of bound and tail-tip vortices develops vortex rings like what is shown in Fig. 2.9. The vortex rings have a net force outward that propels the animal underwater [Videler, 1993].

But not all vortices generated by the lift-based method are converted into an optimal thrust during swimming. The optimality of the vortices can be measured by Strouhal number which shows the structure of the vortices made through the body undulation of fishes. The Strouhal number, St, is a dimensionless parameter. It represents the ratio of unsteady to inertial forces and is defined as [Taylor et al., 2003]

$$St = 2\frac{f\,h}{\overline{\dot{x}}} \tag{2.5}$$

where f is the stroke frequency of the body undulation, h is the heave of the caudal fin and $\overline{\dot{x}}$ is the average cruising velocity of the fish. If $0.25 < St < 0.4$, the vortices behind the caudal fin produce maximum thrust. Note that the Strouhal number is mainly applicable for fishes whose swimming is through their body and caudal fins [Triantafyllou et al., 1993].

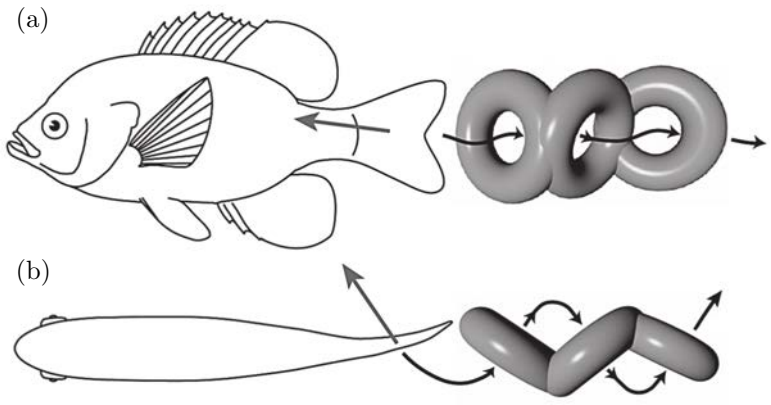

Figure 2.14: Vortex rings left behind a swimming fish, (a) side view and (b) top view [Linden and Turner, 2004].

Although vorticity method in oscillatory and undulatory motions is based on the same principles; the fin path of vorticity method in undulation mode is more similar to Fig. 2.8(d). Out of this category, the fishes like tuna and swordfish could be cited. Cetaceans like whales also swim based on this principle but their flukes oscillate in dorsoventral plane.

2.2.3.3 Propulsive Force Comparison

In order to compare the adaptability of the propulsive forces with respect to the swimming specialities of swimming animals, it is necessary to compare the functionality of the propulsive forces. One of the chief criteria for the comparison is swimming efficiency, called Froude efficiency. Swimming efficiency is expressed as

$$\eta = \frac{P_{\text{use}}}{P_{\text{tot}}}, \tag{2.6}$$

where P_{use} is the useful work done by the fish that pushes the fish forward and generates thrust in the direction of motion. During swimming, the fish pushes the water backward. The backward motion of water imposes an extra work called induced work, P_{ind} that as well as P_{use} constitute the total work of the fish locomotion, P_{tot}.

While swimming, the fish transfers momentum to the water. The mean rate of the transferred momentum to the wake is called thrust, T.

$$T = v_{\text{wake}} \left(\frac{dm_{\text{wake}}}{dt} \right) \tag{2.7}$$

where m_{wake} is the mass of wake or the volume of water that is moved by the fish and v_{wake} is the speed of that wake. Depending on the resistive forces that are acting on the fish, the thrust could provide different swimming speeds for the fish. The multiplication of this speed with the thrust is the useful power of the fish,

$$P_{\text{use}} = T v_{\text{fish}} = v_{\text{fish}} v_{\text{wake}} \left(\frac{dm_{\text{wake}}}{dt} \right), \tag{2.8}$$

where v_{fish} is the fish speed. The induced power, P_{ind}, is also the rate of the kinetic energy, E_{kinetic}, which is transferred to the water.

$$P_{\text{Ind}} = \frac{dE_{\text{kinetic}}}{dt} = \frac{1}{2} v_{\text{wake}}^2 \left(\frac{dm_{\text{wake}}}{dt} \right) \tag{2.9}$$

Accordingly the total power is calculated by

$$P_{\text{tot}} = \left(v_{\text{fish}} + \frac{1}{2} v_{\text{wake}} \right) v_{\text{wake}} \left(\frac{dm_{\text{wake}}}{dt} \right) \tag{2.10}$$

Knowing P_{useful} and P_{total}, the swimming efficiency is obtained as

$$\eta = \frac{v_{\text{fish}}}{v_{\text{fish}} + \frac{1}{2} v_{\text{wake}}} \tag{2.11}$$

Considering (2.11), the thrust generated by the fish drives the fish efficiently if v_{fish} is large in comparison to v_{wake}. In order to increase v_{fish} without increasing thrust, the resistive forces (Sec. 2.2.2) need to be minimized through the appropriate body and/or fin shape for different gaits of swimming. The body and fin shapes appropriate for minimization of the resistive forces are discussed in Sec. 2.3.

In addition to the minimization of the resistive forces, the efficiency could be improved with the same thrust through reducing v_{wake} if a large amount of water are accelerated, see (2.7). In other words, an efficient swimmer slightly increases the speed of a large amount of water instead of drastically increasing the speed of a small amount of water. Hence, the lift-based swimmers such as tuna[1] and bird-wrasse are more effi-

[1] Tunas apply the vorticity method which is actually an undulatory lift-based propulsion.

cient than drag-based ones since they push larger amount of water back. Drag-based swimmers such as eel[1] and angelfish could only push water back in proportion to the size of their fins.

Notice that the undulatory propulsive forces are more efficient than their corresponding oscillatory mechanisms since the undulatory methods accelerate a larger amount of water by their bodies and fins. For instance, tunas whose swimming method is undulatory are more efficient than bird-wrasses with oscillatory lift-based propulsion since the undulation of the last part of the tail peduncle of tunas provide larger displacement for the caudal fin to accelerate larger amount of water.

Beside higher efficiency, the lift-based method has other priorities over drag-based method due to their different duty cycle. As Fig. 2.8 illustrates, in oscillatory motion, drag-based swimmers are generating thrust during only 50% of their fin beating stroke whereas lift-based ones, especially those whose fin beating diagram is similar to Fig. 2.8(d), have 100% duty cycle. This allows lift-based swimmers to obtain higher speed of swimming [Alexander, 2002].

In undulatory swimming, both skin friction and pressure drag in vorticity method are less than those in acceleration reaction force method because of the body movement of the fish in the acceleration reaction force method. During locomotion of the fish, the body will not stay straight-stretched and it will increase both types of drags. While in the vorticity-based swimmers, the body motion is concentrated in the last part of the body while the anterior part of the body remains straight during swimming. Hence, a fish in vorticity method needs less energy for propulsion than a fish in acceleration reaction method.

In drag-based swimming, the speed of pushing water backward in power stroke determines the generation of the thrust. This speed is equal to the difference between the water speed of fish propulsor and the fish itself. The larger this difference, the larger thrust is generated. At the beginning of the motion when fish is stationary, the difference between the propulsor and the fish is large; however, in the middle of swimming, that difference reduces unless the propulsor strokes faster while the propulsor speed has an upper limit. Hence, the drag-based (including acceleration reaction force method) swimmers are privileged for the beginning of the motion or situations that instant acceleration is needed like manoeuvring time.

On the other hand, the lift-based swimmers generate thrust through the speed of the propulsor stroke. If the speed of propulsor with respect to water flow increases,

[1] Eels apply the acceleration reaction force method of swimming which is an undulatory drag-based swimming.

the swimming thrust augments. At the beginning of the motion, the speed of the fish relative to water is zero and, therefore, the propulsive forces are weak. But during swimming, the speed of fish goes up and the propulsors come across the water with higher speed which provides stronger propulsive forces in cruising. Accordingly, the lift-based (including vorticity method) swimmers are adaptable for long-distance swimming [Vogel, 1994].

The comparison of the propulsive forces reveals the role of swimming hydrodynamics on the optimal performance of the fishes. First of all, lift-based swimmers are more efficient than the drag-based swimmers as the former accelerates a larger amount of water. Likewise, undulatory fishes are more efficient than the oscillatory ones since they come across larger amount of water during locomotion. Accordingly, the optimal periodic motion or cruising of fishes requires an undulatory lift-based propulsion. For instance, one of the main reasons for swimming optimality of thunniforms is their undulatory lift-based propulsion method. Even fishes such as ocean sunfishes with MPF swimming mode is optimal for prolonged speed since it has oscillatory lift-based swimming method.

Moreover, the performance of the drag-based swimmers are ideal for instant acceleration such as manoeuvring and fast-start which are transient motion. Accordingly, fishes like pike which has the highest acceleration record among swimming animals use undulatory acceleration reaction force method. And also, the fishes such as angelfish or knifefish that are famous for their manoeuvrability are applying oscillatory and undulatory drag-based swimming mechanisms.

2.3 Body and Fin Shape

To analyse various body shape of fishes, primarily the effects of resistive forces either viscous or pressure drags should be considered. Note that due to the role of Reynolds number, Re, in the description of resistive forces, the body shape effects are discussed here within different ranges of Re.

2.3.1 Body Shape

Depending on Re, streamlines[1] around an object are classified into three types which are laminar, transitional and turbulent. In the laminar flow, the streamlines are roughly parallel to each other. In the transitional one, the flow separation occurs and the

[1] Streamlines are defined as the moving path of a fluid particle in the flow.

vortices are shed. While in turbulent flow, the vortices made due to the flow separation are broken down. To have a laminar flow Re should be very low while in the turbulent flow Re of the object is very high. In between, the flow is transitional [Biewener, 2003].

Reynolds number determines the relative importance of viscous and pressure drag forces. The viscous or skin friction force is produced due to the friction between the flow and the surface of the body. The skin friction drag depends on the surface of the body and viscosity of the fluid. On the other hand, the pressure drag is generated by the gradient of the dynamic pressure in the front and back of the object in the flow. When the flow reaches the back of an object, it is decelerated along the surface. The deceleration is even worse when the flow is separated from the surface of the object since the flow separation could end up in turbulent flow which is irregular and chaotic. The turbulent flow is the main source of energy loss and drop in dynamic pressure.

For small and slow animals like boxfish that have small Re, the viscous drag is more important than the pressure drag. Provided that, to decrease the drag, the surface area should be minimized although it increases the pressure drag. On the other hand, for large and fast animals like swordfish, which have great Re, the pressure drag is more critical than viscous drag. Then swordfish must have a body that reduces its pressure drag. The best way for the reduction of pressure drag is having a streamlined body shown in Fig. 2.15(a) which avoids the flow separation. Comparing with a bluff body illustrated in Fig. 2.15(b), the surface of the streamlined body is increased and, hence, the skin friction drag is enlarged. But since the skin friction drag is not important for higher Re, the resultant drag force is decreased.

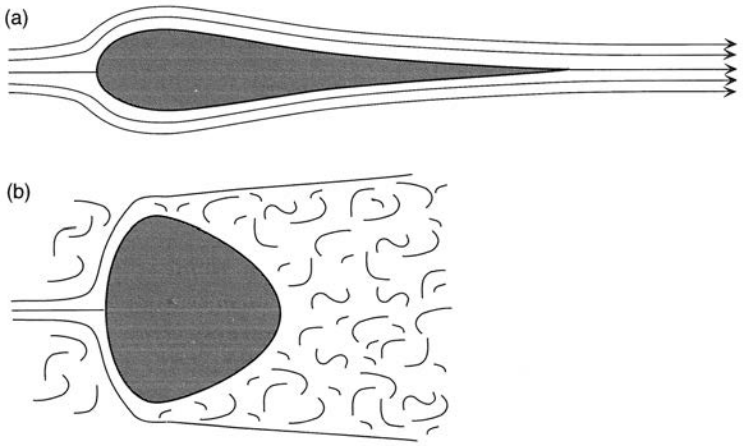

Figure 2.15: The flow around (a) a streamlined body and (b) a bluff body [Biewener, 2003].

In order to have an optimal streamlined body which produces the least drag, there

Table 2.2: The ratio of maximum thickness to length, D/L, of some swimming animals [Videler, 1993]

Swimming Animal	D/L
Fishes	
Bluefin tuna	0.28
Swordfish	0.24
White shark	0.26
Cod	0.16
Mackerel	0.14
Eel	0.05
Cetaceans	
Blue whale	0.21
Bottle-nosed dolphin	0.25
Others	
Emperor penguin	0.26
Harp seal	0.24

is a trade-off between the pressure and skin friction drag. The longer body, the higher skin friction drag and lower pressure drag. The shape of the streamlined body could be justified to submit the minimum drag by considering two elements: the maximum thickness of the animal body, D, and its length, L. In 1956, von Karman tested different streamlined bodies in wind tunnel to find their drag. For all of these bodies, the thickest parts were located in the first third of the body. He showed that the animals with streamlined bodies that have D/L between 0.18 and 0.28 produce less than 10% of the minimum possible drag. Table 2.2 shows D/L of some swimming animals [Videler, 1993].

In addition to the role of the body shape in decreasing resistive forces, the body shape of animals also affects the generation of propulsive forces especially for BCF swimmers whose bodies are involved in propulsive force generation. For instance, as it has been mentioned previously, animals like eel and trout employ undulatory acceleration reaction force method for swimming. In this method of propulsion, the fish needs to push a large amount of water in each propulsive cycle for an efficient swimming. Accordingly, their propulsors, mainly their body toward the tail, need to have a large surface area. Hence, fishes such as eel and trout have deep tail peduncle. Besides the deep tail peduncle, those fishes also need to have a flexible body for undulation. This flexibility requires a compressed body shape in the posterior part which produces undulatory motion with higher amplitude. Anguilliforms, subcarangiforms and carangiforms have this type of body shape; nevertheless, anguilliforms like eels have the most suitable

body shape for undulatory acceleration reaction force.

Despite anguilliforms, the fishes like tunas employ the undulatory vorticity method. Their body undulation is limited to their tail peduncle to provide a higher amplitude for caudal fin stroking. Hence, the tail peduncle does not require to push the surrounding water laterally. Therefore, the tail peduncle of thunniforms like tuna is narrow. The narrow shape of the tail also lessens the produced drag forces during undulation [Lindsey, 1979].

2.3.2 Fin Shapes

Similar to the body shapes of fishes, their fins considerably affect the resistive and propulsive forces as well.

The pectoral fins have two main methods of propulsion, drag- or lift-based swimming, introduced in Sec. 2.2.3. In both aforementioned methods, the fins need to transfer propulsive momentum to the surrounding water. In other words, during drag-based swimming or rowing, the momentum is transferred to water by the surface area of the fins while in lift-based swimming or flapping, the momentum is transferred through the leading edge of the fins. For the sake of efficiency, a larger amount of water in each fin stroke must be accelerated, see Sec. 2.2.3.3. Therefore, the fins in efficient rowing demand large surface area while they need long leading edge for efficient flapping motion.

The suitable shape for rowing and flapping motion could be determined using aspect ratio, AR, which is defined as

$$AR = \frac{S^2}{A} \tag{2.12}$$

where S is the span of the fin and A is its surface area, see Fig. 2.16. The fins with high and low aspect ratios are proper for lift- and drag-based swimming, respectively. For instance, bird-wrasse and angelfish are both labriform swimmers but the former has flapping and the latter rowing motion. Therefore, aspect ratio of pectoral fins of bird-wrasses are higher than that of angelfishes.

Similar to the pectoral fins, the caudal fins have also a significant role in maximizing propulsive forces. The caudal fins which are involved in drag-based swimming need to have low aspect ratio. For example, the undulatory motion of subcarangiforms like trout is a drag-based method. Accordingly, trout fishes have caudal fins with low aspect ratio. On the contrary, the caudal fins which are involved in lift-based swimming need to have high aspect ratio. The vorticity method of thunniforms like tuna is a lift-based

method and tunas have caudal fins with high aspect ratio.

In addition to AR that determines the ratio between the span of the fin and the surface area, the overall shape of the caudal fin also plays an important role for increasing thrust generation since two fins with similar AR could have different performances. For instance, the experimental data has confirmed that backward-curving leading edge produces 8.8 percent drag in comparison with fins without that backward-curve. This is due to the fact that the induced drag made at tail tips is considerably reduced. When the tail tip is not small, some vortices with different speed and direction of propulsive vortex ring will be generated. This works as a resistive force called induced drag [Videler, 1993].

Besides the effects of fins on the fish propulsion, the fin shapes are also justified by the resistive forces. Fishes with high Reynolds number have a streamlined cross-section. That is because of reducing pressure drag. But for fishes with low Reynolds number, viscous drag are more important, and having a streamlined shape for the fins to reduce the pressure drag is not crucial. Slow swimmers like labriforms have flexible pectoral fins to adduct their fins during flapping and rowing to reduce the drag.

So far, the effects of the fin shapes on swimming motion of fishes in horizontal plane are observed. Nevertheless, the fins could also be used for up-down motion. This is more critical for caudal fin shapes since they are mostly responsible for planar propulsion. Caudal fins could be horizontally symmetric, called homocercal, or asymmetric, called heterocercal. Homocercal caudal fin propels the fish forward while heterocercal fins also produce lift force in vertical axis. If the higher half of the fin is larger, then the fin is called epicercal and produces lift upward. On the contrary, when the lower part of the fin is larger, the fin is called hypocercal and the lift force is generated downward. Different types of caudal fin are shown in Fig. 2.16 [Videler, 1993].

Apart from asymmetrical fin shape which produce lift force upward or downward, the asymmetrical musculature of the fins also produce up or down motion. For instance, some types of thunniform swimmers have homocercal caudal fins but the musculature of their caudal fins is asymmetrical. This asymmetry provides sufficient lift force upward to compensate the negative buoyancy of pelagic nature of thunniforms during their continuous swimming [Webb, 1994].

In addition to heterocercal shape and musculature of caudal fins which could be used for generating lift forces towards up and down direction, the pectoral fins of some fishes like sharks provide lift surface for them. These pectoral fins are rather stiff and have high aspect ratio [Videler, 1993].

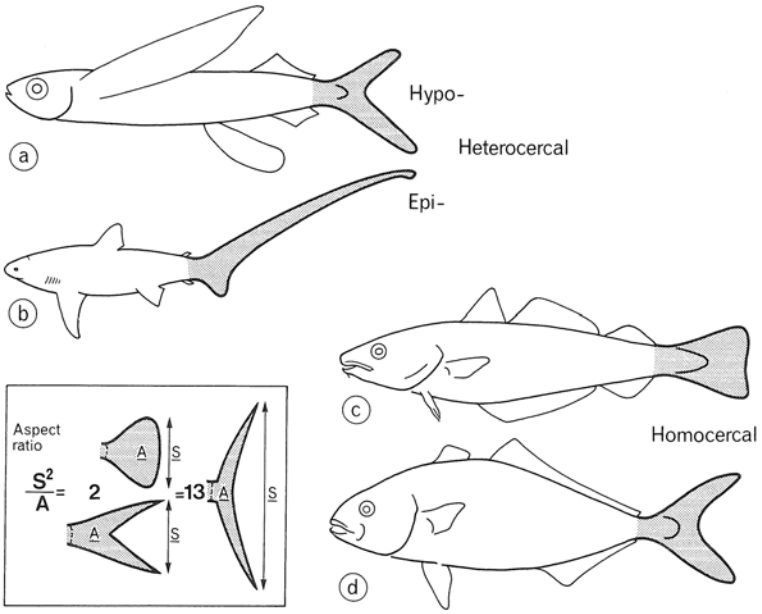

Figure 2.16: Caudal fin shapes could be (a) hypo-heterocercal, (b) epi-heterocercal, (c) homocercal with low AR and (d) homocercal with high AR. [Videler, 1993].

2.4 Summary

Undoubtedly, the marvellous swimming performance of fishes owes to their optimised nature. Nevertheless, fishes are optimized only with respect to their swimming specialities: cruising/sprinting, manoeuvring and accelerating. In the previous sections, these specialities with respect to the swimming gaits, the swimming forces and also the body and fin shapes of fishes are discussed and are summarized in Table 2.3.

The fishes such as tuna whose specialities is in cruising and sprinting are adapted for pelagic lift. They are mainly undulatory BCF swimmers including subcarangiforms, carangiforms and thunniforms.There is an exception of ocean sunfish which is an MPF swimmer, tetraodontiform. Cruising is a periodic motion done through red or slow oxidative muscles whereas sprinting as a transient motion is through fast glycolytic muscles. Cruisers apply lift-based propulsion method which is not suitable for transient motion like fast-start and manoeuvring. Sprinting specialists are mainly drag-based swimmer which is not suitable for periodic motions. The Reynolds numbers corresponding for cruising and sprinting specialists are great and, accordingly, they need to essentially reduce pressure drags. The pressure drag is minimized via the streamlined body shape of these animals. The fin shape of cruising and sprinting specialists are different since they employ two distinct swimming propulsions. The fins of cruisers

Table 2.3: Properties of fish swimming with respect to their specialities. 1 - Swimming propulsors: body and/or caudal fin, BCF, including anguilliforms, ANG, subcarangiform, SBC, carangiforms, CRN, thunniform, THN, osctraciiform, OST, and median and or paired fins, MPF, including rajiform, RJF, diodontiform, DDN, labriform, LBR, amiiform, AMF, gymnotiform, GMN, balistiform, BLS, tetraodontiform, TTR. 2 - Swimming kinematics: station holding, STH, hovering, HVR, slow swimming, SLW, cruising, CRS, sprinting, SPR, fast-start, FST. 3 - Swimming muscles: slow oxidative, SO, fast glycolytic, FG. 4 - Time-based feature of swimming: periodic, PRD, and transient motion, TRN. 5 - Swimming propulsive forces: oscillatory lift-based method, OLM, oscillatory drag-based method, ODM, undulatory vorticity method, UVM, undulatory acceleration reaction method, UAR. 6 - Swimming resistive forces: viscous drag, VD, and pressure drag, PD. 7 - Body/Fin shape: streamlined body shape, STL, short and deep body, SDB, high fin aspect ratio, HAR, low fin aspect ratio, LAR.

SPECIALTY	**1**	**2**	**3**	**4**	**5**	**6**	**7**
Cruising/Sprinting	BCF THN CRN SBC	CRS SPT	SO FG	PRD TRN	UVM UAR	PD	STL & HAR STL & LAR
Accelerating	BCF CRN SBC	FST SPT	FG	TRN	UAR	PD	STL & LAR
Manoeuvring	MPF all BCF OST	HVR SLW	SO	PRD	UAR ODM OLM	VD	SDB & LAR

have crescent shape with high aspect ratio whereas the sprinters need fins with low aspect ratio to have larger surface area.

The accelerators such as pike that has the highest acceleration record among fishes are suitable for fast-start gait of BCF swimmers such as carangiforms and subcarangiforms. The accelerators usually swim on the bottom to suddenly hunt the preys. This gait of swimming needs a transient motion and, thus, white or fast glycolytic muscles are activated during this type of motion. Similar to other transient motion, optimal accelerating motion needs a drag-based swimming. The accelerator fishes apply the acceleration reaction force method. The main resistive force for accelerators is pressure drag and, thus, they have streamlined body. However, to provide large thrust at the beginning of their swimming, they have large caudal area as well as an extended dorsal or anal fins at the posterior part of their body. Similar to the other drag-based swimmers, the caudal fin of the accelerators has low aspect ratio.

The last swimming speciality is manoeuvring which is applied by approximately all

MPF swimmers. They usually live in coral reef areas where precise motion is needed. Manoeuvring specialists usually have hovering and slow swimming gaits of swimming motions. In hovering and slow swimming gaits of swimming which are mainly periodic motions, the red or slow oxidative muscles are applied. The absolute majority of MPF swimmers have both oscillatory and undulatory drag-based swimming motions; however, in some type of manoeuvres such as some rajiforms, labriforms and tetraodontiforms. These fishes have oscillatory lift-based propulsion method. The manoeuvring specialists have mainly large and flexible fin. Due to the slow swimming and small Reynolds number of manoeuvres, they mainly concern about viscous drags and accordingly have short and deep body.

Among all three aforementioned swimming specialists, there are some fishes that are expert in station holding. These fishes could be found in the category of MPF swimmers including rajiforms and balistiforms with flat shape, and BCF swimmers such as carangiforms and anguilliforms. The formers are usually flat and parallel to the substratum. The others have compressed body shape and have sufficient fins or flexible propulsors to hold their position through grasping the substratum.

Chapter 3

State of The Art

In the previous chapter, it is discussed that the optimal performance of fishes is within their swimming specialities which are determined by swimming gait, swimming force, and body and/or fin shape of the fishes. Swimming gait of fishes could be understood by their swimming modes which are either body and/or caudal fin (BCF) or median and/or paired fin (MPF), Fig. 2.2. Accordingly, through detecting of the swimming mode of fishes, their swimming specialities are recognized.

Analogous with fishes, capabilities of the biomimetic robots are also recognizable from their swimming modes. For instance, the robots that are inspired from labriforms are optimized and specialized for manoeuvring while fast swimmers are among thunniforms. Hence, in this chapter the robots are presented based on their swimming modes to be BCF-form, Sec. 3.1, and MPF-form fish robots, Sec. 3.2. As well as the swimming modes, the fish robots are further investigated with respect to their actuation mechanism and body shape in Sec. 3.3.

3.1 BCF-Form Fish Robots

The existing swimming robots are largely inspired by BCF mode of swimming. This mode includes five subgroups that are distinguished by their undulatory and/or oscillatory swimming. For all of these subgroups of BCF swimmers, corresponding robots are designed and constructed.

3.1.1 Anguilliforms

Anguilliforms like eel and lamprey are the most undulatory fishes among BCF swimmers. Whole anguilliforms' body participates in undulatory motion with large ampli-

tude. In some cases, the amplitude increases towards the caudal fin [Lindsey, 1979]. The travelling wave made by anguilliforms' body is short and more than 1 in a body length. 1.7 waves per body-length is reported in some fishes [Alexander, 2002].

In order to make undulatory motion, the muscles in both sides of vertebral column are activated. One side is contracted while the other is relaxed and to some extent stretched. This creates a bending in the body shape started from the anterior segment of the body. The bending moves along the body towards the tail by gradually stretching the contracted muscles and contracting the muscle of the other side [Lindsey, 1979].

In terms of shape, anguilliforms like eels have long and thin shape. They usually have taper shape, cylindrical shape for anterior part while the posterior part is laterally compressed. Their body span is expanded by the tail. They also have a small or rounded caudal fin with low or moderate aspect ratio. Some anguilliforms do not possess caudal fin [Lindsey, 1979].

Anguilliforms are not fast and efficient swimmers in comparison with other BCF swimmers; however, the long and thin body allows them to live in habitats with coral reef like the bottom of the sea [Lindsey, 1979]. Anguilliforms tend to have the minimum recoil since they generate more than 1 wave per body-length which minimizes the lateral forces. Besides, they are capable of backward swimming [Sfakiotakis et al., 1999].

Considering the aforementioned type of body shape as well as backward and manoeuvrability capabilities, anguilliform-like robots are adapted robots for motion planning underwater [McIsaac and Ostrowski, 2003]. Two swimming robots from this category could be observed in this section.

Ayers et al. [2000] have developed a biomimetic lamprey robot shown in Fig. 3.1(a). This robot includes a rigid head, a flexible body and a passive tail. The flexible body is actuated by shape memory alloy artificial muscles. The artificial muscles are propagated on either side of the body. Actuation of these muscles in sequence provides the rhythmic lateral undulation of the robot which generates swimming motion of the robot. The robot could propel backward by reversing its rhythmic undulation.

Recently, Boyer et al. [2009] have started to develop an eel-like swimming robot using parallel mechanism. This robot has 12 vertebrae with 3 degrees of freedom of rotation for each vertebrate. All these identical vertebrae have parallel mechanism but are mounted in series together. For the skin of the robot, rubber rings with intermediate rigid section is used in order to provide easy distortion and also resist the pressure of the water around it.

3.1.2 Subcarangiforms

Similar to anguilliforms, whole body of subcarangiforms like trout participates in undulatory motion; however, the amplitude of the undulation is larger at posterior half or one-third of the body. In this swimming mode, the body has a sinusoidal motion and the tip of the snout is oscillating with moderate amplitude.

In terms of shape, subcarangiforms are more rounded and heavier than anguilliform. They have a fairly deep tail peduncle. Their caudal fin has low aspect ratio with straight or slightly inward curve-shaped margin at posterior part. Their caudal fin is flexible and able to change its area by 10% during different stages of swimming.

The speed of subcarangiforms highly depends on the body undulation. The caudal fin does not affect the speed of the fish in this mode; however, it could be used for high acceleration, fast turning and high-speed maneuverability. In order to increase the speed of motion greater than 1 or 2 body-lengths per second, these fishes do not enlarge the amplitude of undulation but the undulation speed and accordingly beating frequency of the caudal fin increase. Yet, the maximum frequency produced by a subcarangiform fish depends on its size. The larger the fish, the smaller the undulation frequency [Lindsey, 1979].

Trout is an example of subcarangiforms developed by Salume [2010] shown in Fig. 3.1(b). The 0.5-meter artificial trout has three main parts: a nose cover, a middle flange and a silicone tail. All the electronics and actuation components are inside the nose cover and the flange. The propulsion is made in the posterior part of the robot using a rotational actuator. In other words, a DC motor is connected to a plate by two flexible steel cables while the plate is casted inside the tail. A sinusoidal rotation of the motor causes undulation of the tail to propel the robot.

(a) Lamprey robot (b) Trout robot

Figure 3.1: Two fish robots inspired by anguilliforms and subcarangiforms

As it has been described, Salmuae does not follow the traditional procedure to

develop a swimming robot using multiple linkages. Instead, Salumae has implemented work done by Alvarado [2007] to develop a propulsor part of the robot mimicking the morphology of a real fish, in particular, the geometry, stiffness and stiffness distribution of the body, and the caudal fin.

3.1.3 Carangiforms and Thunniforms

The next group of BCF swimmers, carangiforms like Mackerel, propels through undulation of the last third of their body. The thrust is mainly produced by the caudal fin. The undulation wavelength is never completed in a body length. Thus the lateral forces cannot be cancelled out and cause the tendency of the fish to recoil by sideslipping and yawing.

The recoil tendency of carangiforms is controlled in two ways. The amplitude of undulation increases just close to the caudal fin where the body span of the fish is greatly reduced. This reduction which is called narrow necking lessens the energy that is dissipated through displacing water around the tail peduncle. The recoil is further controlled by increasing the mass and the body span of the fish at the anterior part. The body span of the fish could be increased by stiff median fins which increase the resistance of the fish to sideways displacement.

In terms of shape, carangiforms have more rigid anterior part compared with anguilliforms and subcarangiforms. The tail peduncle is narrow and flexible. Carangiforms have also stiff and forked shape caudal fins with high aspect ratio. The area of the caudal fin in this mode is not controllable similar to the previous modes. The angle of inclination of the caudal fin also changes when the caudal fin reaches its maximum lateral motion to always have a backward-facing component during motion [Lindsey, 1979].

The carangiforms are more efficient and faster than the previous swimming modes; although, its turning and manoeuvrability are limited because of the rigidity of the anterior part of their body [Sfakiotakis et al., 1999].

Usually the fastest and the most efficient carangiforms are categorized as thunniforms like tuna [Colgate and Lynch, 2004]. Although, this is not a fully representative definition for thunniforms since they apply different kind of hydrodynamic propulsion in comparison with carangiforms.

Thunniforms generate undulatory wave significantly by the very last part of their tail peduncle. The wavelength of undulation is long, and wide at trailing edge of the

caudal fin. They provide thrust mainly by their stiff caudal fin[1]. The angle of attack of the caudal fin changes once it reaches its maximum amplitude in order to maximize the thrust.

Thunniforms have quite streamlined body shape. The anterior part of their body is heavy, inflexible and often circular in cross section. The posterior part including the tail peduncle is lighter and flexible. The tail peduncle is strengthened by the keels located at either sides of the peduncle. Due to the keel, the tail peduncle is wider than it is deep. In addition to strengthening the tail peduncle, the keels have an important role in decreasing the drag during rapid lateral motion of the tail.

In addition to keels, there exist five to eleven finlets along the body. These finlets are located above and beneath the body and serves to reduce drag. The drag decreases since the finlets avoid separation of the boundary layer around the body. The body is connected to the caudal fin with the narrow neck of the tail peduncle.

Thunniforms' caudal fin is crescent-shape with high aspect ratio[2]. Their caudal fin is stiff; however, it shows a slight flexibility during powerful stroke. The span of the caudal fin does not change except for some type of thunniforms which have very small change. During the stroke of the caudal fin, the centre of the caudal fin is leading and the tips are following.

Among fishes, thunniforms are the fastest and the most efficient swimmers[3]. However, taking hydrodynamic characteristic into account, thunniforms are adapted for pelagic swimming with calm waters. Accordingly, thunniforms do not perform well in turbulent waters like streams, tidal rips and so on. They are not also capable of slow swimming, turning, manoeuvring and rapid accelerating [Sfakiotakis et al., 1999]. In comparison with carangiforms, thunniforms are less reluctant to have sideways recoils. This is due to heavy body at anterior part, the narrow neck of the tail peduncle and the high-aspect ratio caudal fin [Lindsey, 1979].

Note that cetaceans have quite similar swimming mechanisms of thunniforms. The only difference between cetaceans and thunniforms is the shape of their tail. Cetaceans have horizontal fluke while thunniforms have vertical caudal fin. Due to the similarity in swimming mechanisms, dolphin-like robots are also discussed in this section. In addition, since the swimming mechanisms of carangiforms and thunniforms are quite similar, a number of works done based on thunniforms is called carangiforms in literature. In fact, in many cases the robots mimicking carangiforms and thunniforms

[1] 90% of thrust is produced by the caudal fin
[2] Large span and short chord
[3] Thunniforms could be up to 90% efficient

are not distinguishable. Accordingly, in the following paragraphs the examples of both subcategories are discussed together.

As previously indicated, RoboTuna was built at MIT in 1994 [Triantafyllou and Triantafyllou, 1995]. This robot is the prominent example of thunniform-mimetic robots. Six years later, RoboTuna was improved as RoboTuna II [Beal, 2003; Jakuba, 2000]. Being carriage mounted and using external power support, these robots mimic the swimming mechanism of a bluefin tuna. RoboTuna have eight linkages while six links are independently actuated. Figure 3.2 shows RoboTuna and RoboTuna II.

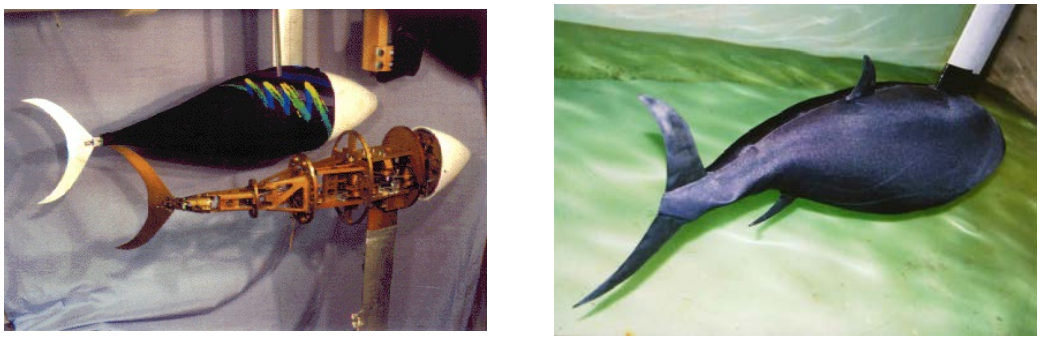

(a) RoboTuna I (b) RoboTuna II

Figure 3.2: Tuna-like robots built at MIT.

At MIT, another fish-like robot, RoboPike, was built [Triantafyllou et al., 2000]. As its name indicates, this robot is inspired by a pike. On the contrary of the previous robots, this robot is a free swimming robot. RoboPike has three degrees of freedom (DOF), two of which are for producing undulation and one DOF is for changing the angle of the pectoral fins. RoboPike is actuated by DC servo motors. While the undulation is to propel the robot, the pectoral fins are employed as rudders.

Inspired by RoboTuna, Vorticity Control Unmanned Undersea Vehicle (VCUUV) was developed in 1997. Similar to RoboPike, VCUUV is a free swimming robot using its tail for propulsion and pectoral fins for steering. Using hydraulic power unit, VCUUV has four active links to create undulation. This fish robot is able to go up and down under water and avoid obstacles [Anderson and Chhabra, 2002; Liu and Hu, 2004].

In addition to RoboTuna and VCUUV that are tuna-mimetic robots, Kim and Youm [2004] and Lashkari et al. [2010] have constructed two tuna-like robots called PoTuna and ARTEMIS. PoTuna is 1 m and 25 kg and actuated with one motor through a 2-link mechanism. The robot is also able to go up and down, and turn using the lift surface of the pectoral fins and the ventral fin, respectively. ARTMIS swims through

undulation of a 3-link tail. The tail mechanism of ARTEMIS is a scotch yoke with rack and pinion mechanism which is actuated by only one DC motor. ARTEMIS is able to turn and change its swimming speed through position and speed of control of its motor, respectively.

The mackerel-mimetic robot, BASEMACK1, developed by Lee et al. [2007] is an example of carangiform robots. BASEMACK1 has three links forming tail peduncle. The first link is attached to its front body (head) and the last one is attached to the caudal fin. The caudal fin which is shaped based on real mackerel tail is made from 1 mm thick flexible metal. All the links are actuated by DC servo-motors. BASEMACK1 has mimicked mackerel geometrically.

Regarding carangiforms, several fish robots have been developed at University of Essex [Liu et al., 2004, 2005]. The robots are in two groups of G and MT and produce undulatory motion using multi-linkages. Figure 3.3 illustrates the fish robots model G9 and MT1. For more information the reader is referred to [Liu, 2006].

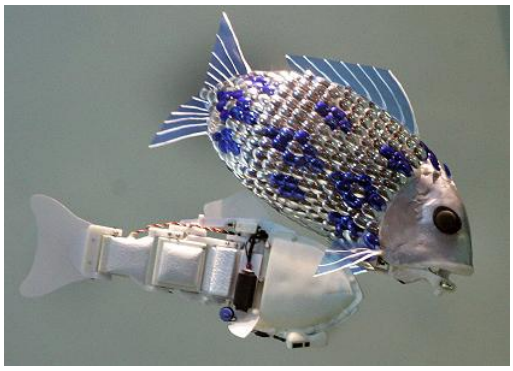

(a) Model G9 [Beciri, 2009]

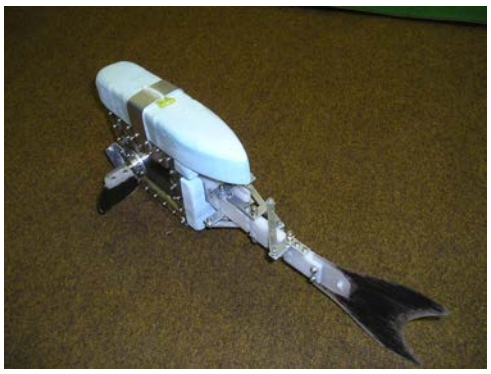

(b) Model MT1 [Liu, 2008]

Figure 3.3: Fish robots developed at the University of Essex.

At University of Washington, a group of robotic fishes have also been developed that have characteristic of a carangiform robot [Morgansen, 2003; Morgansen et al., 2007]; however, they could use their pectoral fins for surfing and diving. At Beihang University, several robotic fishes, SPC series, have been developed [Liang et al., 2011; Wang et al., 2005]. These torpedo body shape robots swim using 2-link caudal fin. Besides caudal fin, the robot makes benefit of two fixed dorsal and anal fins for stabilization. SPC series robots are built to study the performance of tail fin. Robofish and SPC-III developed at University of Washington and Beihang University are illustrated in Fig. 3.4.

Festo Company has also constructed a pneumatically actuated fish robot called

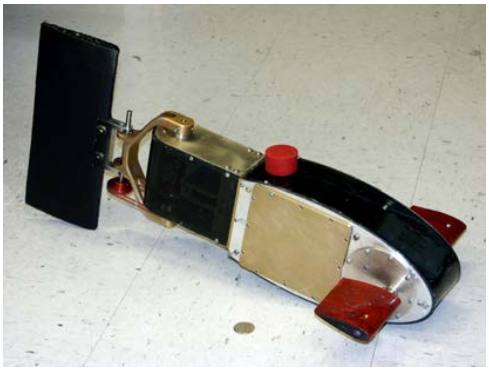

(a) Robofish [Morgansen et al., 2007]

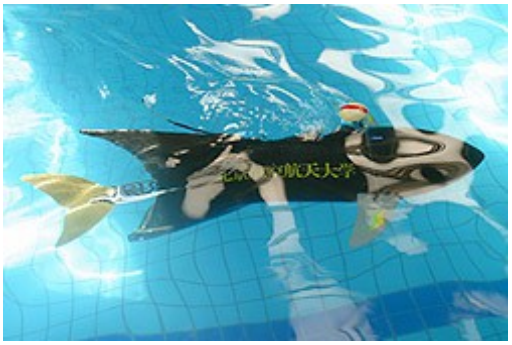

(b) SPC-III [SPC]

Figure 3.4: Fish robots built in University of Washington and Beihang University.

Airacuda which could be categorized in carangiform swimming robots [fes, 2013]. On the contrary of the majority of the BCF-mimetic robots that actuate the caudal fin through linkages, Airacuda is actuated by four muscles: two muscles used for actuation of the tail and the other two are employed for steering. The length of Airacuda is 1 m and its weight is 4 kg. The robot is also able to go up and down using a water tank inside the body.

Besides fish-like robots, a number of dolphin-like robots have been developed initially by Nakashima and Ono [2002]. They built a three linkages robot. Using spring and damper at joints, they made the robot self-propelled. Soon after, Nakashima et al. [2004] built a new dolphin robot that use DC motor in the first joint while the next joint is passive. The new robot was able to have three-dimensional motion. In 2005, Dogangil et al. built a pneumatically driven four-link robot [Dogangil et al., 2005]. Afterwards, Yu et al. [2007a] built a five-link dolphin robot actuated by five DC servo motors. However, in order to increase the efficiency, Yu et al. [2007b] designed a two-motor driven scotch yoke mechanism for undulation of the tail. The length of the crank in this mechanism is adjustable. Figure 3.5 shows uncoated dolphin robot built by Yu et al. [2007b].

The existing carangiform- and thunniform-mimetic robots are not limited to what have been mentioned in this section. However, similar works are described here. For instance, works done by Mason and Burdick [2000], Saimek and Li [2004], Kim et al. [2007] and Mohammadshahi et al. [2008] are not mentioned. But there are other fish robots which have their undulation caused by multi-linked actuation that correspond to thunniforms.

Figure 3.5: Uncoated dolphin robot developed by Yu et al. [2007b].

3.1.4 Ostraciiforms

Ostraciiforms are the only purely oscillatory BCF mode. The caudal fin is the only propulsor for this mode which has pendulum-like oscillation around the connection point between the caudal fin and the tail peduncle. Ostraciiforms oscillate their caudal fin by alternatively contracting the muscles on either sides of the tail peduncle. This mode does not perfectly match any living fish. Some fishes like boxfish can employ this mode of swimming beside other mode like MPF mode.[1] This mode of swimming is usually applied as an auxiliary propulsion system.

Ostraciiforms have different body shape, although their body is inflexible. Ostraciiforms like boxfishes do not have streamlined body shape in order to decrease the resistive forces. In this mode, the caudal fin is to a certain extent stiff with low aspect ratio.

The propulsors of thunniforms and ostraciiforms are rather similar, nevertheless the hydrodynamic characteristic of these two swimming modes are completely different. Ostraciiforms have low hydrodynamic efficiency. This mode of swimming is usually used for slow swimming among fishes, e.g. scabbard and crestfish [Lindsey, 1979].

To name an ostraciiform robot, Micro Autonomous Robotic Ostraciiform (MARCO) designed and fabricated by Kodati et al. [2008] could be mentioned. MARCO is inspired by a boxfish. This fish robot shown in Fig. 3.6 has a pair of 2-DOF pectoral fins and a single DOF caudal fin. The design of the pectoral fins is according to the actual boxfish shape while hydrodynamic experiments are considered for the design of the tail shape. MARCO uses its pectoral fins for steering the motion while the caudal fin propels the robot. Noting that the robot mimics a real boxfish, MARCO has also a

[1] Due to this, sometimes ostraciiforms are categorized in MPF swimming mode since some ostraciiforms like boxfish use their median or paired fin to swim. To illustrate, in [Colgate and Lynch, 2004] ostraciiforms are categorized as MPF swimmers.

body shape quite similar to its corresponding actual fish in nature. The robot is highly manoeuvrable by making benefit of its pectoral fins. Added to that, the pectoral fin could also work as lifting surfaces for the robot which is valuable for up-down motion.

Figure 3.6: MARCO inspired by a boxfish as an ostraciiform Kodati et al. [2008].

On the contrary of the BCF-form robots whose caudal fins are modelled with a flat and flexible shape, Esposito et al. [2012] have developed a fish robot inspired from bluegill sunfish that swims by a caudal fin that is moving with its fin rays. This robot is produced based on the biological studies done by Flammang and Lauder [2009] and Flammang and Lauder [2008] on the caudal fin of a bluegill sunfish. The caudal fin is made by six fin rays to mimic five kinematic pattern used by sunfishes; although, sunfishes have 19 fin rays. The fin rays are controlled independently through low stretch tendon connected to rotational servo motors. The stiffness and size of the fin rays are scaled down from the real fish. The main body of the robot is designed to be streamlined, see Fig. 3.7.

3.2 MPF-Form Fish Robots

MPF swimmers categorized in seven groups based on their propulsors and their types of motion. Similar to BCF mode, the propulsors in MPF swimming mode has two types of motion, oscillatory and undulatory. In oscillatory mode, the fins could have rowing and/or flapping motion. In rowing motion, the fins move forward horizontally and backward broadside. In fact, the propulsion forces are generated during backward stroke of the fins. In flapping motion, the fins go up and down almost similar to flapping wings of birds. This provides a net force in both up and down strokes [Sfakiotakis et al.,

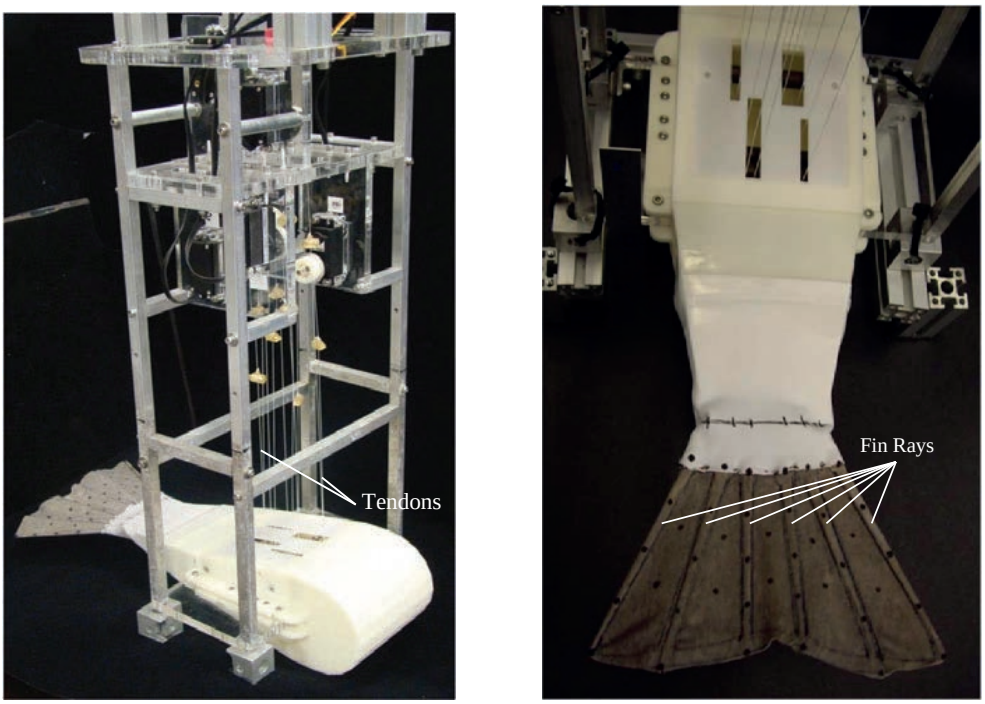

(a) Side view (b) Top view

Figure 3.7: The flexible caudal fin which is actuated by the fin rays [Esposito et al., 2012].

1999], see Sec. 2.2. Labriforms and tetraodontiforms have oscillatory fin motions.

In undulatory mode, the fins have more complicated motion. Undulatory fins are made of several fin rays which are connected to the body at their bases. The rays could be moved independently and are connected together by a flexible membrane. In comparison with the body undulation, the fin undulation could reach higher frequencies up to 70 Hz but with smaller amplitude. The fishes whose swimming motions are through their undulating fins cannot reach high speed. On the other hand, undulating fins enable the fishes to have precise controllability and manoeuvrability. In addition, the fins allow a fish to have both forward swimming and backward swimming without turning. The undulating fins do not occupy a large area during swimming. Accordingly, they are suitable for swimming in confined spots in the water. Rajiforms, diodontiforms, amiiforms, gymnotiforms and balistiforms have undulatory fin motions [Lindsey, 1979].

Many MPF-mimetic robots and mechanisms are developed thus far. However, some of the MPF subgroups such as diodontiforms, balistiforms and tetraodontiforms do not have any corresponding robots. In this section, all subgroups are discussed because of their potential to be designed.

3.2.1 Rajiforms

Rajiforms swim using enlarged pectoral fins which are the lateral expansion of the body. The pectoral fins of the rajiforms could have two types of locomotion, undulatory or oscillatory. In undulation mode, the amplitude of undulation increases from the anterior part to the posterior to create wave [Sfakiotakis et al., 1999]. In oscillation mode, however, the fins behave like flapping wings of birds in the air in order to create a wave with higher amplitude.

Rajiforms like eagle rays and mantas have larger pectoral fins in comparison with rajiforms like stingrays. The former have pretty oscillatory motion while the latter has undulatory motion. Undulatory rajiforms are more adapted for sedentary life while the oscillatory swimmers are more capable of free-swimming life.

Willy and Low [2005] have developed a stingray-like robot which has undulation mode, while Gao et al. [2007, 2009] have developed BHRay-I and BHRay-II inspired by manta ray with oscillatory motion of fins.

To create the undulation, Low and Willy [2005] designed two flexible pectoral fins. The fins include fin rays where they are separately controlled. To actuate the fins, ten servo motors are used while a crank is attached to the end of each motor to play the role of fin rays. All the rays are also connected together using a flexible membrane made of thin acrylic sheet between each two rays. Figure 3.8 illustrates the swimming mechanism developed by Low and Willy.

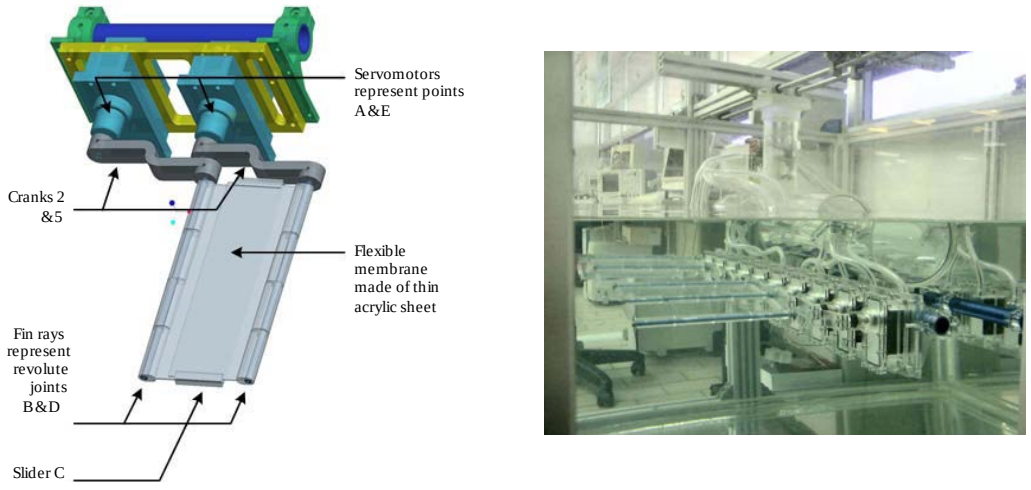

(a) CAD model for two fin rays connected together

(b) Rajiform robot made of nine lateral fins

Figure 3.8: Model of fin mechanism mimicking rajiforms [Low and Willy, 2005].

In order to design BHRay-I, two 1-DOF fins actuated by a servo motor are employed. The pectoral fins are made of carbon fibre pipe, a silicone rubber board and reinforcing aluminium. The carbon fibres placed at the leading edge of the fins are actuated by motors. Then the flexible silicone rubber passively generates phase difference which is critical for an efficient thrust production of the fins. However, due to the non-adjustable flapping parameters, amplitude and frequency, Gao et al. [2009] enhanced their previous design using two servo motors working for the fins individually. They called the new version, BHRay-II. BHRay-I and BHRay-II are shown in Fig. 3.9.

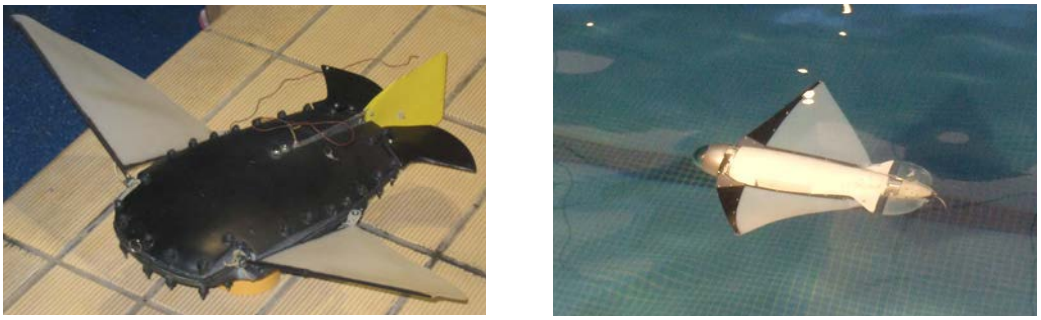

(a) BHRay-I [Gao et al., 2007] (b) BHRay-II [Gao et al., 2009]

Figure 3.9: Fish robots inspired by manta ray.

3.2.2 Diodontiforms

Similar to rajiforms, diodontiforms like porcupine fishes propel through their broad pectoral fins. But their pectoral fins are vertical and undulatory. Their undulation may be made of 2 wavelengths at each instant.

Diodontiforms are able to have up-down motion using the vertical component of forces made by pectoral fins. In addition to undulation, the pectoral fins could have flapping motion in labriform swimming mode. The combination of these two swimming modes enables fishes like porcupine to have slow but precise manoeuvrability.

3.2.3 Labriforms

Similar to rajiforms and diodontiforms, labriforms swim by their pectoral fins; however, labriforms have oscillatory and narrower pectoral fins. Among labriforms both types of oscillation could be found such as angelfishes whose pectoral fins have rowing motion and bird-wrasses whose pectoral fins have flapping motion.

Most of labriforms have comparable prolonged speed with that of BCF mode swimmers. For providing high prolonged speeds, the pectoral fin frequency becomes similar to the beating frequencies of the caudal fin of BCF swimmers. Like other swimming modes, this mode could also be combined with other swimming mechanism like ostraciiforms. Many fish also use their pectoral fins for only slow swimming and/or position holding [Lindsey, 1979].

As the most important MPF swimmers, labriforms are highly manoeuvrable. This is due to their ability in controlling pectoral fins independently and producing backward thrust. However, labriforms are low efficient swimmers in comparison with carangiforms and thunniforms. Several labriform-mimetic robots have been developed like Bass II [Kato, 2000], Bass III [Kato et al., 2000] which is enhanced version of Bass II, and BoxyBot [Lachat et al., 2005].

BASS II mimics the swimming mode of a real black bass using two-motor driven mechanical pectoral fins (2MDMPF). These pectoral fins could have feathering motion and lead-lag motion. The combination of those two types of motions enables the robot to have forward and backward swimming, and also turning in horizontal plane. Substituting 2MDMPF with 3-motor driven mechanical pectoral fin (3MDMPF) in design of BASS III provides flapping motion for the pectoral fins. Flapping motion is to create the vertical swimming of the robot. BASS II and BASS III are shown in Fig. 3.10.

Kato et al. [2003] have continued their work on analysing the swimming performance of an underwater robot which make benefits of the pectoral fins for its locomotion. They have designed and fabricated a robot called PLATYPUS which has two pairs of 3MDMPFs. PLATYPUS with 1.36 m length, 0.12 m diameter and 14.5 kg weight is constructed to have more precise manoeuvrability than BASS-III. The cord and span of the fins in this robot are 0.1 m and 0.08 m, respectively. The robot uses ground power supply and transfers the data of its sensors through a cable to a computer on the ground. PLATYPUS has experienced different configurations in another works of [Kato et al., 2006].

Regarding three aforementioned types of motion for pectoral fins including flapping, rowing and feathering, Low et al. [2007] have also designed a mechanism using a single motor and planetary gear assembly to provide all those motions for a labriform fish robot.

BoxyBot (3.11) in is another fish robot from labriform category. The fish robot has a pair of 1-DOF pectoral fins and one tail. The combination of motion of those fins and the tail provide forward and backward swimming as well as turning motion of the robot. Although swimming mode of the robot is inspired by the boxfish; the robot does not

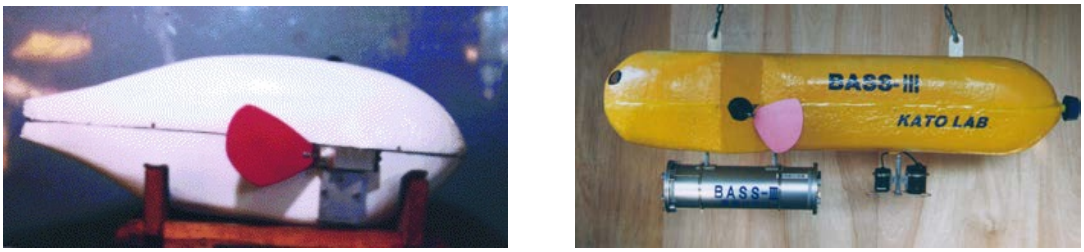

(a) BASS II (b) BASS III

Figure 3.10: Fish robots developed mimicking black bass [Kato].

mimic the shapes of boxfish fins and tail. It should be noted that BoxyBot is capable of having different swimming modes. For instance, using the tail as a rudder and the fins as propeller, BoxyBot is employing labriform swimming mode. Conversely, using the fins as steering tools and the tail as propeller, BoxyBot has switched to ostraciiform swimming mode. Besides the capability of the robot in switching its swiming modes, the high maneuvrability of the robot is considerable. Yet the robot is a planar robot and does not have ability for diving. Fankhauser and Ijspeert [2010] have improved the design of BoxyBot specifically through the design of fins in order to get faster and more efficient swimming.

Figure 3.11: BoxyBot as a labriform- or ostraciiform-mimetic robot [Lachat et al., 2005].

Eventually, Sitorus et al. [2009] made a robotic fish which its pectoral fins are able to have all pectoral fin motion of a labriform fish including rowing, flapping and feathering motion. All of these types of motion are generated by two couples of servo motors, each couple for one fin. The robot and pectoral fins are made from plastic while the fin bases

are from wood. This robot with 2.5 kg weight is only able to swim on the water surface with the maximum speed of 0.03 m/s during the flapping motion of the pectoral fins.

The existing labriform-mimetic robots are designed based on flat and flexible pectoral fins; however, the pectoral fins of a labriform fish are made from fin rays. Accordingly, Palmisano et al. [2007] designed a pectoral fin inspired from a bird-wrasse fin which is made from 5 fin rays[1] each of which is designed to be deformable differently and 3D printed using ABS material. The rays are connected together with a silicone skin and actuated with 4 servo motors. The pectoral fin mechanism is tested close to the surface of water to keep the electronic part out of water. Using this mechanism, the curvatures generated by the fin are actively controlled.

3.2.4 Amiiforms

Bowfin is an example of fish in amiiform swimming mode. The propulsion system of amiiforms is based on the undulation of their long dorsal fin. During undulation, up to 7 waves could be seen in their dorsal fins. They show different ranges of undulation amplitude. This swimming mode faultlessly matches the swimming motion of the African freshwater fish, Gymnarchus niloticus.

In terms of shape, amiiforms do not usually have any anal or caudal fin. Their body is straight while swimming. Pectoral fins could also be employed in some fish of this group. Amiiforms have elongated dorsal fin with up to 200 fin rays. Although there are amiiforms with short dorsal fins with nearly 19 fin rays.

Fishes such as ribbonfishes could swim similar to amiiforms during slow swimming but for rapid manoeuvring, they could have intermittent body undulation or employ swimming mode like subcarangiform [Lindsey, 1979].

Gymnarchus niloticus as an amiiform inspires the undulating fin, RoboGnilos, designed and fabricated by Hu et al. [2009]. The mechanism consists nine fin rays connected to an individual motor. The motors are independent to have adjustable amplitude, frequency and phase. All the rays are connected together by a membrane surface. Figure 3.12(a) shows RoboGnilos.

3.2.5 Gymnotiforms

Gymnotiform have similar swimming characteristic of amiiforms except gymnotiform employ undulating anal fin instead of dorsal fin. This type of swimming can be seen among south American electric fishes.

[1] In nature, each pectoral fin of a bird-wrasse consists 14 fin rays or ribs.

Gymnotiform have elongated anal fins. They do not possess dorsal and caudal fin. There exist some gymnotiforms with very small caudal fin. Like amiiforms, they have straight body.

Gymnotiforms are able to have backward as well as forward swimming by reversing the direction of rapid undulation of their anal fins with short wavelength [Lindsey, 1979].

In this category, MacIver et al. [2004] have developed an undulating fin mechanism in order to investigate the swimming of a black ghost knife fish through its anal fin. The fin is 53 cm long and consists of 13 fin rays each of which controlled by a small digital servo motor. Similarly, a robot inspired by ghost knife fish is fabricated by Curet et al. [2011a,b]. The robot swims through an undulating anal fin with 32 fin rays actuated with 32 motors. The fin rays are connected together by bilayer of lycra. The elastic module of this fin sheet is roughly similar to the module of the real fish membrane between the rays. This fabricated anal fin is 32.6 cm long and 3.4 cm high. The robot is used for investigation of the counter-propagating waves of the fin during station-holding and hovering. Two travelling waves are moving from the head to the tail and the tail to the head and meet each others in the middle line of the undulating fin.

Similarly, Epstein et al. [2006] have designed and constructed a fish robot inspired by a black ghost knifefish. Their mechanism shown in Fig. 3.12(b) has eight fin rays. Each ray is connected to a mitre gear actuated individually by a radio-controlled servo motor. The fin rays are connected together by a thin sheet of latex.

In addition, Low and Willy [2005] have applied their aforementioned undulating fin mechanism to mimic swimming mode of a gymnotus carapo fish or a black ghost knifefish called later on Nanyang knifefish (NKF-I) robot. On the contrary of the robot described in [Epstein et al., 2006], the rotational axis in NKF-I is perpendicular to longitudinal wave direction since the fin rays are directly actuated by motors. Low and Yu improved their NKF-I presented in Fig. 3.13(a) to a modular and reconfigurable robot called NKF-II. This version of NKF has three main parts: buoyancy tank, motor compartment and undulating fin module. For more information about the improvment the reader is referred to [Low, 2009; Low and Yu, 2007]. Siahmansouri et al. [2011] have built a robot with six fin rays that has improved NKF robot series using two separate servomotors that could control the depth and direction of the robot. Figure 3.13(b) Siahmansouri et al.'s work.

(a) RoboGnilos developed by Hu et al. [2009]

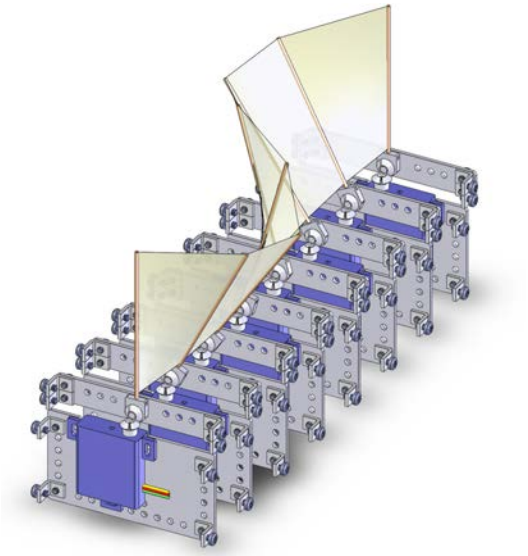

(b) Undulating fin developed by Epstein et al. [2006]

Figure 3.12: Two undulating fin mechanisms.

3.2.6 Balistiforms

Propulsion through simultaneous undulation of both dorsal and anal fins is described by balistiforms. The dorsal and anal fins are inclined sometimes 90°. The horizontal components of forces produced by dorsal and anal fins propel the fish forward. During undulation, several half-sized waves could be observed on the fins of balistiforms.

The body of balistiforms is deep, incompressible and inflexible. The shape of the caudal fin is alterable. The caudal fin could be 2.5 times of its compressed size. Balistiforms have elongated dorsal and anal fins. Nevertheless, there are balistiforms with short dorsal and anal fin which have slender body shape.

Balistiforms are able to go forward, backward, upward and downward through undulation of their dorsal and anal fins independently. For maximum forward speed, they unfold their caudal fin. In order to increase speed, balistiforms like flat fish use both anguilliform and balistiform swimming modes together.

3.2.7 Tetraodontiforms

Similar to balistiforms, tetraodontiforms like puffer fishes use its dorsal and anal fins for propulsion, but they flap their fins side-to-side. These fins are usually flapping in unit like a caudal fin in ostraciiform mode which is separated into two parts.

Tetraodontiforms could be thought as the continuation of balistiforms where the

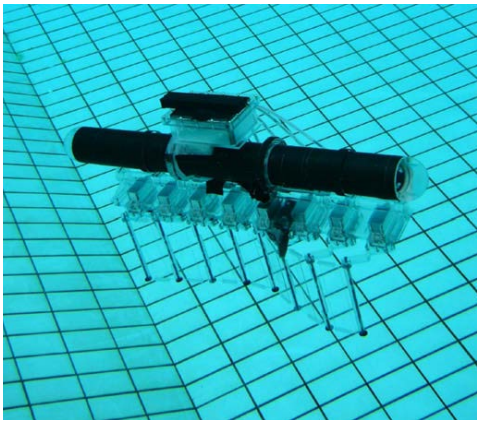

(a) NKF-I [Low, 2009]

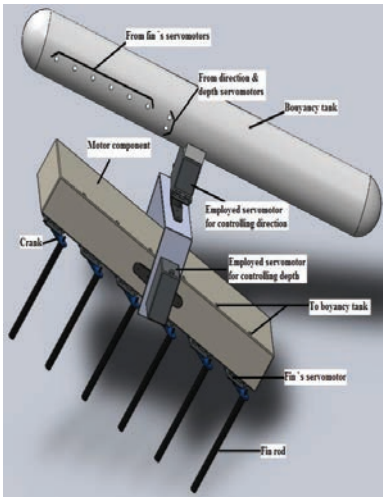

(b) Mechanism developed by Siahmansouri et al. [2011]

Figure 3.13: NKF-I and its improved version by Siahmansouri et al. [2011]

wavelength of undulation is considerably high [Sfakiotakis et al., 1999]. The extreme example of tetraodontiforms can be seen in ocean sunfish that propel using its high dorsal and anal fins. Ocean sunfishes have no caudal fins and tail propulsion.

Note that this mode of swimming could also be combined with other swimming modes like labriform.

3.3 Discussion

The existing robotic fishes are classified based on their swimming mode such as anguilliforms, labriforms and so on. These modes show the swimming capabilities of the robots for optimal swimming. For instance, anguilliform-mimetic robots are highly capable of manoeuvring among narrow areas, and, hence, they are designed and constructed for optimal manoeuvring. However, the optimality of swimming will be improved by taking some other aspects of fish robots into account by designing the most appropriate actuation mechanism and designing suitable body and fin shape for fish locomotion.

3.3.1 Actuation System

One of the primary aspect of robotic fishes is their actuation system which is powered using either conventional or alternative actuators. Conventional actuators include hy-

draulic and pneumatic actuation systems, and electric motors. Alternative actuators include shape memory alloys (SMAs), piezoelectric materials, ionic polymer metal composite (IPMC), dielectric elastometer actuators (DEAs) and so forth. Smart actuators are small, light and easy adaptable to any type of mechanisms.

Among existing fish robots, hydraulic and pneumatic actuators are used by Anderson and Chhabra [2002] and Dogangil et al. [2005]. Electric motors are employed by Hu et al. [2009]; Kodati et al. [2008]; Liang et al. [2011]; Liu et al. [2005]; Low and Willy [2005]; Morgansen et al. [2007]; Triantafyllou et al. [2000]; Triantafyllou and Triantafyllou [1995]. In order to transfer the power of the conventional actuators to propulsors of the robots, different mechanisms could be designed which depends on the fish swimming mode. Oscillatory fish robots have simple mechanism as their propelling fins are directly actuated by the motor. On the contrary, undulatory fish robots could have more complicated construction such as using linkages in series or in parallel.

In BCF swimming mode, the undulation is produced by a number of links connected in series. Each link then could be actuated either directly or passively by a phase lag. The phase lag is to create traveling wave. In MPF mode, the undulation is caused by several parallel links which are connected by a flexible membrane. In other words, the parallel links play the role of fin rays in an undulatory fin. In some of the developed fish robots, the flexibility is made by the connection of each two rays by a flexible mechanism [Low and Willy, 2005] while others have all rays connected together by a flexible sheet, for instance [Epstein et al., 2006; Hu et al., 2009]. In both BCF and MPF modes, the links are rigid except in [Triantafyllou et al., 2000] which three bendable links are employed.

On the contrary of the link system, the mechanism introduced in the previous section for trout robot has unique features. A motor is connected to a plate casted inside a composite tail. The sinusoidal rotation of the motor provides the undulation of the tail [Salume, 2010].

Despite conventional actuators, alternative or smart actuators are not widely employed in robotic fishes. Some robotic fishes using smart actuators are listed here. SMAs are employed in construction of a lamprey robot [Ayers et al., 2000], an eel-like robot [Low et al., 2006] and a tuna-like robot [Suleman and Crawford, 2008], piezoelectric actuators are used in a mackerel-mimetic robot [Heo et al., 2007] and its improved version [Nguyen et al., 2010], IPMC actuators are used in [Mbemmo et al., 2008] and [Cha et al., 2013], and DEAs are employed in a fish-like robot [Jordi et al., 2010]. This robot is actually an air fish and cannot swim underwater. The interested reader in smart actuators used in robotic fishes is referred to [Shinjo, 2005] and [Chu et al.,

2012].

Conventional actuators, most of the times, need other parts for transferring their power to the propulsors. The presence of these extra parts requires large space for actuation system. In addition, this type of actuators could provide large torque efficiently. Accordingly, conventional actuators are often used in large robots.

Hydraulic and pneumatic systems could execute a high rate of energy with respect to their weight; however, the main concern about using these systems for fish robots are their large size and the lag in their control systems [Mavroidis et al., 2000]. In comparison with hydraulic and pneumatic actuators, electric motors produce smaller torque. Nevertheless, due to relatively small size, easier controllability, especially for manoeuvring robots, and also the easy storage of their energy medium including recharging batteries, the electric motors are extensively used in various type of large fish robots [Mavroidis et al., 2000].

On the other hand, smart actuators are small and sometimes they work analogous to a muscle for the robot. The smart actuators, also, produce small torque. This small torque as well as small actuator size make the small actuator a proper choice for as small robots as 14 mm microrobot [Shi et al., 2010]. Among them SMAs are the fastest actuators and IPMCs are the most suitable actuators for micro robots less than 50 mm [Chu et al., 2012].

3.3.2 Body Shape

The purpose of producing robots inspired by fishes is to mimic their swimming mechanisms to have efficient underwater robots. Yet mimicking the body shape of aquatic animals has a crucial role in the enhancement of the efficiency and the performance of the robot. This is even more significant when the fish body is undulating.

Accordingly, many existing fish robots are mimicking the geometry of fish bodies such as [Boyer et al., 2009; Triantafyllou and Triantafyllou, 1995; Yu et al., 2007a]. In order to do that, the skeleton of fish robot is made by either a flexible spiral or some rigid rings around the undulating body such a way that there is a sufficient distance between each two rings. This distance causes the flexibility of the body whereas rigidity of rings increases the resistance of body against water pressure when the body is covered by a flexible material.

Beside geometry, in some cases like [Salume, 2010], the body stiffness of the real fish is also taken into account. In [Salume, 2010], the work done in [Alvarado, 2007] is applied to develop a flexible composite model as the propelling part of the robot. The

composite model is capable of adjusting its size, geometry and stiffness based on real corresponding trout.

3.4 Summary

Till now, numerous fish robots have been built. These robots have diverse ranges of actuation mechanisms. The diversity of the robots is mainly due to their swimming modes. In total, fishes could have two distinguishable swimming modes which originate in their active propulsors during locomotion. The majority of fishes apply their body and/or caudal fin (BCF) for swimming where the median and/or paired fins (MPF) are employed by the others. BCF and MPF swimming modes are classified further into several swimming forms. Every swimming form has its own swimming capabilities. The robots inspired from each form have its swimming characteristics. Accordingly, categorizing the robots with respect to their corresponding swimming forms reveals their capabilities.

Swimming forms of fishes have their dedicated swimming propulsor, shape and swimming capabilities. After introducing these three properties of all swimming forms, these properties are also investigated in the corresponding robot in each category. The state of the art shows that the absolute majority of the robot has mimicked only the swimming mechanisms of fishes. The geometrical and specifically biological aspects of fishes are mainly ignored in the design.

The mechanical design of each robot is also investigated. Since most fish robots have BCF-form robots, especially carangiforms and thunniforms, the actuation mechanism of the robot needs to generate undulatory motion. This motion is usually made up of several links in series that are actuated with several actuators mainly electric motors. A few robots in this category have made undulatory motion with only one actuator. The undulation mechanism for MPF-form is more complicated. The links in undulatory MPF swimmers are usually in parallel and act like fin rays. The actuation system to generate oscillatory motion is simpler except in some labriform-mimetic robots that have mimicked all types of pectoral fin motions at once.

As well as swimming forms and mechanical design, the actuation system of the biomimetic swimming robots are also discussed in this chapter. Both conventional and alternative actuators are applied for the development of fish robots; however, the usage of conventional actuators is rather widespread. Alternative actuators are mainly employed by micro-robots which are beyond the scope of the current project. Among conventional actuators, the robots are essentially actuated with electric motors due to

their mall size and easier controllability. Hydraulic and pneumatic actuators are also employed by some robot makers to develop robot in cruising mode. This is due to the large torque produced by these two actuators.

Chapter 4

Design

The primary step of creating novel biomimetic swimming robots is its design. The swimming robots could have problematical design if an appropriate shape and swimming mechanism are not selected for them. The optimal shape and swimming characteristics of biomimetic swimming robots depend on their corresponding fishes.

It has been discussed in the previous chapters, depending on the nature of fishes and their habitats, fishes have optimal swimming which is determined by their swimming specialities. In chapter 2, three main swimming specialities of fishes, cruising/sprinting, accelerating and manoeuvring, are investigated with respect to several points such as their swimming gait.

The existing fish-mimetic robots are inspired from one type of fish and, hence, have one swimming specialities. For instance, [Anderson and Chhabra, 2002], [Kim and Youm, 2004] and [Lashkari et al., 2010] are made to have cruising capabilities while [Kodati et al., 2008] and [Fankhauser and Ijspeert, 2010] are designed and constructed for manoeuvrability purposes. This single speciality raises an issue which is the failure of the robots in performing marine tasks. For instance, monitoring pipelines under water needs a robot with navigation capability for long distances due to the great length of the pipelines. On the other hand, the robot needs to have close distance with the pipelines for inspection. This requires a robot with manoeuvrability abilities among coral reefs and narrow areas. Accordingly, for accomplishing marine tasks with one single robot, it needs to be able to have multiple gaits of swimming.

In order to design a robot with multiple gaits of locomotion including cruising and manoeuvring, the hydrodynamic and biological aspects of tuna and bird-wrasse are investigated. Tuna is well-known candidate for cruising mode of swimming while bird-wrasse is a manoeuvrable fish. After investigation of the optimal swimming char-

acteristics of tuna and bird-wrasse, the combination of their swimming specialities is observed for design of UC-Ika 2. UC-Ika 1 is also designed as a single gaited robot inspired from tuna which is suitable for cruising mode only.

In this chapter, the swimming characteristics of tuna and bird-wrasse is discussed in Sec. 4.1 and 4.2. Moreover, the design of UC-Ika 1 is described in Sec. 4.3 while the design of UC-Ika 2 is presented in Sec. 4.4.

4.1 Swimming Specialities of Tuna

The investigation of the capabilities of tuna, shown in Fig. 1.5(b) , in swimming could be accomplished by studying swimming gait, swimming forces and body (and fin) shape of tunas.

4.1.1 Swimming Gait

The swimming gait of tuna is defined with respect to their swimming propulsors, kinematics, muscles and time-based locomotion behaviour.

Tuna is a thunniform fish which swim through undulation of the posterior part of its tail peduncle and caudal fin. The wavelength of undulation is long, and wide at trailing edge of the caudal fin. They provide thrust mainly by their stiff caudal fin[1]. The angle of attack of the caudal fin changes once it reaches its maximum amplitude in order to maximize the thrust [Lindsey, 1979].

Tuna is specialised for cruising kinematics of motion which distinguishes a part of swimming that a fish has a sustainable speed for more than 200 minutes without fatigue [Webb, 1994].

In terms of muscles, tuna swims using the red or slow oxidative muscles which have low power output and are, thus, non-fatiguing. The non-fatiguing nature of red muscles suits them for sustainable swimming [Webb, 1994].

Tuna is mainly capable of periodic motion or steady motion which continues in a long period of time to navigate long distances [Sfakiotakis et al., 1999].

4.1.2 Swimming Forces

The dynamic behaviour of the fish robot is influenced by two main forces: hydrostatic and hydrodynamic forces. Hydrostatic forces are more essential for depth control while hydrodynamic ones are used for swimming. However, to facilitate the swimming model

[1] 90% of thrust is produced by the caudal fin

with minimum energy dissipation, hydrodynamic forces need to be produced with respect to several factors. These factors are introduced as optimal swimming factors.

4.1.2.1 Hydrostatic Forces

Hydrostatic forces such as weight and buoyancy play crucial roles in the stability of fishes. The weight, W, is defined as the mass multiplied by the gravitational constant, $M_\mathrm{f}\, g$. On the other hand, the buoyancy, B, is defined by Archimedes' law as the displaced mass of water multiplied by the gravitational constant, $\rho_\mathrm{w}\, V_\mathrm{f}\, g$, where V_f is the fish volume and ρ_w is the density of water.

In order to keep the position of the robot stable under water, W and B need to be equal. Additionally, the centres of mass and buoyancy must be vertically aligned while the centre of buoyancy should be above that of the weight. This assures the attitude stability of the robot. As a pelagic fish, tuna has almost neutral buoyancy [Videler, 1993].

4.1.2.2 Hydrodynamic Forces

Hydrodynamic forces such as resistive and thrust forces vary from fish to fish, see Sec. 2.2. For a tuna-like robot, the main resistive force is associated with the pressure drag while the main thrust force is associated with the lift force [Alexander, 2002]. Accordingly, the pressure drag and lift forces need to be decreased and increased, respectively, in order to have an efficient swimming.

The pressure drag is the result of the pressure gradient along the body. In order to decrease this drag, the shape of the animal is a determining factor. The best overall shape of swimming animals is streamlined bodies with the diameter of thickest part, d, and fish length, l. Streamlined bodies with d/l between 0.18 and 0.28 produce less than 10% of the minimum possible drag [Videler, 1993].

Regarding propulsive forces, tunas use vorticity method for swimming. In this method, tuna fishes generate lift forces through shedding vortices around the tips of its caudal fin [Videler, 1993]. These vortices make two forward and lateral forces. The forward force is the thrust of the fish while the lateral forces will cancel out each other in a complete fin stroke. The vortex rings behind a fish is shown in Fig. 4.1.

Larger vortex rings provide greater thrust forces. To enlarge the vortex rings, the caudal fin and the very last part of the tail peduncle make a travelling wave, see Fig. 4.2. The speed of the travelling wave must be greater than the speed of the fish [Sfakiotakis et al., 1999]. The undulatory motion requires the caudal fin to change its orientation

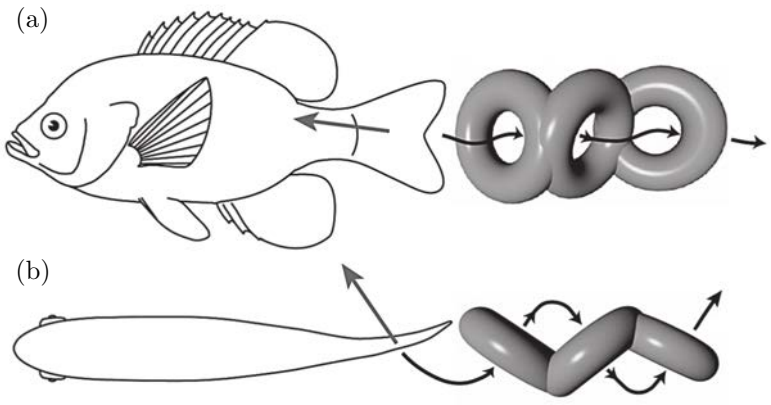

Figure 4.1: Vortex rings left behind a swimming fish, (a) side view and (b) top view [Linden and Turner, 2004].

once it reaches its maximum heave.

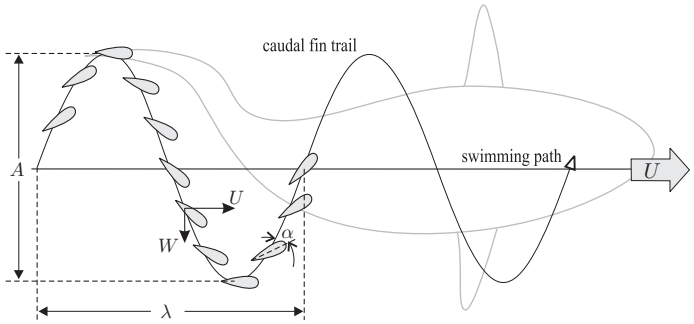

Figure 4.2: Traveling wave generated by undulatory motion of fish with the overall fish swimming speed, U, the lateral speed of the caudal fin, W, the instantaneous angle of attack of the caudal fin, α, the undulation amplitude, A, and the undulation wave length, λ [Sfakiotakis et al., 1999].

4.1.2.3 Optimal Generation of Swimming Forces

While the optimised design regarding the shape of the body and the caudal fin enhances the swimming performance of a fish robot, there exist other decisive factors of designing an efficient swimming robot. Two main criterions are taken into account in this thesis: Strouhal number and Froude efficiency.

The Strouhal number is a factor that shows the structure of the vortices made through the body undulation of fishes. The Strouhal number, St, is a dimensionless

parameter. It represents the ratio of unsteady to inertial forces and is defined as

$$St = 2\frac{f\,h}{\bar{\dot{x}}} \tag{4.1}$$

where f is the frequency of the body undulation, h is the heave of the caudal fin and $\bar{\dot{x}}$ is the average cruising velocity of the fish. If $0.25 < St < 0.4$, the vortices behind the caudal fin produce maximum thrust. Note that the Strouhal number is applicable for fishes whose swimming is through the lift-based methods including vorticity method, see Sec. 2.2 [Triantafyllou et al., 1993].

The Froude efficiency is another important factor to evaluate the swimming behaviour of fishes. This factor relates the useful power used for propulsion to total kinetic energy of the fish which is the mean rate of transferred momentum to the wake around the fish. Froude efficiency is defined by

$$\eta = \frac{\overline{F_{Cx}}\;\bar{\dot{x}}}{P_{\text{total}}}, \tag{4.2}$$

where $\overline{F_{Cx}}$ is the thrust and $\bar{\dot{x}}$ is the mean velocity of the fish. P_{total} is the total kinetic energy of the fish [Lighthill, 1960]. In this paper, P_{total} is obtained through the following expression

$$P_{\text{total}} = \overline{F_{Cx}}\;\bar{\dot{x}} + \overline{F_{Cy}}\;\bar{\dot{y}}, \tag{4.3}$$

where $\overline{F_{Cy}}$ is the force to generate vortex wake and $\bar{\dot{y}}$ is the mean lateral speed of the caudal fin. Derivations of $\overline{F_{Cx}}$ and $\overline{F_{Cy}}$ are presented in Chapter 5. A tuna fish could be up to 90% efficient while a screw propeller fish robot is at most 50% efficient [Yu and Wang, 2005].

4.1.3 Body and Fin Shape

One of the main sources of the swimming optimality of fishes is their optimal shape. However, the optimality of body shape is essentially determined by resistive forces whereas fin shapes are optimised with respect to the propulsive forces.

Tuna has quite streamlined body shape. The anterior part of its body is heavy, inflexible and often circular in cross section. The posterior part including tail peduncle is lighter and flexible. The tail peduncle is strengthened by the keels located at either sides of the tail peduncle. Due to the keels, the tail peduncle is wider than it is deep. In addition to strengthening the tail peduncle, the keels have an important role in

decreasing the drag during rapid lateral motion of the tail [Lindsey, 1979].

The main fin of tuna for swimming is its caudal fin. Tuna's caudal fin is crescent-shape with high aspect ratio[1], see Fig. 4.3. Its caudal fin is stiff; however, it shows a slight flexibility during powerful stroke. During the stroke of the caudal fin, the centre of the caudal fin is leading and the tips are following [Lindsey, 1979].

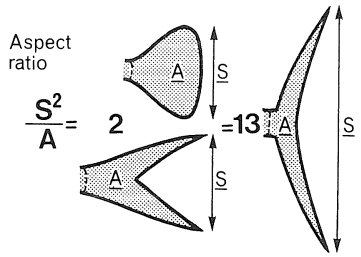

Figure 4.3: Caudal fins with similar aspect ratio but different shape [Videler, 1993].

During undulation of tuna, the fluid around the fish is pushed and pulled laterally. These accelerations and decelerations of the fluid result in escalation of energy dissipation and reduction of swimming efficiency. Since the undulation of tuna is initiated in its tail peduncle, the joint between the caudal fin and the tail peduncle is narrow to reduce this energy dissipation. In other words, the smaller surface of the tail peduncle helps tuna to move smaller volume of water laterally. This saves the energy of tuna in cruising.

4.1.4 The Combination of Swimming Characteristics of Tuna and Bird-Wrasse

Considering the swimming gait and swimming forces as well as body and fin shape, tuna is an appropriate candidate for efficient cruising. However, for adding the manoeuvring gait to a tuna-mimetic robot, several design factors must be kept in mind.

- Tuna has BCF swimming mode which means that the caudal fin and the tail peduncle are engaged to the cruising gait of swimming.
- Tuna has vorticity method of swimming. This mode does not tolerate any turbulence of water during cruising since turbulent water avoids the vortex generation and decreases the swimming power and efficiency.
- Body shape of tuna fishes is streamlined in order to minimize the pressure drag.

[1] Large span and short chord

- Their tail peduncle has narrow neck at its joint to caudal fin. This is due to the fact that tuna needs to decrease the drag of lateral motion of their tail. With the same reason, tuna fishes do not have any long and posteriorly extended dorsal and anal fins.

Among manoeuvrable fishes, bird-wrasses are selected for the second gait of swimming because of two main reasons. Primarily, bird-wrasses are from labriform category of swimming mode and actuated with their small pectoral fins. The non-activated tail for manoeuvring inspired from labriforms does not interfere cruising motion of the robot through the tail inspired from tunas. Moreover, bird-wrasses have lift-based swimming which is compatible with vorticity method of tuna swimming. Using drag-based swimming like angelfish which has similarly labriform swimming mode increases the drag of motion.

4.2 Swimming Specialities of Bird-Wrasses

Similar to tuna, optimal swimming of bird-wrasse is investigated through discussing the swimming gait, swimming force and the shape of them. Figure 1.5(a) illustrates a typical bird-wrasse.

4.2.1 Swimming Gait

The swimming gaits of bird-wrasse are defined with respect to their swimming propulsors, kinematics, muscles and time-based locomotion behaviour.

Bird-wrasses are labriform fishes which swim through the oscillation of their pectoral fins. Labriforms have two types of fin motion, either rowing like angelfish or flapping like bird-wrasse [Lindsey, 1979].

Bird-wrasses are capable of hovering and slow swimming kinematics of motion. In hovering, the fish has zero water speed with non-zero ground speed. Slow swimming is different from hovering with non-zero water speed. Beside these two swimming kinematics, bird-wrasses have comparable prolonged speed. The fish speed greater than cruising speeds and smaller than sprinting is called prolonged speed [Webb, 1994].

In terms of muscles, similar to the majority of MPF swimmers, the bird-wrasses employ mainly red fibres during swimming. White muscles are used among MPF swimmers for adducting the fins to reduce the drag [Webb, 1994].

From swimming kinematics of bird-wrasses, it could be understood that they could have both periodic and transient motion. However, due to the flapping motion of their

pectoral fins, they are more capable of periodic motion rather than transient motion.

4.2.2 Swimming Forces

Swimming forces are divided into two groups, resistive and propulsive forces. Bird-wrasses deal with pressure drag as their main source of resistive forces. This is due to the relatively high Reynolds number of bird-wrasses. Fishes with high Reynolds number need to minimize the pressure drag rather than the skin friction drag. The description of resistive forces are presented in Sec. 2.2.2.

Regarding the propulsive forces, bird-wrasses have oscillatory flapping mode which is considered as a lift-based mechanism. This mechanism consists of up-stroke and down-stroke, see Fig. 4.4.

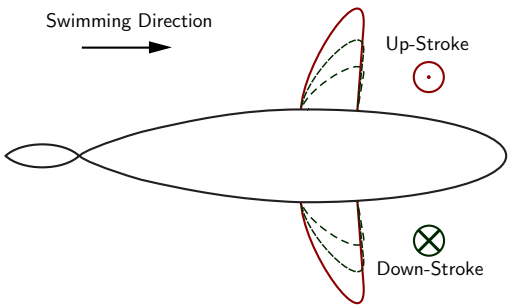

Figure 4.4: The flapping motion of pectoral fins of bird-wrasses.

In both strokes, the vortices are made at the leading edges of the fins. As shown in Fig. 4.5, these vortices are in the shape of vortex rings and push the fish forward. The surface area of the fins is not involved in the propulsion.

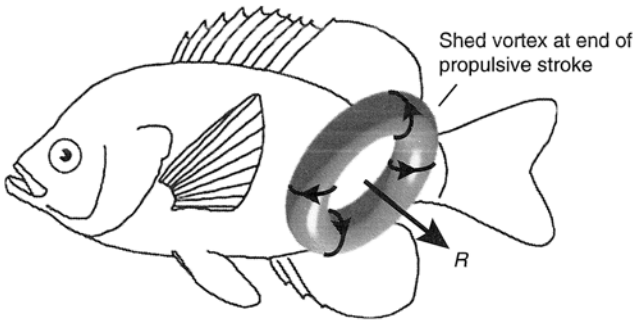

Figure 4.5: Votex rings generated by pectoral fins [Biewener, 2003].

The pectoral fins of a bird-wrasse do not behave similarly in the up- and down-

strokes. The speed of up-stroke is greater than down-stroke. Having higher speed of stroking during up-stroke than that of down-stroke, most of the thrust is generated during the up-stroke of the fins. The path of the flapping pectoral fins is shown in the Fig. 4.6.

Figure 4.6: The pathway of flapping pectoral fins of bird-wrasses (U is the overall swimming speed) [Alexander, 2002].

The lift-based mechanism and generation of vortex rings are further discussed in Sec. 2.2.3.

4.2.3 Body and Fin Shapes

For optimal swimming, fishes have also optimal body and fin shape. However, the optimality of body shape is essentially determined by resistive forces whereas fin shapes are optimised with respect to the propulsive forces [Lindsey, 1979].

Bird-wrasse needs to minimize the pressure drag. In order to do so, bird-wrasses have streamlined and compressed body shape. The compressed shape of the body enables the fish to generate less drag and to be more flexible for turning and manoeuvring. On the contrary of several fishes like tuna that have narrow neck at the posterior part of their tail peduncle, the bird-wrasses have deep tail peduncle extended by dorsal and anal fins. The deep tail peduncle of bird-wrasses is used for steering of the fish.

Bird-wrasses swim through the lift-based mechanism of their pectoral fins [Biewener, 2003]. Accordingly, the pectoral fins of bird-wrasses need to have high aspect ratio, which means large span and short chord, since in lift-based mechanism the propulsion is made by the leading edge of the fins. Enlarging the surface area of the fins decreases the thrust generation and increases the drag forces. Notice that, bird-wrasses adduct their pectoral fins during their motion to decrease the drag forces further.

The caudal fin of bird-wrasses, however, has low aspect ratio since the caudal fin with the aid of the tail peduncle and dorsal and anal fins are used for steering of the fish during manoeuvring [Lindsey, 1979].

4.3 Design of UC-Ika 1

Figure 4.7 illustrates UC-Ika 1 which is only capable of cruising gait of swimming. Considering the cruising gait, UC-Ika 1 is a tuna-like robot and mimicked the swimming characteristics of tuna. This robot must be able to have planar cruising motion. It does not have any capabilities for manoeuvring and up-down motion.

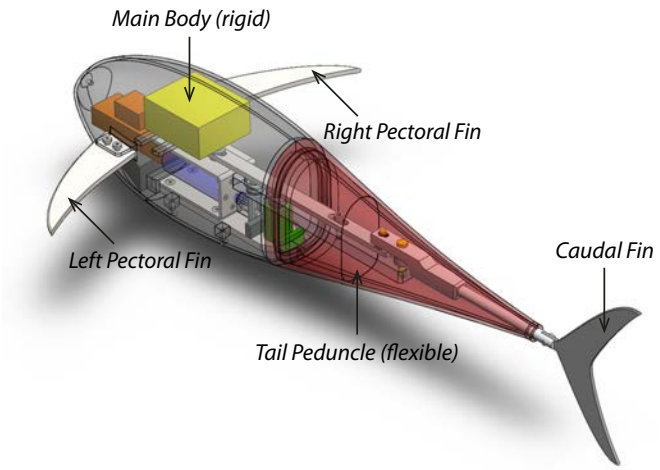

Figure 4.7: The CAD design of UC-Ika 1

4.3.1 Shape

The robot consists of two main parts: the main body and the tail. The main body is designed as a rigid part and contains all stationary components such as batteries, microcontroller, and DC motor. The pectoral fins are fixed to the body and, in this prototype, are rigid as well. The tail includes a flexible tail peduncle and a rigid caudal fin. Inside the tail peduncle, the undulation actuation mechanism is located. The mechanism connects the DC motor with the caudal fin, see Fig. 4.7.

The design of UC-Ika 1 allows investigation of all aforementioned swimming characteristics of a tuna which are necessary for the stable and efficient cruising motion of the robot. UC-Ika 1 is neutrally buoyant with an approximate weight of 4 kg while the centre of buoyancy is above that of the mass (Fig. 4.8).

Figure 4.8 also shows that the overall shape of UC-Ika 1 is streamlined with d and l of 147 mm and 610 mm, respectively. Accordingly, the body shape of the robot has d/l equal to 0.24 which is within the optimal range for streamlined bodies, 0.18-0.28 [Videler, 1993]. For further information, the reader is referred to Sec. 2.3.

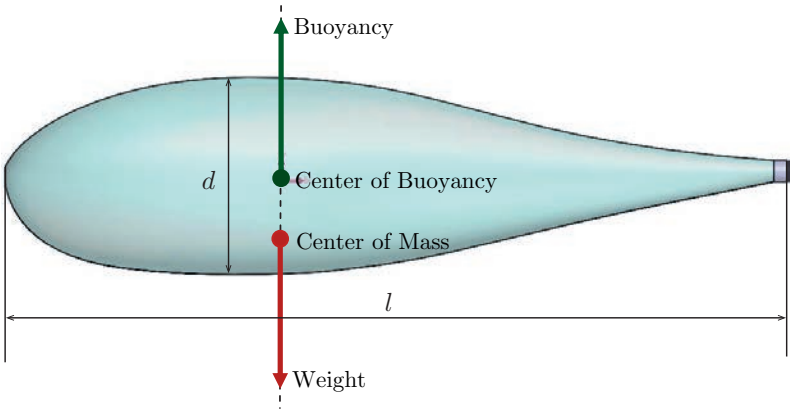

Figure 4.8: The overall body shape of UC-Ika 1

Moreover, in order to have efficient cruising, the tail peduncle skin is designed to be flexible. The tail peduncle at the connection to the caudal fin is narrow with peripheral of 64 mm. The caudal fin is designed to be lunate shaped with aspect ratio, S^2/A, of 6.4 where S is 170 mm and A is equal to 4500 mm^2.

4.3.2 Cruising Mechanism

The undulation of the tail is determined by the kinematic mechanism illustrated in Fig. 4.9. This mechanism has distinguishing features. First of all, the mechanism is actuated by one DC motor. This allows assembling of the motor inside the main body close to the centre of mass in order to decrease the weight of the tail peduncle. When the tail peduncle is light, the robot swinging is controllable due to the small mass moment of inertia at posterior part of the robot.

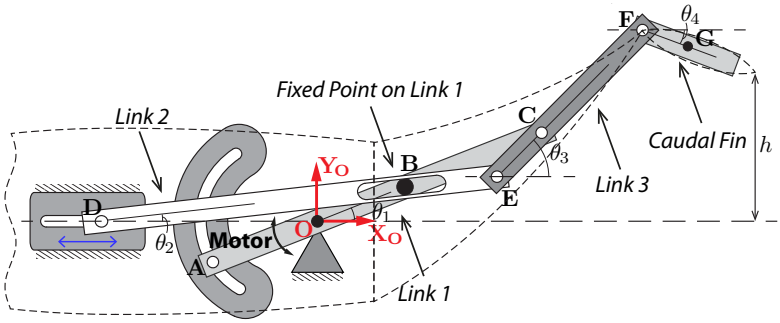

Figure 4.9: The link mechanism of the tail peduncle

The second distinguishing feature is the passive control of the third link. In other

words, θ_3 in Fig. 4.9 is dependent on the motion of the rest of the link system and is determined by θ_1. Accordingly, less degrees of freedom need to be controlled.

The third important feature of the mechanism is owing to its suitability for mimicking the real tuna cruising. The existing tuna-mimetic robots have swimming mode of carangiforms like mackerel. Carangiforms undulate from last third of their body while the lift-based propulsion system of thunniforms like tuna is confined to the very last part of their body close to the caudal fin [Sfakiotakis et al., 1999]. Thus the tail mechanism must avoid excessive motion of the tail peduncle near the rigid body and minimises the associated energy dissipation.

Considering the kinematics of the tail design, Fig. 4.9, θ_1 with an amplitude of 7 degrees cause a heave of 17 mm of point C. On the other hand, the motor oscillation of 14 degrees of θ_3 yields a heave of 56 mm for point F. The short heave for point C and long one for point F, while the tail mechanism is not optimised, is a quite satisfactory result for a tuna-like undulation. The CAD design of tail mechanism of UC-Ika 1 is shown in Fig. 4.10.

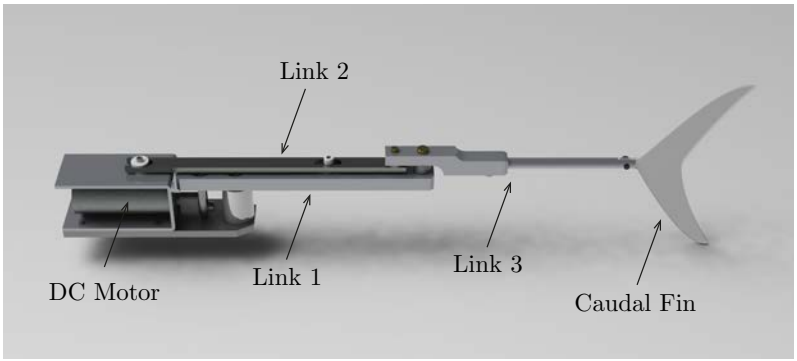

Figure 4.10: The CAD design of tail mechanism of UC-Ika 1

4.4 Design of UC-Ika 2

UC-Ika 2 is designed to be specialised for cruising and manoeuvring. Taking the swimming specialities of tuna for cruising and bird-wrasse for manoeuvring as well as up-down motion capability into account, UC-Ika 2 is designed as shown in Fig. 4.11.

The design issues of UC-Ika 2 to combine tuna and bird-wrasse are discussed in details with respect to the shape, cruising, manoeuvring and up-down motion mechanism of UC-Ika 2.

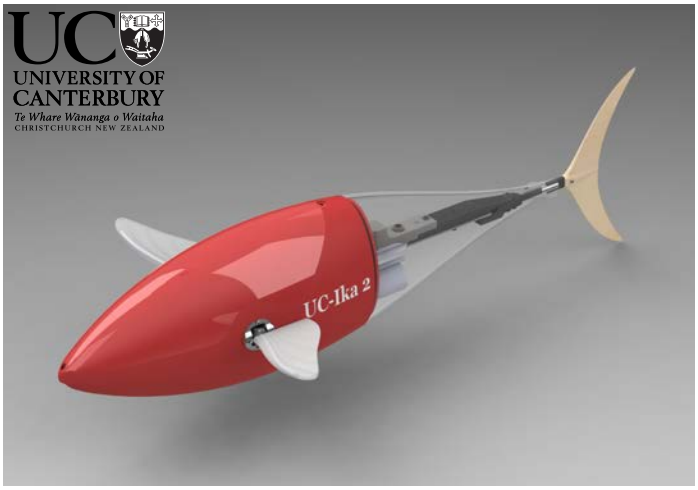

Figure 4.11: The CAD design of UC-Ika 2

4.4.1 UC-Ika 2 Shape

The robot consists of two main parts: main body and tail. The main body is designed as a rigid part and contains all stationary components such as batteries, microcontroller, and DC motors. The pectoral fins and their actuation mechanisms are also a part of the main body. Moreover, the actuation mechanism of buoyancy control system is located inside the main body. The tail includes a flexible tail peduncle and a rigid caudal fin. Inside the tail peduncle, the undulation actuation mechanism is located.

The body shape of UC-Ika 2 is inspired from both aforementioned fishes. Those parts of the main body that is necessary for optimal cruising is mimicking tuna while the rest is inspired from bird-wrasse. UC-Ika 2 has a streamlined body shape with deep and compressed body shape scaled from tuna and bird-wrasse. The body shape of tunas are described in previous section.

The tail part including tail peduncle and caudal fin is used for cruising mode inspired from a tuna. Accordingly, the tail peduncle has a narrow neck at its connection to the caudal fin. The caudal fin is stiff with high aspect ratio. The pectoral fins resemble the bird-wrasse fins with different scale. The fins have 5 ribs with a flexible material surrendering the ribs to guarantee the flexibility of the fins, see Fig. 4.12.

4.4.2 Cruising Mechanism

The cruising mechanism of UC-Ika 2 is similar to its previous version (Fig. 4.9). However, the tail mechanism is optimised using PSO algorithm described in Chapter 6.

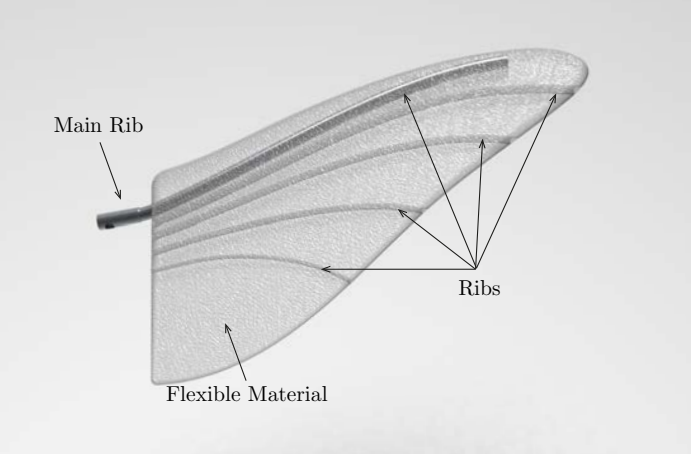

Figure 4.12: The CAD design of pectoral fins of UC-Ika 2

This mechanism is actuated by a DC motor which is located inside the main body. The rest of the mechanism including three links is inside the flexible tail peduncle. The motor directly actuates link 1 but the other links are passively actuated through geometrical constraints shown in Fig. 4.13.

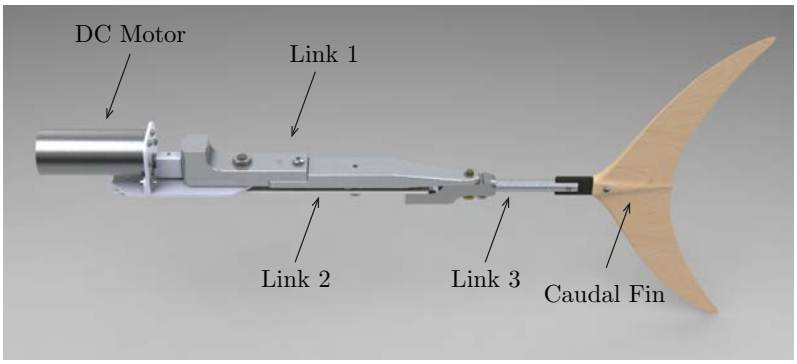

Figure 4.13: The CAD design of tail mechanism of UC-Ika 2

This mechanism is capable of mimicking the optimised undulatory swimming of tunas. Moreover, since tunas change their caudal fin orientation at the end of each stroke, a flexible joint between the caudal fin and the tail peduncle is designed.

4.4.3 Manoeuvring Mechanism

The pectoral fin actuation mechanism is actuated with two independent separate DC motors. Each DC motor is connected to a cam and slider mechanism which is connected the link rod. One of the ribs of each pectoral fin is connected to the link rod, see

Fig. 4.14.

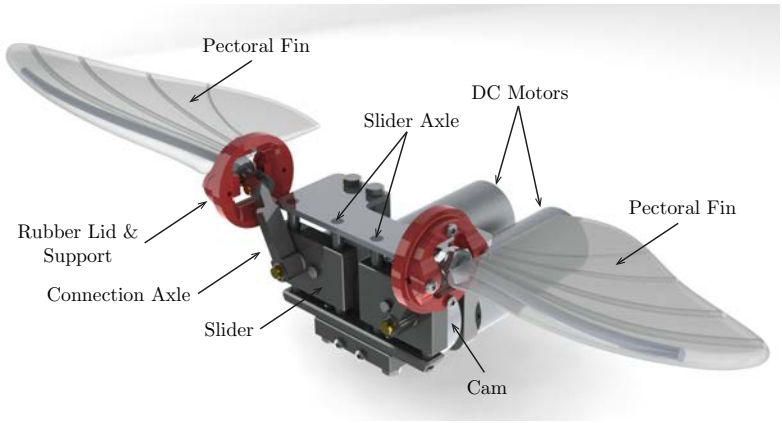

Figure 4.14: The CAD design of pectoral fin actuation system of UC-Ika 2

This mechanism converts the rotational motion of the motor into the flapping motion of the fins with different up- and down-stroke speed, similar to bird-wrasse flapping motion shown in Fig. 4.6.

4.4.4 Up-Down Motion Mechanism

Static depth control through playing with the buoyancy and the weight of the robot is targeted for up-down motion. Indeed, a mechanism similar to ballast control system of submarines is designed to change the weight of the robot through filling and draining its container with water. The mechanism as shown in Fig. 4.15 is consisted of a DC motor, a cylinder and a gear system that converts the rotational motion of the motor into translational motion of the piston in the cylinder. The buoyancy control system also makes benefit of two mechanical switches that turn off the motor when the cylinder is filled with or drained from water.

4.5 Summary

The design of two fish robots are described in this chapter. The first robot, UC-Ika 1, is designed to be specialised for cruising mode of swimming while the second one, UC-Ika 2, is designed for multiple gaits of swimming. UC-Ika 2 is specialised for cruising and manoeuvring modes of swimming. This robot is also able to have up and down motion.

In order to design UC-Ika 1, the swimming characteristics of tuna is considered.

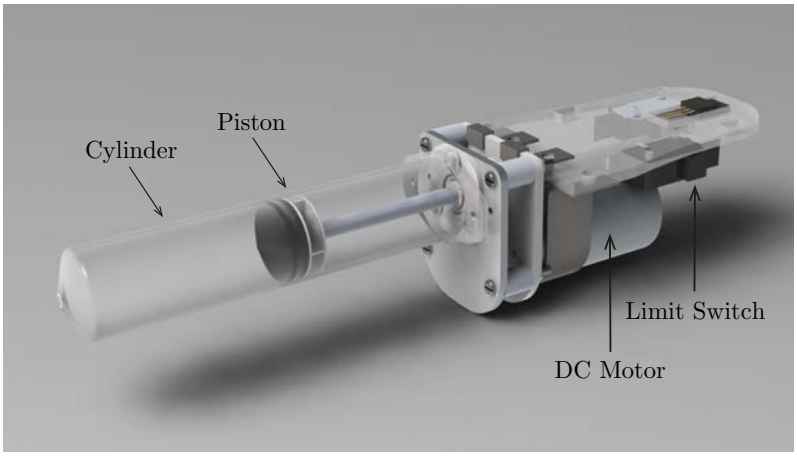

Figure 4.15: The CAD design of buoyancy control system of UC-Ika 2

Tuna is an efficient fish in cruising mode which employs the very last part of its tail and caudal fin for undulatory swimming. The pectoral fins of tuna do not have an essential role for cruising. Therefore, a tail mechanism is designed to mimic the undulatory motion of tuna. The main body is designed to be rigid while the tail is flexible. The overall body shape of the robot is streamlined resembling tuna. Since the robot must only have planar motion, it is designed to be neutral buoyant.

The design of UC-Ika 2 is more complicated than UC-Ika 1 since the swimming characteristics of both tuna and bird-wrasse are considered. The cruising mode of UC-Ika 2 is inspired from tuna and accordingly the tail mechanism of UC-Ika 1 is optimised and employed for this robot too. The manoeuvring mode of fish is inspired from bird-wrasse. Bird-wrasse uses its pectoral fins for manoeuvrability. Hence, an actuation system for two flapping pectoral fins is designed. A buoyancy control system is also designed to enable the robot to go up and down. In terms of shape, the caudal fin is inspired from tuna and the pectoral fins from bird-wrasse. This robot has streamlined, deep and compressed body shape inspired from tuna and bird-wrasse.

Chapter 5

Mathematical Modelling

Subsequent to the design, the swimming behaviour of the robot requires analytical modelling since it is necessary to analyse their swimming behaviour and improve their performance. Modelling of robotic fishes is challenging due to the complication of the fluid-structure interaction which can be obtained only through computational fluid dynamics (CFD). Hence CFD is employed for modelling of swimming motion in [Anton et al., 2009; Liu et al., 1996; Zhang et al., 2006]. Although CFD can reliably capture the fluid-structure interaction, this method cannot be employed for control and optimisation purposes.

Besides CFD which is purely a fluid dynamics approach for modelling, the majority of models have mechanical approach based on works done by Wu [1961] and Lighthill [1960, 1970]. Wu [1961] modelled the fish as a two-dimensional waving plate. Based on the inviscid aerodynamic theory, slender body theory, Lighthill [1960, 1970] presented the *elongated body theory* (EBT). Assuming quasi-static conditions, the EBT defines the propulsion of a fish via the sinusoidal wave travelling along the fish body. This method is mainly applicable for anguilliform-like robots whose travelling wave has the constant amplitude from head to tail. Accordingly, Lighthill introduced a *large-amplitude elongated body theory* which is suitable for modelling of carangiforms with different body wave amplitudes [Lighthill, 1971].

The majority of the existing models of fish swimming rely on Lighthill's work. For instance, Harper et al. [1998] proposed a design of tail dynamics with optimal spring constant for actuation of an oscillating fin. Similarly, Barrett et al. [1996] developed a form of travelling wave using Lighthill's description for the wave as

$$y_{\text{body}}(x,t) = \left(c_1\, x + c_2\, x^2\right) \sin\left(k\, x + \omega\, t\right) \tag{5.1}$$

where y_{body} is the lateral displacement of the body, x is the body displacement along the main axis, c_1 and c_2 are linear and quadratic coefficients of wave amplitude envelopes, k and ω are the body wave number and frequency. k and ω are defined as $k = 2\pi/\lambda$ and $\omega = 2\pi f$ where λ is the wave length.

Since (5.1) is applicable to carangiform and thunniforms, the mathematical modelling of those two aforementioned fishes is extensively modelled by means of (5.1) that is also called trajectory approximation [Nguyen et al., 2013]. Yu et al. [2004] developed a model for a four-link carangiform-like robot using the travelling wave expression. Yu and Wang used their simplified propulsive model for optimisation of link-length-ratio of their robotic fish [Yu and Wang, 2005]. Yan et al. [2008] also studied the effects of parameters such as frequency, amplitude, wave length, phase difference and coefficient of wave amplitude envelopes on the robot cruising speed by using travelling wave form of (5.1). The adoption of the trajectory approximation could be also found in [Liu et al., 2004].

Trajectory-based models such as [Yan et al., 2008; Yu et al., 2004] use only the experimental observations of the body shape of real fishes during swimming and apply those observations for modelling of the body form of the swimming robots. These models are purely kinematics-based models and cannot fully represent the robot motion since the role of propulsive and resistive forces are ignored.

Beside trajectory approximation method, others have modelled the fish swimming taking both kinematics and dynamics of the robots into account. For instance, McIsaac and Ostrowski [2002, 2003] have developed a five-link robot using Lagrangian method. In other words, an eel-like robot with odd number of links are modelled. The simplified hydrodynamic forces of links are adopted from [Ekeberg, 1993]. Multi-body anguilliform robot is also considered by Xu and Niu [2011a,b] where the number of link system could be even too. Similar to McIsaac and Ostrowski, Xu and Niu have employed the simplified swimming force model of Ekeberg [1993] and Lagrange method for dynamic analysis.

The trajectory approximation is mainly used for carangiform-like robots and dynamic modelling is applied to anguilliform-like robot locomotion. However, carangiform-like robot are also modelled dynamically such as [Liu et al., 2008; Mason, 2003; Morgansen, 2003; Morgansen et al., 2007; Wang and Tan, 2013; Yu et al., 2006; Zhou et al., 2008]. The models obtained using both dynamics and kinematics of the robots is more reliable since the essential role of hydrodynamic forces are observed. However, the usage of the current dynamic models are limited due to the following assumptions.

- The robots are assumed to be made of a chain of links in series while the swimming motion of fish robots can be through diverse mechanisms. For example, UC-Ika 1 & 2 are designed and constructed to generate undulatory motion with three links that are not in series. One of the links is directly actuated by the DC motor and the other links are actuated passively.

- The models are built up with the assumption of steady or quasi-steady state condition. These two state conditions assume that the flow around the caudal fin has constant speed. Nevertheless, the speed of flow is variable and depends on the swimming behaviour of the fish robot.

- The existing models consider that the links are in contact with the surrounding fluid and the hydrodynamic forces are acting directly on them. This assumption is not reliable since most of the times the robot is covered by a skin layer.

This chapter presents a comprehensive, distinct mathematical model for UC-Ika 1 & 2. The model has 4 DOFs that represent the dynamic behaviour of the robot in cruising gait of swimming resembling a tuna. The model adopts the modified hydrodynamic force model of Nakashima et al. [2003]. Most of the existing mathematical models have considered the fluid inertia as an added mass to the mass of the fish which is appeared in the left-hand side of the dynamic equations of motions. In this model, the fluid inertia force is directly employed as a force in the right-hand side of the equation. This simplifies the derivation of the equations. The hydrodynamic forces are then calculated considering those DOFs and variable speed of flow around the fish. This variability submits a more representative model, although it is vulnerable by the constant parameters of the equations including frequency and amplitude of undulation wave.

In the remainder of this chapter, the mechanical design of UC-Ika 1 in the cruising mode is described in Sec. 5.1. The kinematics of tail actuation mechanism and the fish robot is presented in Sec. 5.2. Sec. 5.3 describes the hydrodynamic forces engaged in swimming. The governing equations of motion of the fish robot is derived in Sec. 5.4.

5.1 Mechanical Design

The mechanical design of both versions of UC-Ika have similar cruising mechanisms[1] and are described in Chapter 4. However, the mechanical design of UC-Ika 1 is briefly

[1]The only difference between UC-Ika 1 & 2 in cruising mode is their sizes and dimensions.

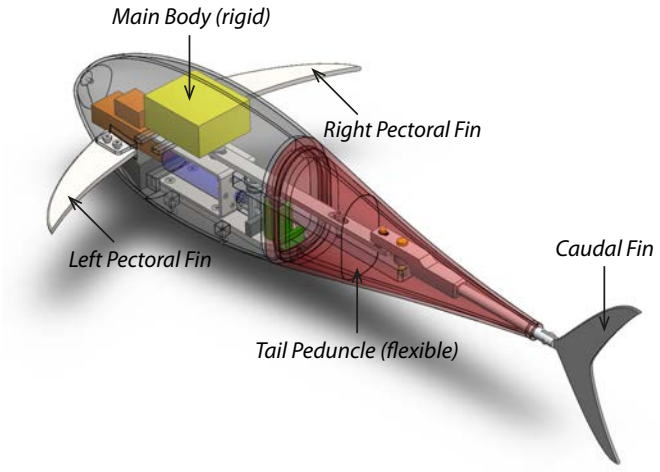

Figure 5.1: CAD design of fabricated fish robot

described for the sake of reminding.

As illustrated in Fig. 5.1, UC-Ika 1 is composed of main body, tail peduncle, pectoral fins and caudal fin. The main body is rigid and contains all electronics including microcontroller, batteries, sensors and DC motor. The pectoral fins are fixed to the main body and do not have any motion. Since both UC-Ika 1 & 2 cruise by means of the undulatory motion of their tail, the tail is the flexible part of the design where the actuation mechanism of the fish robot for cruising mode except the DC motor is located. The actuation mechanism is described in details in Sec. 5.2. The crescent-shaped caudal fin is connected to the tail using a rubber which is employed to complete the undulation of the tail[1]. The rubber is then modelled with an angular spring.

UC-Ika 1 is designed and fabricated to investigate the swimming performance of a tuna-mimetic robot during cruising motion. To do so, the undulation of the tail and the caudal fin is symmetrical to cancel out the lateral forces and propel the fish robot forward. In addition, since the cruising mode is one type of planar motion, UC-Ika 1 excludes any mechanism that could take the fish upward or downward in the water like buoyancy control system, inclination of tail or rotation of pectoral fins.

5.2 Kinematics

Undulatory motion of the tail of tuna fishes plays a significant role in their efficient cruising. Accordingly, the tail mechanism of tuna-mimetic robots needs to generate

[1]The undulation of a tuna-like robot like UC-Ika 1 is shown in Fig. 4.2

this undulatory motion, often, using a number of links that are connected together in series such as [Liu et al., 2005; Yu et al., 2007b]. However, UC-Ika 1 & 2 differ from the existing tuna-mimetic prototypes since they make benefit of a tail mechanism, shown in Fig. 5.2, whose links are not in series. The tail peduncle of UC-Ika 1 & 2 is consisted

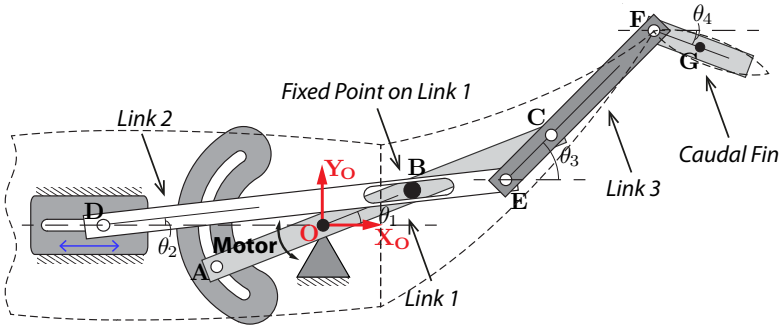

Figure 5.2: Link Mechanism of Tail Peduncle

of three links. All these three links are actuated by a single DC motor by means of the kinematic mechanism depicted in Fig. 5.2. This mechanism has novel design since it could make undulatory motion through generating different angles for its links while whole mechanism is actuated with only one motor.

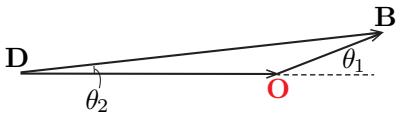

Figure 5.3: Vector analysis to obtain the first expression of 5.2.

Through kinematical analysis (see Fig. 5.3), the relationship between the links of the tail mechanism with respect to the relative reference frame placed at point O is provided with following expressions.

$$\begin{aligned}
\overline{DO} - \overline{DB}\cos\theta_2 &= -\overline{OB}\cos\theta_1 \\
\overline{DB}\sin\theta_2 &= \overline{OB}\sin\theta_1 \\
\overline{EC}\cos\theta_3 &= \overline{DO} - \overline{DE}\cos\theta_2 + \overline{OC}\cos\theta_1 \\
\overline{EC}\sin\theta_3 &= -\overline{DE}\sin\theta_2 + \overline{OC}\sin\theta_1
\end{aligned} \tag{5.2}$$

Solving the previous expressions, four unknown parameters, $\overline{DB}$, $\overline{DO}$, θ_2 and θ_3, can be obtained. Substituting the unknowns in the following expression, the displacement

of points F during a complete cycle of rotation of the motor is obtained.

$$\begin{cases} X_F = \overline{MO} + \overline{OC}\cos\theta_1 + \overline{CF}\cos\theta_3 \\ Y_F = \overline{OC}\sin\theta_1 + \overline{CF}\sin\theta_3 \end{cases} \tag{5.3}$$

Derivatives of expressions 5.2 determine the $\dot{\theta}_1$ and $\dot{\theta}_3$ which are angular velocities of link 1 and link 3, respectively. The velocity of point F is then obtained as follows.

$$\begin{cases} \dot{X}_F = -\overline{OC}\,\dot{\theta}_1\sin\theta_1 - \overline{CF}\,\dot{\theta}_3\sin\theta_3 \\ \dot{Y}_F = \overline{OC}\,\dot{\theta}_1\cos\theta_1 + \overline{CF}\,\dot{\theta}_3\cos\theta_3 \end{cases} \tag{5.4}$$

Similarly, angular acceleration of the links, $\ddot{\theta}_1$ and $\ddot{\theta}_3$, and the acceleration of point F is obtained.

$$\begin{cases} \ddot{X}_F = -\overline{OC}\,\ddot{\theta}_1\,\sin\theta_1 - \overline{CF}\,\ddot{\theta}_3\,\sin\theta_3 \\ \qquad\quad -\overline{OC}\,\dot{\theta}_1^2\,\cos\theta_1 - \overline{CF}\,\dot{\theta}_3^2\,\cos\theta_3 \\ \ddot{Y}_F = \overline{OC}\,\ddot{\theta}_1\,\cos\theta_1 + \overline{CF}\,\ddot{\theta}_3\,\cos\theta_3 \\ \qquad\quad -\overline{OC}\,\dot{\theta}_1^2\,\sin\theta_1 - \overline{CF}\,\dot{\theta}_3^2\,\sin\theta_3 \end{cases} \tag{5.5}$$

Through X_F, Y_F, $\dot{X}_F$, $\dot{Y}_F$, $\ddot{X}_F$ and $\ddot{Y}_F$, the undulatory motion of the tail mechanism is analysed. Besides that the relationship between the angular position of link 1 and link 3 is revealed by

$$\lambda = \theta_1/\theta_3. \tag{5.6}$$

λ depends on the sizes of the links of the tail mechanism including $\overline{DE}$, $\overline{OB}$, $\overline{BC}$, $\overline{EC}$ and $\overline{CF}$.

Knowing the behaviour of point F with respect to the relative reference frame and using λ, the fish robot model can be expressed by four links in series where the angular motion of third link, $\overline{CF}$, is dependent on second link, $\overline{OC}$. The schematic sketch of the fish robots is depicted in Fig. 5.4.

Considering Fig. 5.2, the overall swimming performance of the robots is analysed with regard to the absolute reference frame. Due to the importance of point G, centre of the caudal fin, for calculation of hydrodynamic forces, the position of point G is expressed by

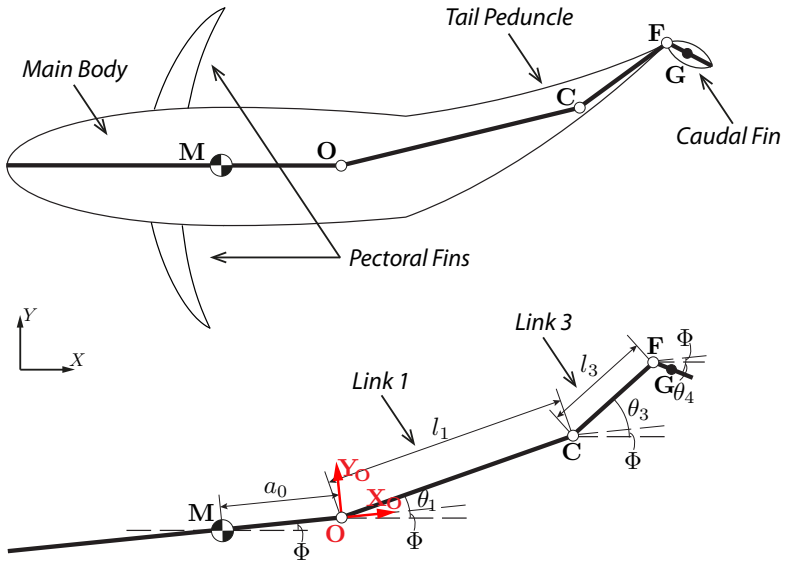

Figure 5.4: The schematic sketch of UC-Ika 1 & 2 in cruising mode

$$\begin{aligned} X_G =& X + \overline{MO}\cos(\Phi) + \overline{OC}\cos(\theta_1+\Phi) \\ &+ \overline{CF}\cos(\theta_3+\Phi) + \overline{FG}\cos(\theta_4), \end{aligned} \tag{5.7}$$

$$\begin{aligned} Y_G =& Y + \overline{MO}\sin(\Phi) + \overline{OC}\sin(\theta_1+\Phi) \\ &+ \overline{CF}\sin(\theta_3+\Phi) + \overline{FG}\sin(\theta_4), \end{aligned} \tag{5.8}$$

where X, Y , Φ and θ_4 are DOFs of the model: translations X and Y of centre of mass in X and Y directions, the rotation Φ about the centre of mass of the robots and the rotation θ_4 of the caudal fins. The centre of mass of the fishes is at point M. θ_1 is the actuation angle provided by means of the DC motor as

$$\theta_1 = A\sin(2\pi f t), \tag{5.9}$$

where A, f and t are amplitude, frequency and time, respectively. θ_3 in expressions (5.7-5.8) can be replaced by $\lambda\,\theta_1$.

Note that, the resultant velocity of point G, defined as U, is an important parameter for derivation of hydrodynamic forces acting on the fin. U is obtained from two forward and lateral components of velocity at centre of the caudal fins, point G, and employed

in next section. U is expressed by

$$U = \sqrt{\left(\dot{X}_G^2 + \dot{Y}_G^2\right)}. \tag{5.10}$$

5.3 Hydrodynamic Forces

The hydrodynamic forces are considered based on the following assumptions:

- The main body rotation is negligible. Accordingly, the lateral lift forces generated through the rotation of the main body is neglected.
- Only the caudal fin is responsible for propulsion. Since nearly 90% of propulsion forces is generated by the caudal fin, this assumption is a reasonable.

Taking aforementioned assumptions into account, the main hydrodynamic forces acting on the fish robots are shown in Fig. 5.5.

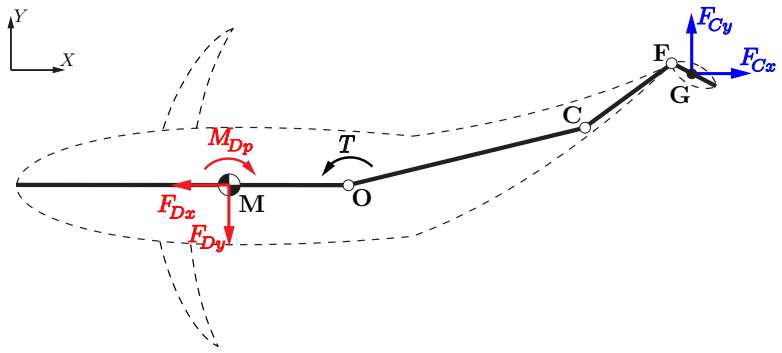

Figure 5.5: The free-body diagram of the forces acting on UC-Ika 1

5.3.1 Forces on Main Body of Fish Robot

In general, two main hydrodynamic forces are acting on the fins, which are lift and drag forces. However, lift forces are not considered since the main body is symmetric relative to $X - Z$ plane and its rotation is negligible. The drag forces of the main body

are then [Batchelor, 1967],

$$F_{Dx} = C_{Dx}\frac{\rho\, S_x}{2}\dot{X}^2, \tag{5.11}$$

$$F_{Dy} = C_{Dy}\frac{\rho\, S_y}{2}\dot{Y}^2, \tag{5.12}$$

$$M_{Dp} = \frac{1}{8}\, C_{Dp}\rho \left(\frac{(L_0 - L_1)^4}{L_1} + L_1^3\right) S_y\dot{\Phi}^2, \tag{5.13}$$

where S_x and S_y are fish robot projected areas, C_{Dx} and C_{Dy} are the drag coefficients of fish robots along X and Y directions, respectively. C_{Dp} is also yaw drag coefficient [Liu et al., 2008]. ρ is the water density. L_0 is the distance between the center of mass of the robots, point M, and L_1 is the distance between point M and point F.

5.3.2 Forces on Caudal Fin

A number of hydrodynamic models for fish swimming have been presented such as waving plate theory [Wu, 1961]. However, the most suitable model for carangiform-like robots with small lateral motion of the tail is elongated body theory introduced by Lighthill [1960]. Based on Lighthill's theory, Nakashima et al. [2003] have described the lift and fluid inertial forces by

$$F_L = 2\pi\rho S C_C U^2 \sin\alpha\cos\alpha, \tag{5.14}$$

$$F_I = \pi\rho S C_C^2(\dot{U}\sin\alpha + \dot{\alpha}U\cos\alpha), \tag{5.15}$$

where S and $2C_c$ are span and the chord of the caudal fins, respectively. α is the instantaneous angle of attack defined by following expression

$$\alpha = \theta_4 + \arctan\left(\frac{\dot{Y}}{\dot{X}}\right). \tag{5.16}$$

Figure 5.6 depicts the free-body diagram of the caudal fins showing the inertial and lift forces.

When flow is passing an object, at least, two main forces are exerted on it: lift and drag forces. The drag force is also made with the pressure drag and the skin friction drag. In terms of the caudal fin, the lift force is calculated by (5.14). However, the skin friction drag is really small due to the very small surface area of the caudal fin with respect to the whole body. The pressure drag is also neglected since the caudal fin is

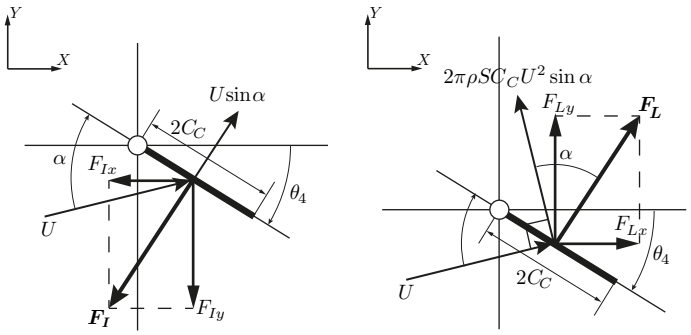

(a) Fluid Inertial Force (b) Lift Force

Figure 5.6: The free-body diagram of the caudal fin showing lift and fluid inertial forces

thin and has streamlined body shape (see Sec. 2.2.2).

The fluid inertial force is the force exerted on the caudal fins by the fluid around it when water is accelerated and decelerated. Fluid inertial force is calculated by (5.15).

With (5.14) and (5.15), F_{Cx} and F_{Cy} are obtained as

$$F_{Cx} = (F_L - F_I)\sin\theta_2, \tag{5.17}$$

$$F_{Cy} = (F_L - F_I)\cos\theta_2. \tag{5.18}$$

F_{Cx} and F_{Cy} are the thrust and the lateral force generated by the fish robots during swimming.

5.4 Governing Equations of Coupled Fluid Mechanics Structure

The robot has four DOFs including translations X and Y of centre of mass in X and Y directions, the rotation Φ about the centre of mass of the robots and the rotation θ_4 of the caudal fins. The input to the system is the motor torque, T. The motor torque is load independent and is proportional to the angular velocity and frequency (see Fig. 5.7). Although the load acting on the motor is fluctuating, it is assumed to be a small value. Thus a constant motor torque is considered and its corresponding frequency, f, is calculated by

$$f = \frac{N}{2\,\pi} = -2.278\ T + 16.755. \tag{5.19}$$

where N is the rotational speed of motor in radian per second. Then f is substituted into expression (5.9) which represents the angular motion of link 1, θ_1. Besides f, θ_1 has oscillation amplitude, A, which is constrained kinematically by the tail mechanism.

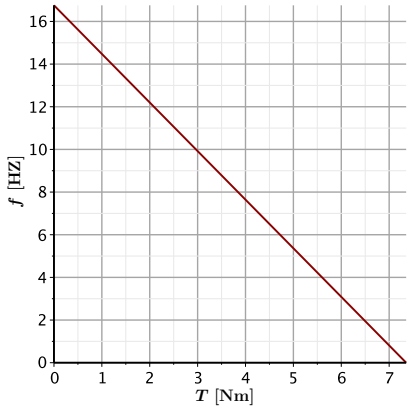

Figure 5.7: The relationship between the frequency and torque of the motor

Substituting A and f into expression (5.9), θ_1 is employed as the input to the dynamic model of the robots.

Considering the 4 DOFs, four equations of motion are derived applying Newton's second law.

$$\begin{aligned} M\,\ddot{X} &= F_{Cx} - F_{Dx}, \\ M\,\ddot{Y} &= F_{Cy} - F_{Dy}, \\ I_M\,\ddot{\Phi} &= (X_G - X)\;F_{Cy} - (Y_G - Y)\;F_{Cx} - M_{Dp}, \\ I_c\,\ddot{\theta}_4 &= (X_G - X)\;F_{Cy} - (Y_G - Y)\;F_{Cx} - k\;(\theta_4 - \theta_3)\,. \end{aligned} \tag{5.20}$$

where M is the total mass of the fish robots about the centre of mass, I_M is the total mass moment of inertia of the robots about their centre of mass, I_c is the mass moment of inertia of the caudal fins about point M, and k is the spring constant of the rubber connecting the caudal fins to the tail peduncles.

Substituting the hydrodynamic forces into the equations of (5.20) yields a coupled nonlinear system of the fluid mechanics structure. Accordingly, the system is solved applying the numerical Runge-Kutta Fehlberg method. The simulation result using the aforementioned equations of motion are presented in Chapter 7.

5.5 Summary

In this chapter, the cruising mode of two fish robots (UC-Ika 1 & 2) from the category of carangiforms and thunniforms are mathematically modelled. The model makes benefits of kinematics and dynamics of fish robots. The model has four DOFs: translations in X and Y directions, the rotation around the centre of mass of the robots, Φ, and the rotation of the caudal fins about their joint to the tail peduncles, θ_4. The robots swim through undulatory motion of their body and caudal fin. The undulatory motion is generated by the tail mechanism that is actuated by a single DC motor.

As the first step of modelling, the tail mechanism of the robots is kinematically analysed with respect to the relative reference frame. Then the swimming behaviour of the robots with respect to the absolute reference frame is investigated. This swimming behaviour is associated with hydrodynamic forces that are acting upon the fish robots. Finally, the governing equations of motion of the robot are derived. Substituting the hydrodynamic forces into the equations of motion yields the coupled nonlinear system which is solved using Rung-Kutta Fehlberg method.

Chapter 6

Efficiency-Based Optimisation

6.1 Introduction

Using the mathematical model of the cruising mode of swimming of robots, the robot needs to be simulated using its dynamic equations of motion. However, there are a number of constant parameters in the equations including sizes of different parts of the robot, amplitude and so on whose values need to be substituted. At this stage, an important issue arises: how to decide on the best values for those parameters. To address this problem several approaches could be applied.

Some robotic fish developers have analysed different parts of the robot separately. For instance, they experimentally test different sizes of the fish fins and select the best one after the comparison of them together. Similarly, Kodati et al. [2008] have taken hydrodynamic experiment into account to design caudal fin of their fish called MARCO while the pectoral fins are analogous to a real boxfish.

This method that analyses a fish partly, not wholly, is not an ideal approach since the effectiveness of each part of fish robots needs to be investigated in connection with the whole body and the swimming behaviour of the fish. For example, based on hydrodynamic analysis of fish swimming, a manoeuvrable angelfish requires fins with large surface area and low aspect ratio in order to have an efficient swimming whereas a fast swordfish needs a caudal fin with small surface area and high aspect ratio. Both aforementioned types of fins are highly efficient but with respect to their natures: being manoeuvrable or being high-speed swimmer.

In addition to the previous approach, some researchers have tried to scale the real fish size and tail beat for their robots such as [Anderson and Chhabra, 2002; Gao et al., 2009; Triantafyllou et al., 2000; Yu et al., 2007b] where the shape and geometry of

fish robots are mimicked. Even more, Salume [2010] has developed a trout robot that resembles the morphology of the real fish in geometry, stiffness and stiffness distribution of the body and the caudal fin.

Although preferable compared to the previous method, the method of scaling down the real fish ignores the fact that the fish robots are developed based on their locomotion types for limited purposes like coastal monitoring, pollution search and so on. Whereas in nature the exercise physiology of swimming animals is compromised according to their natural demands like respiration, digestion and reproduction which are not issues of developing fish robots. For instance, bird-wrasses have an elongated beak which is useful for its type of catching prey. The size of this elongated beak does not affect bird-wrasse locomotion. Hence mimicking body shape of a bird-wrasse with its elongated beak does not optimise the robot motion.

Yet there are many other aquatic robot developers who have not explained explicitly why specific shape and values for, e.g., the sizes and the tail beat of their fish robot are selected. For instance, BoxyBot [Lachat et al., 2005] is a well-known robot for its manoeuvrability. However, BoxyBot could have superior performance if it had optimised values for the shape and the size of its body and fins. The majority of robotic fishes like [Epstein et al., 2006; Kato et al., 2000; Liang et al., 2011; Low and Willy, 2005; Morgansen et al., 2007] could be classified in this group since they are mainly mimicking the swimming mode of real fishes rather than their morphologies.

Considering the disadvantages of the aforementioned methods, this chapter has introduced a method for determination of constant parameters of a robotic fish. This method includes optimising the constant parameters of the mathematical model of the fish robot using Particle Swarm Optimisation (PSO) algorithm. In this method, all different parts of the robot are optimised simultaneously. Moreover, the robot could be optimised for dissimilar purposes. For example, the fish robot could be optimised for efficient and fast swimming.

In Sec. 6.2, the background of PSO algorithm is discussed. The algorithm itself is introduced in Sec. 6.3. In Sec. 6.4, the application of PSO algorithm to the robotic fish is observed. In this section, the particles and fitness function of PSO algorithm are defined. In Sec. 6.5, the optimisation result is presented. Eventually, in the last section, this chapter is summarised.

6.2 Background

Optimisation is one of the most important problems in engineering. This problem cannot be always addressed via analytical methods like gradient decent. For instance, multi-modal functions cannot be optimised using gradient method since there are a number of local optimal solutions. To address this problem, evolutionary algorithms (EA) are attractive approaches since they are capable of solving large and complex problems [Yu and Gen, 2010a].

EAs are stochastic-search algorithm inspired by natural evolution. EAs initiate optimisation by a group of solutions called population. The performance of each individual in the population is then evaluated using a fitness function. Then the population behaviour is evolved analogous to the nature [Yu and Gen, 2010b]. EAs like genetic algorithm (GA), particle swarm optimisation (PSO) and differential evolution (DE) all go through similar algorithms.

So far various types of EAs have been proposed started from 1960 [Yu and Gen, 2010a]. All of them have their own pros and cons. Among the proposed methods, PSO algorithm that relies on swarm intelligence (SI) has shown more suitability for complex optimisation purposes. SIs are inspired by the social behaviour of animal species like birds, fish and ants. Due to self-organizing nature of SIs, they are suitable for dynamic problems. Note that, in addition to PSO, there is another main SI-based algorithm called ant colony optimisation (ACO). ACO is not discussed in this paper since ACO is apt to discrete optimisation problems [Yu and Gen, 2010b].

As a SI-based algorithm, PSO is inspired by the social behaviour of birds within a flock. In the other words, each bird in the swarm modifies its motion with the information obtained from other members of the swarm, its own experience and its current direction of motion. This makes the basic intuitive ideology of PSO algorithm. Kennedy and Eberhart invented PSO algorithm in 1995. They defined birds as particles in the algorithm where the direction of motion of each bird is represented by particle's velocity.

Many authors have compared the performance of PSO with many other EAs and global optimisation methods. For instance, PSO is compared with GA in [Abraham et al., 2006; Hassan et al., 2005; Kachitvichyanukul, 2012]. The results point out that PSO with its simple conceptual structure is comparable favourably with other global optimisation methods in its speed of convergence, its computational efficiency and its capability to optimise complex and nonlinear functions.

6.3 PSO Algorithm

PSO algorithm has two inherent components: particles and fitness function which must be defined for every optimisation problem. Each particle has a position, $x_i(t)$, which represents a solution to the fitness function. In each iteration, the particles' positions are updated with the particles' velocities of that iteration, $v_i(t)$, which shows the directions of motion of the particles. The velocities of the particles are computed considering three factors: velocities of the particles toward the best experienced position of the swarm called *gbest*, velocities of the particles toward the best experienced position of each particle called *pbest* and the previous particles' velocities[1]. Figure 6.1 shows the behaviour of each particle within a swarm conceptually.

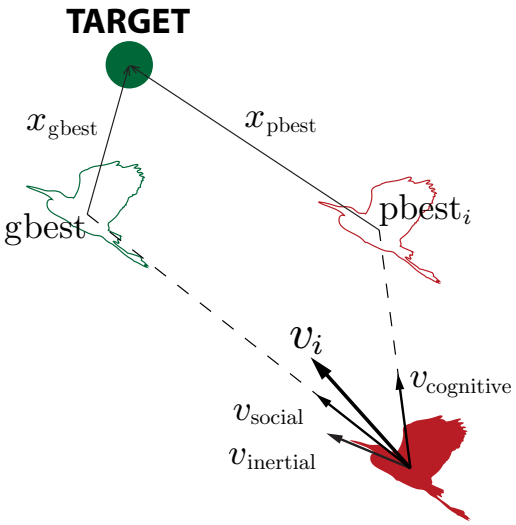

Figure 6.1: The concept of a particle's behaviour in PSO algorithm.

PSO algorithm includes following steps [Shi and Eberhart, 1999]:

1. Initialize the swarm by randomly dedicating a value for the position, $x_i(t)$, and velocity, $v_i(t)$, of each particle.

2. Evaluate the performance of each particle based on its current position using a fitness function, F.

3. Compare the value of fitness function of each particle to its best, $pbest_i$, so far.

[1] Note that the position and the velocity in the algorithm do not have their physical properties.

If the new value is better than $pbest_i$, then

$$pbest_i = F\left(x_i\left(t\right)\right) \tag{6.1}$$

$$x_{pbest_i} = x_i\left(t\right) \tag{6.2}$$

4. Compare $pbest_i$ to global best performance, $gbest$. If $pbest_i$ is smaller than $gbest$, then

$$gbest = F\left(x_i\left(t\right)\right) \tag{6.3}$$

$$x_{gbest} = x_i\left(t\right) \tag{6.4}$$

5. Update the velocity of each particle based on following function:

$$v_i\left(t\right) = w\, v_i\left(t-1\right) + c_1\, r_1\left(x_{pbest_i} - x_i\left(t\right)\right) + c_2\, r_2\left(x_{gbest} - x_i\left(t\right)\right) \tag{6.5}$$

Where w called inertia weight represents the influence of the previous speed of the particle on the new speed. Large w helps the swarm to explore new areas in the search space; however, it slows down the speed of convergence. Inertia weight can be constant, variable and adaptive using some approaches like fuzzy controllers.

c_1 and c_2 are cognitive and social constants which do not have an essential impact on the convergence of the algorithm. Nevertheless, they could change the speed of convergence. By default $c_1 = c_2 = 2$ but experiments show that $c_1 = c_2 = 1.49$ facilitates the algorithm with better results. Yet there is a study that reveals that $c_1 + c_2 \leq 4$ provides better results if $c_1 > c_2$ [Abraham et al., 2006]. r_1 and r_2 are random constants.

6. Update the position of each particle according to following function:

$$\begin{aligned} x_i\left(t\right) &= x_i\left(t-1\right) + v_i\left(t\right) \\ t &= t+1 \end{aligned} \tag{6.6}$$

7. Go back to step 2. This process should be repeated until convergence is reached.

The flowchart shown in Fig. 6.2 illustrates the aforementioned steps.

Instead of *gbest*, the best experienced position of the local particles called *lbest* could be also employed to update the particles' velocities. Accordingly, step 4 and 5 of the

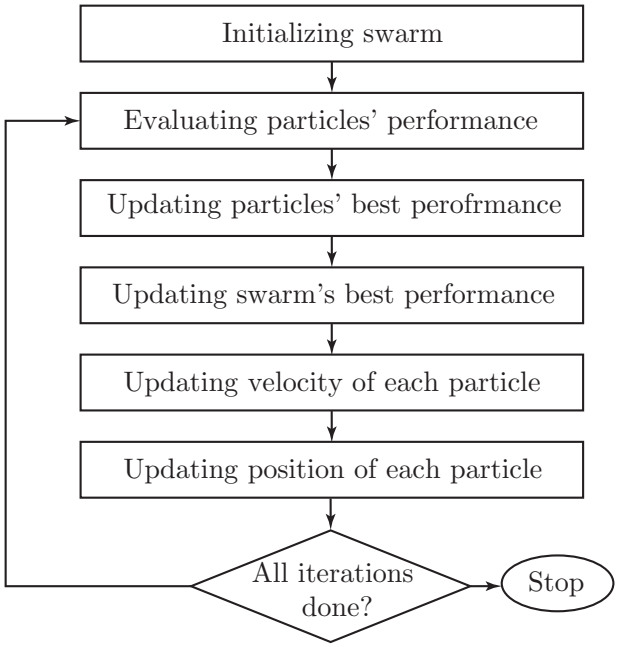

Figure 6.2: PSO flowchart

PSO algorithm should be changed. To introduce the neighbourhood of each particle, a number of topologies have been recommended. Using *lbest* decreases the possibility of premature convergence for PSO algorithm; however, it slows down the speed of convergence considerably. Therefore, in this project *gbest* is applied for optimisation.

6.4 Application

In order to optimise the cruising gait of UC-Ika 2, the model introduced in Chapter 5 is employed[1]. Accordingly, the cruising gait of UC-Ika 2 is modelled with following equations of motion.

$$\begin{aligned} M\,\ddot{X} &= F_{Cx} - F_{Dx}, \\ M\,\ddot{Y} &= F_{Cy} - F_{Dy}, \\ I_M\,\ddot{\Phi} &= (X_G - X)\;F_{Cy} - (Y_G - Y)\;F_{Cx} - \;M_{Dp}, \\ I_c\,\ddot{\theta}_4 &= (X_G - X)\;F_{Cy} - (Y_G - Y)\;F_{Cx} - k\;(\theta_4 - \theta_3)\,. \end{aligned} \tag{6.7}$$

[1]Note that the model introduced in Chapter 5 is based on the cruising mechanism of UC-Ika 1 & 2. Therefore, the model is employed to optimise the cruising mode of UC-Ika 2.

PSO algorithm is applicable to the aforementioned model through proper definition of two intrinsic components of the algorithm including particles and fitness function.

6.4.1 Particles

In (6.7), there are seven unknown parameters that have crucial effect on optimisation of the fish robot. The parameters are $\overline{EC}$, $\overline{CF}$, $\overline{OB}$, $\overline{DE}$ and $\overline{MO}$ which are sizes of the links shown in Fig. 6.3 as well as A and A_4 which are the amplitudes of link 1 and the caudal fin, respectively[1].

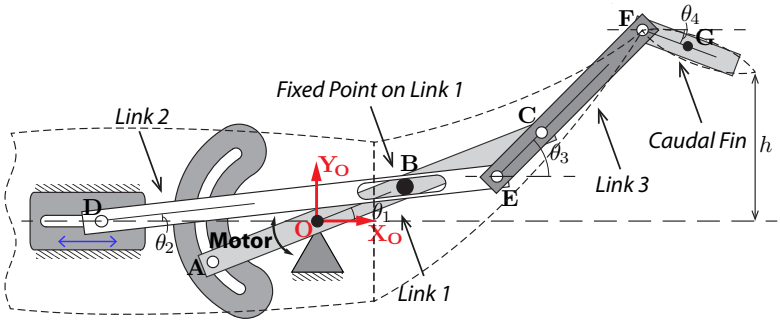

Figure 6.3: The link mechanism of the tail peduncle

The aforementioned parameters are defined as the dimensions of each particle's position. In this particular application of PSO algorithm, five particles are introduced whose positions have seven dimensions which are the unknown parameters of (6.7). Hereafter, the particles and accordingly their parameters are optimised using a fitness function.

Note that the overall shape and dimensions of the robot including a, b, L_1 and L_2 which are vertical semi-axis of the main body, horizontal semi-axis of the main body, length of the main body and length of the tail are not selected for optimisation since they are reference sizes. In other words, all parameters of the robot which incorporate to the swimming mechanism inside the robot are modified based on the shape and dimensions of the robot.

[1]One should bear in mind that due to the passive actuation of the caudal fin, A_4 is not directly used in the equations of motion of the fish robot. A_4 affects the spring constant of the caudal fin whose value is experimentally obtained.

6.4.2 Fitness Function

Since UC-Ika 2 needs an efficient cruising performance, efficiency is considered to serve as the fitness function in this application of PSO algorithm. Efficiency could have various definitions but in terms of swimming efficiency, Froude efficiency is the most well-known definition which is extensively employed to evaluate the efficiency of fishes. Froude efficiency relates the useful power used for propulsion to total kinetic energy of the fish which is the mean rate of transferred momentum to the wake around the fish. Froude efficiency is defined by

$$\eta = \frac{\overline{F_{Cx}}\ \bar{\dot{x}}}{P_{\text{total}}}, \tag{6.8}$$

where $\overline{F_{Cx}}$ is the thrust and $\bar{\dot{x}}$ is the mean velocity of the fish. P_{total} is the total kinetic energy of the fish [Lighthill, 1960]. P_{total} is obtained through the following expression as

$$P_{\text{total}} = \overline{F_{Cx}}\ \bar{\dot{x}} + \overline{F_{Cy}}\ \bar{\dot{y}}, \tag{6.9}$$

where $\overline{F_{Cy}}$ is the force to generate vortex wake and $\bar{\dot{y}}$ is the mean lateral speed of the caudal fin. Derivations of $\overline{F_{Cx}}$ and $\overline{F_{Cy}}$ are presented in Chapter 5.

Experimentally speaking, Froude efficiency is a reliable criterion for optimisation of the fish swimming motion. However, calculating Froude efficiency through a simplified mathematical model will not yield a desired result. For instance, the model assumes that no hydrodynamic force is generated by the tail peduncle while a tuna generate 10% of its swimming thrust by its tail peduncle [Sfakiotakis et al., 1999]. Moreover, during the simulation the model uses a constant drag for different heaves of the tail peduncle. This assumption is not also confirmed by the nature observations since a straight-stretched fish encounters 3-5 times less drag than an undulatory fish [Webb, 1994].

To address the aforementioned problem, a PB function is defined which helps to find out the efficient cruising within the optimal range of Strouhal number. The Strouhal number is a factor that shows the structure of the vortices made through the body undulation of fishes. The Strouhal number, St, is a dimensionless parameter. It represents the ratio of unsteady to inertial forces and is defined as

$$St = 2\frac{f\,h}{\bar{\dot{x}}} \tag{6.10}$$

where f is the frequency of the body undulation, h is the heave of the caudal fin and $\overline{\dot{x}}$ is the average cruising velocity of the fish. If $0.25 < St < 0.4$, the vortices behind the caudal fin produce maximum thrust. This optimal range of St is obtained based on experimental observations of real fishes. Bear in mind that the Strouhal number is mainly applicable for fishes whose swimming is through their body and caudal fins [Triantafyllou et al., 1993].

PB function is defined to guide the particles of the algorithm towards the optimal range of undulatory swimming. Then within this range, the most efficient cruising is calculated. The algorithm of PB function is presented as follows.

Algorithm 1 Calculate Pbest

function PB($\overline{F_{Cx}}, \overline{\dot{x}}, P_{\text{total}}, f, h$)
  $\eta := \overline{F_{Cx}}\ \overline{\dot{x}}\,(P_{\text{total}})^{-1}$
  $St := 2\,f\,h\,\left(\overline{\dot{x}}\right)^{-1}$
  if $St > 0.35$ **then**
    $k := (80\ (St - 0.325))^{-1}$
  else if $St < 0.30$ **then**
    $k := (80\ (0.325 - St))^{-1}$
  else
    $k := 2$
  end if
  return $k\eta$
end function

6.5 Results

The optimisation is carried out with Maple 16.00. The differential equations of motion of the fish robot are solved applying the numerical Runge-Kutta Fehlberg method. After 63 iterations and selecting ρ_1 and ρ_2 as random constants between 0-2, the PSO algorithm submits the best particle including the most optimal parameters. The values of the constant parameters used in the dynamic equations of UC-Ika 2 after optimisation are given in Table 6.1.

6.6 Summary

In order to optimise the swimming performance of the fish robots, this chapter has presented a method of optimising all different parameters of the fish robot, simultaneously.

In this method, the optimal values of the constant parameters present in the equations of motion of the robots must be obtained. Accordingly, an optimisation algorithm, PSO algorithm, from EAs category is selected since they are capable of optimising large and complex system.

PSO algorithm have two intrinsic components: particles and fitness function. Particles are solution of the system which are evaluated using fitness function. In terms of fish robots, particles are solution of the dynamic equations of motion. Dimensions of particles are the constant parameters that need to be optimised.

Fitness function is also defined based on Froude efficiency and Strouhal number of the fish motion. Froude efficiency shows the swimming efficiency of the robot while Strouhal number determines the optimal structure of vortices left behind the robot. In order to combine Froude efficiency and Strouhal number, a PB function is defined. Using PB function, the most efficient solution of the fish swimming within the optimal range of Strouhal number is achieved.

Table 6.1: Constant parameters of UC-Ika 2 after optimisation

Tail Mechanism	
Distance between point M and O	$\overline{MO} = 0.077$ m
Posterior part of link 1	$\overline{OC} = 0.180$ m
Posterior part of link 3	$\overline{CF} = 0.069$ m
Anterior part of caudal fin	$\overline{FG} = 0.030$ m
Anterior part of link 1	$\overline{AO} = 0.030$ m
Distance between point M and B	$\overline{OB} = 0.089$ m
Length of link 2	$\overline{DE} = 0.228$ m
Anterior part of link 2	$\overline{EC} = 0.026$ m
General Parameters	
Mass	$M_0 = 7.426$ kg
Mass moment of inertia	$I_0 = 0.667$ kgm^2
Vertical semi-axis	$a = 0.100$ m
Horizontal semi-axis	$b = 0.075$ m
Tip to point M length	$L_0 = 0.273$ m
Projected area along X	$S_x = 0.021$ m^2
Projected area along Y	$S_y = 0.126$ m^2
Caudal Fin	
Mass	$M_c = 0.120$ kg
Mass moment of inertia	$I_c = 0.001$ kgm^2
Span	$S = 0.372$ m
Chord	$C_C = 0.024$ m
Spring constant	$k = 12.191$ Nm/rad
DC Motor	
Amplitude	$A = \pi/18$ rad
Frequency	$f = 1.5$ Hz
Forces	
Density of water	$\rho = 998$ kg/m^3
Body drag along X	$C_{Dx} = 0.4$
Body drag along Y	$C_{Dy} = 0.85$
Body drag rotational Φ	$C_{Dp} = 0.85$

Chapter 7

Simulation

To analyse the swimming performance of the fish, its behaviour needs to be simulated using the dynamic equations of motion (5.20) derived in Chapter 5. These equations determine the swimming behaviour of fish robot in cruising mode of swimming while the pectoral fins are not activated during locomotion of the robot.

The constant parameters of the equations of (5.20) are evaluated twice for UC-Ika 1 & 2. The parameters of UC-Ika 1 are experimentally selected while the constant parameters of equations of motion of UC-Ika 2 is optimised for an efficient cruising (see Chapter 6).

The simulation is carried out with Maple 16.00. The differential equations of motion of the fish robot are solved applying the numerical Runge-Kutta Fehlberg method.

In this chapter, the simulation results of cruising motion of UC-Ika 1 & 2 are presented in Sec. 7.1 and 7.2.Then the swimming performance of the robots is compared in Sec. 7.3 using Froude efficiency and Strouhal number. The chapter is concluded in Sec. 7.4.

7.1 Simulation of UC-Ika 1

The hydrodynamic forces generated by the motion of the caudal fin play the crucial role in the swimming performance of the fish robot. However, those forces are significantly affected by the kinematics of point F which is actuated by link 1 of the tail mechanism (see Fig. 5.2).

Considering Fig. 5.2, in order to analyse the motion of point F, angular displacement, velocity and acceleration of links 1 and 3 are computed. By substituting the sizes of the links given in Table 7.1 into expressions (5.2), θ_3 is obtained. Figure 7.1

depicts θ_1 and θ_3 for 2 seconds.

Table 7.1: Kinematic parameters

Links	Length [m]
$\overline{MO}$	0.081
$\overline{OC}$	0.165
$\overline{CF}$	0.18
$\overline{FG}$	0.03
$\overline{AO}$	0.03
$\overline{OB}$	0.082
$\overline{DE}$	0.22
$\overline{EC}$	0.025

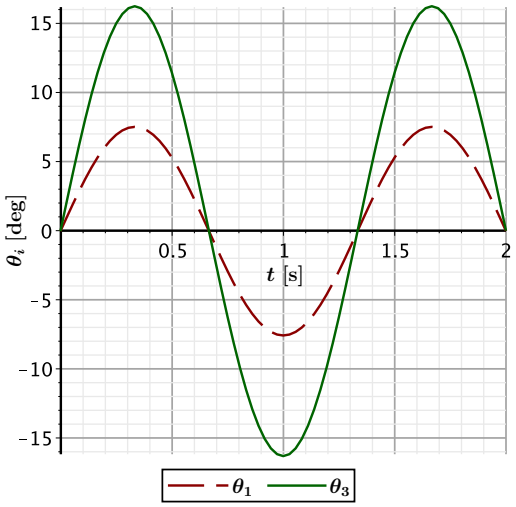

Figure 7.1: Angular motion of link 1 and link 3

As shown in Fig. 7.1, the amplitudes of θ_1 and θ_3 are 7.5° and 16.177°, respectively. Thus, by using expression (5.6), λ is achieved to be equal to 2.146.

Similar to angular displacement, angular velocity and acceleration of links 1 and 3 are calculated whose amplitudes are $\left|\dot{\theta}_1\right| = 47.124$ deg/s, $\left|\dot{\theta}_3\right| = 101.113$ deg/s, $\left|\ddot{\theta}_1\right| = 296.088$ deg/s^2 and $\left|\ddot{\theta}_3\right| = 645.373$ deg/s^2.

The displacement, velocity and acceleration of point F with respect to the relative reference frame are obtained using $\dot{\theta}_1$, $\dot{\theta}_3$, $\ddot{\theta}_1$ and $\ddot{\theta}_3$. The trajectory of motion of point F is depicted in Fig. 7.2.

Once the dynamic behaviour of the tail mechanism is analysed, the swimming performance of the robot could be observed. The analysis of the tail mechanism submits

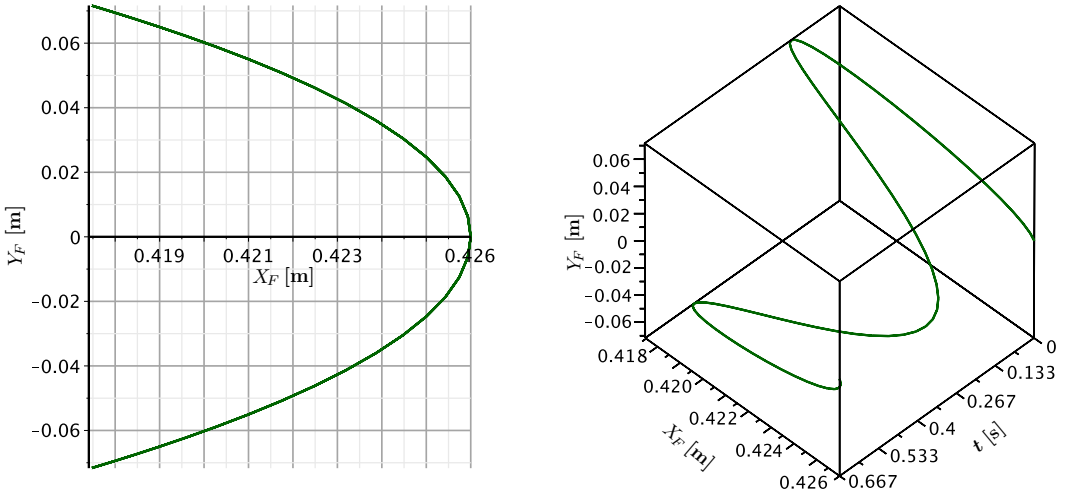

(a) 2D plot

(b) 3D plot considering time

Figure 7.2: Displacement of point F

the value of λ. Substituting λ and the constant parameters given in Table 7.2 into equations of motion, (5.20), reveals the capabilities of the robot in planar motion. It also illustrates how the caudal fin behaves during swimming.

While the model verifies that the robot is swimming forward along X, illustrated in Fig. 7.3, it also shows the slight periodic motion of the robot in Y direction. In the other words, the robot has lateral periodic motion with an amplitude of 0.025 m (see Fig. 7.4). Note that although the translational motion along X shown in Fig. 7.3 seems to be linear after transient time, it is made from very small oscillations due to the change of speed shown in Fig. 7.5.

The robot has a transient motion for 30 s to reach an average cruising speed of 0.29 m/s; although, the cruising speed of the robot is oscillating between approximately 0.28 m/s and 0.30 m/s (see Fig. 7.5). This periodic characteristic of cruising speed is due to the fact that the propulsive forces in a cycle of undulation of the tail is changing.

The simulation of cruising motion of UC-Ika 1 also reveals its periodic lateral speed (see Fig. 7.6). This result is expected from the lateral displacement of the robot, Fig. 7.4, since at the maximum and minimum lateral displacements of the robot, the lateral speed is zero.

The model also indicates that the robot is swinging around its centre of mass with a maximum rotation of 3.98° from its cruising axis (see Fig. 7.7).

In addition to the aforementioned results, Figure 7.8 illustrates that the caudal fin

Table 7.2: Parameters

General	Mass	$M_0 = 4.12$ kg
	Mass moment of inertia	$I_0 = 0.299$ kgm^2
	Vertical semi-axis	$a = 0.075$ m
	Horizontal semi-axis	$b = 0.06$ m
	Tip to point M length	$L_0 = 0.213$ m
	Frontal projected area	$S_x = 0.014$ m
	Lateral projected area	$S_y = 0.078$ m
Caudal Fin	Mass	$M_c = 0.05$ kg
	Mass moment of inertia	$I_c = 0.0007$ kgm^2
	Span	$S = 0.17$ m
	Chord	$C_C = 0.028$ m
	Spring constant	$k = 9.62$ Nm/rad
DC Motor	Amplitude	$A = \pi/24$ rad
	Frequency	$f = 1.5$ Hz
Forces	Density of water	$\rho = 998$ kg/m^3
	Body drag along X	$C_{Dx} = 0.4$
	Body drag along Y	$C_{Dy} = 0.85$
	Body drag rotational Φ	$C_{Dp} = 0.85$

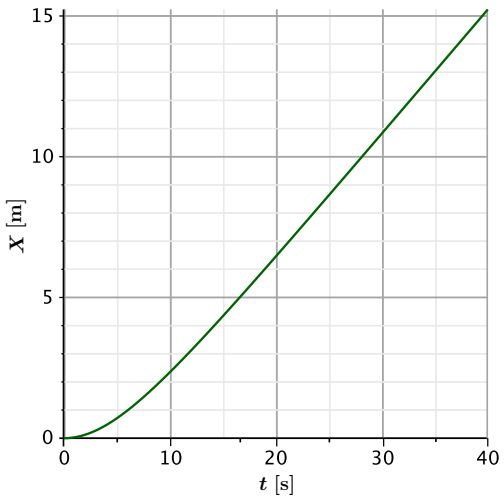

Figure 7.3: Translational motion of the fish robot along X Axis

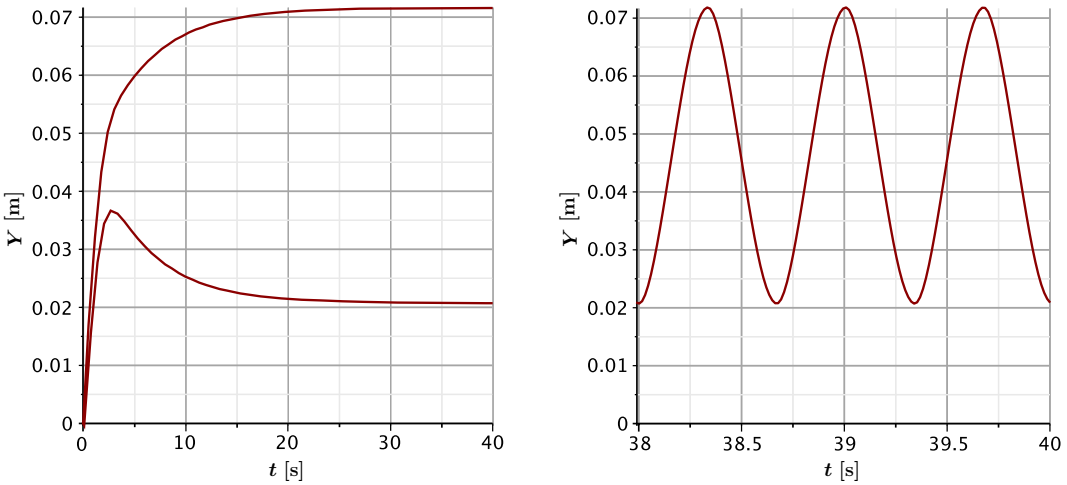

(a) The envelope of lateral motion (b) Lateral steady state motion

Figure 7.4: Translational motion of the fish robot along Y Axis

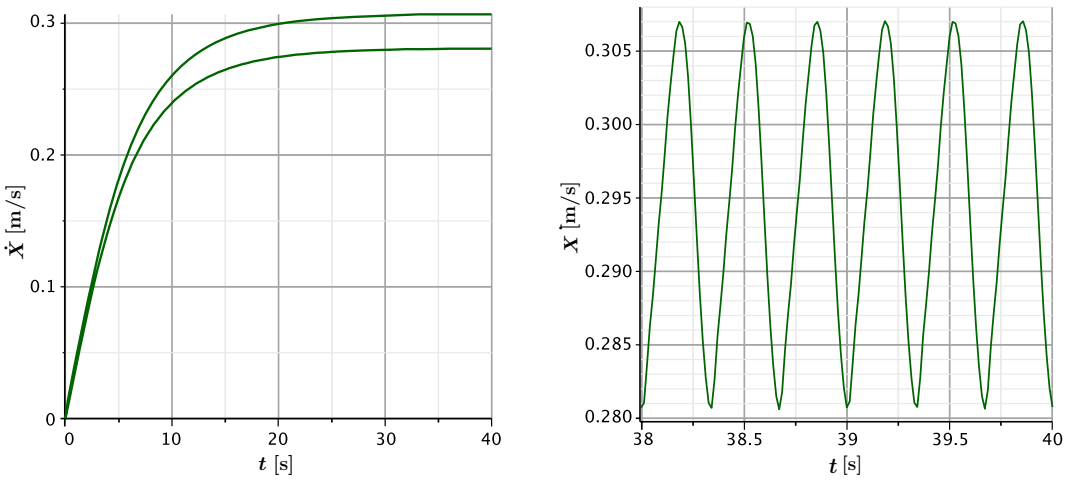

(a) The envelope of forward speed (b) Crusing steady state speed

Figure 7.5: Speed of the fish robot along X Axis

has a periodic motion of amplitude 18.7° which is an ideal amplitude angle of attack for optimal thrust production [Anderson et al., 1998], although UC-Ika 1 is not optimised.

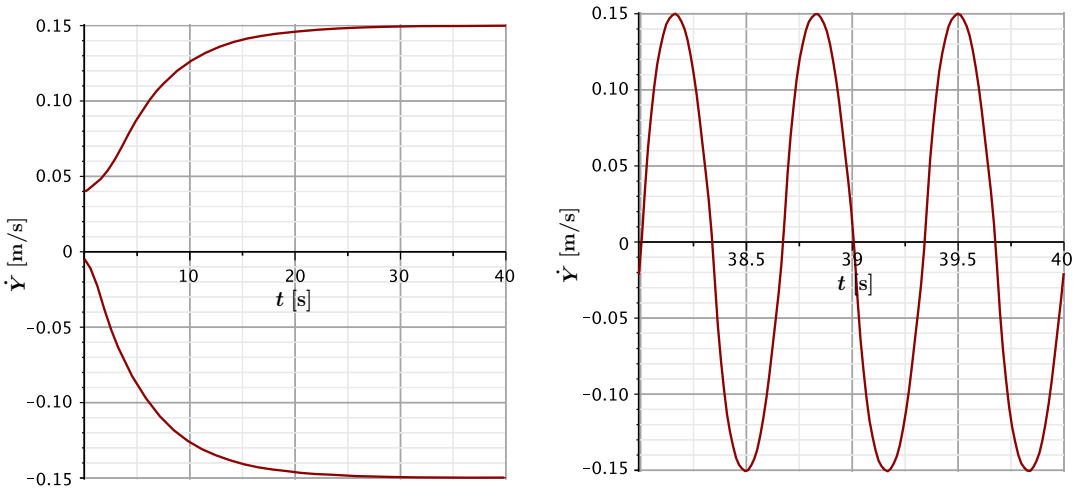

(a) The envelope of lateral speed

(b) Lateral steady state speed

Figure 7.6: Speed of the fish robot along Y Axis

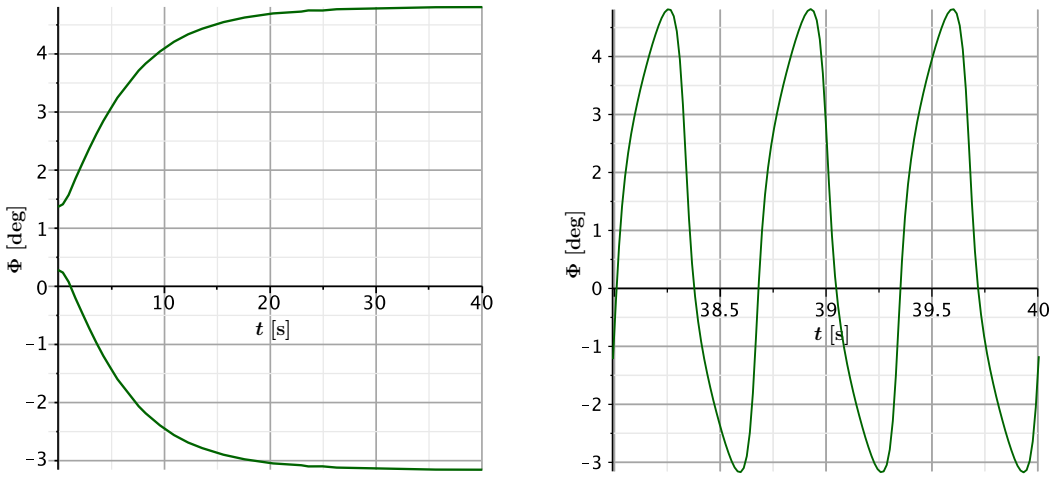

(a) The envelope of swinging motion

(b) The swinging motion of the robot in steady state condition

Figure 7.7: Fish swinging around its centre of mass

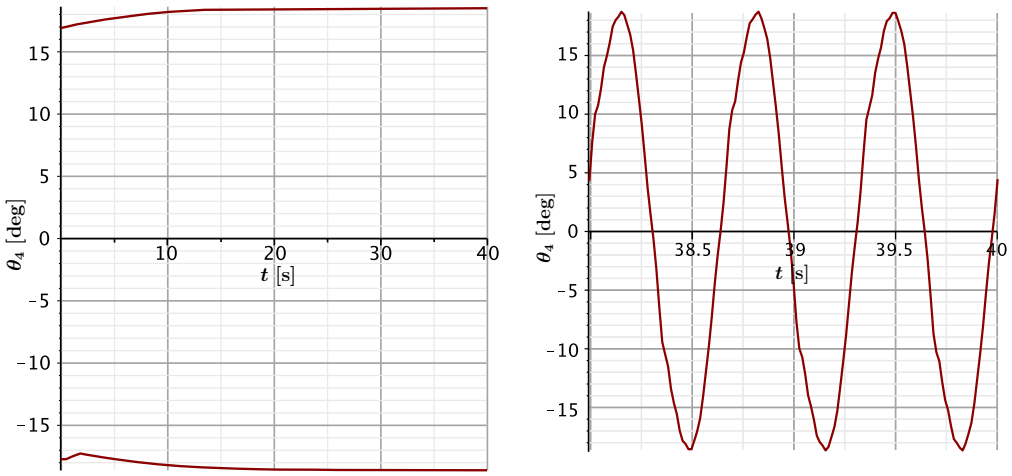

(a) The envelope of oscillation of the caudal fin (b) The periodic motion of the caudal fin in steady state condition

Figure 7.8: Caudal fin rotation around point F

7.2 Simulation of UC-Ika 2

On the contrary of UC-Ika 1, which has non-optimised parameters, UC-Ika 2 makes benefits of its optimised constant tail system[1]. The parameters of UC-Ika 2 after optimisation is presented in Table 7.3.

Similar to UC-Ika 1, for simulation of UC-Ika 2 the kinematic analysis of tail mechanism must be done. However, the main difference between the aforementioned robots is the relationship between the angular displacement of their links 1 and 3 revealed by λ ($= \theta_3/\theta_1$). λ in UC-Ika 1 is equal to 2.146 while it is equal to 2.130 for UC-Ika 2.

The simulation reveals that UC-Ika 2 passes nearly 13 m after 40 seconds (see Fig. 7.9). Despite Fig. 7.9 that shows linear motion of the robot, the trend line of the robot displacement is made of slight periodic motion.

The periodic motion of the robot in cruising could be better understood by considering the speed of the robot in this direction. Fig. 7.10 illustrates the envelope of forward speed and nearly steady state speed of the robot. As Fig. 7.10 shows, the robot has a cruising speed of 0.25 m/s while the forward speed is oscillating between 0.24 and 0.26 m/s. The robot also has a transient time of 35 seconds.

The simulation also shows that the robot has lateral periodic motion with an am-

[1]The optimisation process of UC-Ika 2 with its dynamic equations of motion is described in Chapter 5.

Table 7.3: Constant parameters of UC-Ika 2 after optimisation

Tail Mechanism	Distance between point M and O	$\overline{MO} = 0.077$ m
	Posterior part of link 1	$\overline{OC} = 0.180$ m
	Posterior part of link 3	$\overline{CF} = 0.069$ m
	Anterior part of caudal fin	$\overline{FG} = 0.030$ m
	Anterior part of link 1	$\overline{AO} = 0.030$ m
	Distance between point M and B	$\overline{OB} = 0.089$ m
	Length of link 2	$\overline{DE} = 0.228$ m
	Anterior part of link 2	$\overline{EC} = 0.026$ m
General	Mass	$M_0 = 7.426$ kg
	Mass moment of inertia	$I_0 = 0.667$ kgm^2
	Vertical semi-axis	$a = 0.100$ m
	Horizontal semi-axis	$b = 0.075$ m
	Tip to point M length	$L_0 = 0.273$ m
	Projected area along X	$S_x = 0.021$ m^2
	Projected area along Y	$S_y = 0.126$ m^2
Caudal Fin	Mass	$M_c = 0.120$ kg
	Mass moment of inertia	$I_c = 0.001$ kgm^2
	Span	$S = 0.372$ m
	Chord	$C_C = 0.024$ m
	Spring constant	$k = 12.191$ Nm/rad
DC Motor	Amplitude	$A = \pi/18$ rad
	Frequency	$f = 1.5$ Hz
Forces	Density of water	$\rho = 998$ kg/m^3
	Body drag along X	$C_{Dx} = 0.4$
	Body drag along Y	$C_{Dy} = 0.85$
	Body drag rotational Φ	$C_{Dp} = 0.85$

plitude of 0.015 m (see Fig. 7.11). Since in a complete cycle of undulation, the lateral forces generated by the undulatory motion of the robot cancel out each other, the lateral position of the robot does not change in cruising. However, an offset in the transient time exists. This offset is discussed in Sec. 7.3.

As expected from the lateral displacement of UC-Ika 2, it generates lateral forces

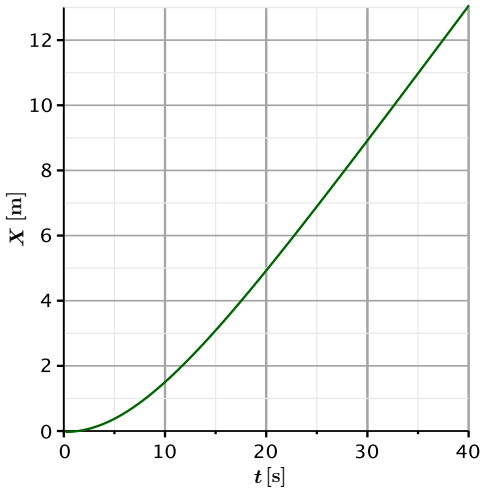

Figure 7.9: Translational motion of UC-Ika 2 along X Axis

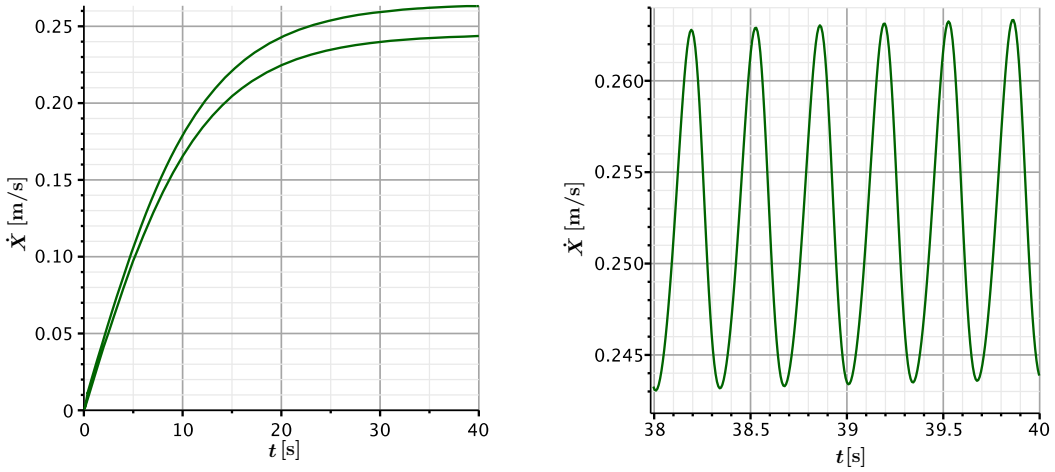

(a) The envelope of forward speed

(b) Crusing steady state speed

Figure 7.10: Speed of UC-Ika 2 along X Axis

which cancel out each other in each complete cycle which causes the lateral periodic speed of the robot with an average speed of zero (see Fig. 7.12). The lateral speed of the robot is oscillating between -0.10 and 0.10 m/s while its average in a complete cycle of undulation is zero.

The robot is also swinging about its centre of mass with a maximum angular displacement of 2.02° from its cruising axis (see Fig. 7.13). Similar to the lateral motion, the robot has an offset at the beginning of the motion. The offset of the angular

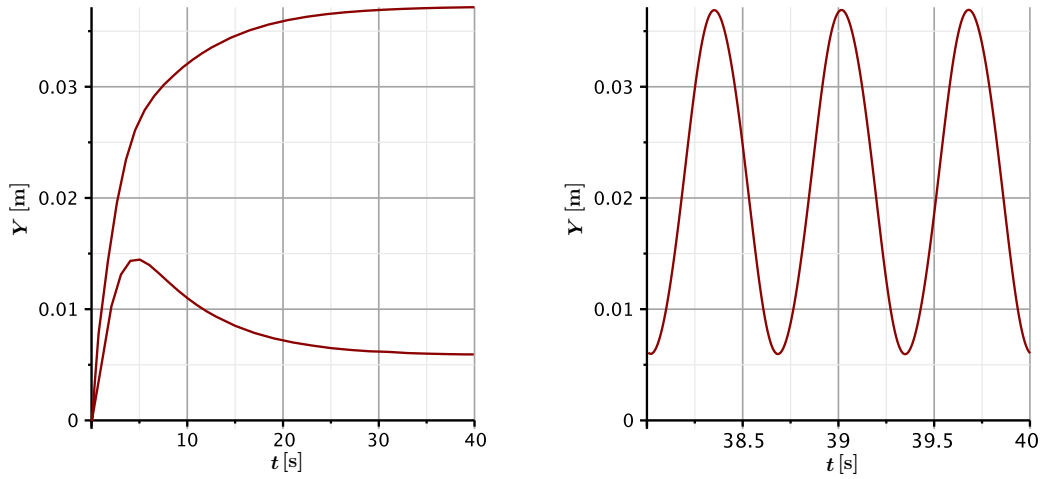

(a) The envelope of lateral motion (b) Lateral steady state motion

Figure 7.11: Translational motion of UC-Ika 2 along Y Axis

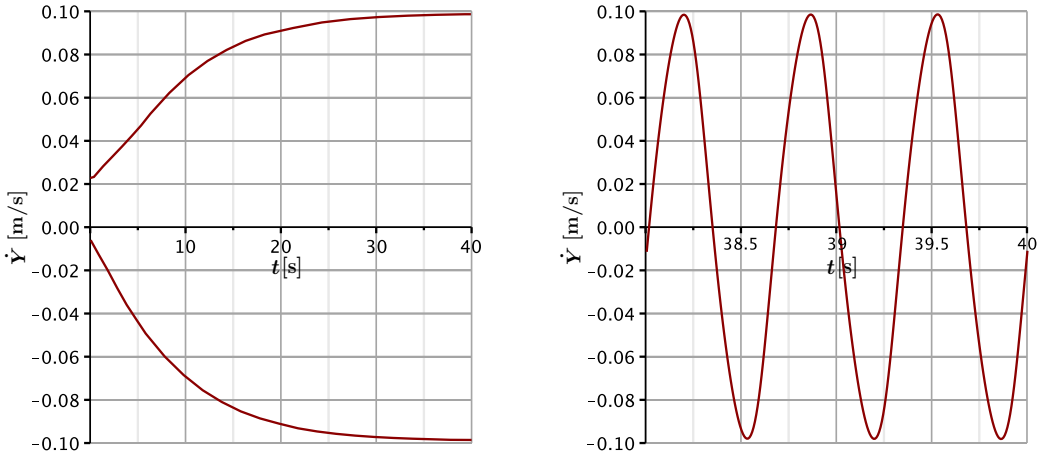

(a) The envelope of lateral speed (b) Lateral steady state speed

Figure 7.12: Speed of UC-Ika 2 along Y Axis

displacement has the same reason as the offset of the lateral displacement which is explained in Sec. 7.3.

In addition to the aforementioned results, Figure 7.14 illustrates that the caudal fin has a periodic motion of amplitude 23.60° which is an ideal amplitude angle of attack for optimal thrust production [Anderson et al., 1998].

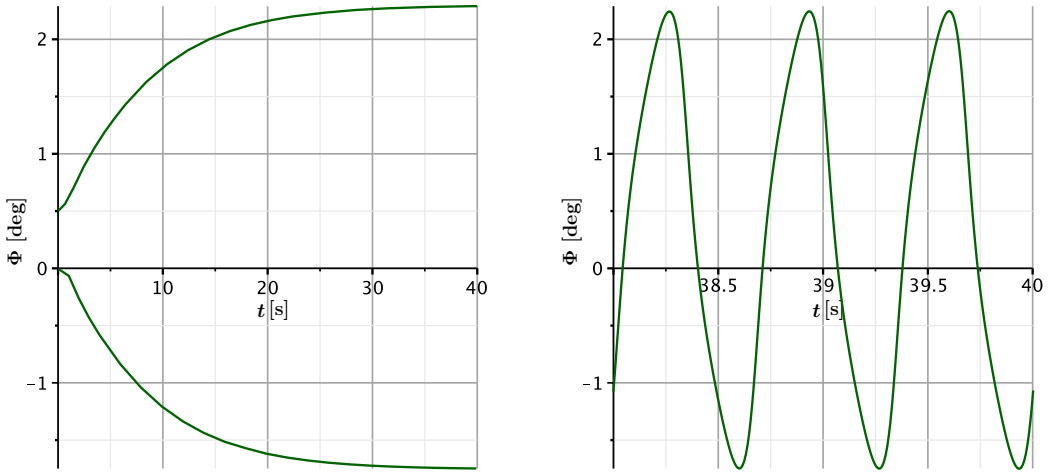

(a) The envelope of swinging motion

(b) The swinging motion of the robot in steady state condition

Figure 7.13: The swinging motion of UC-Ika 2 about its centre of mass

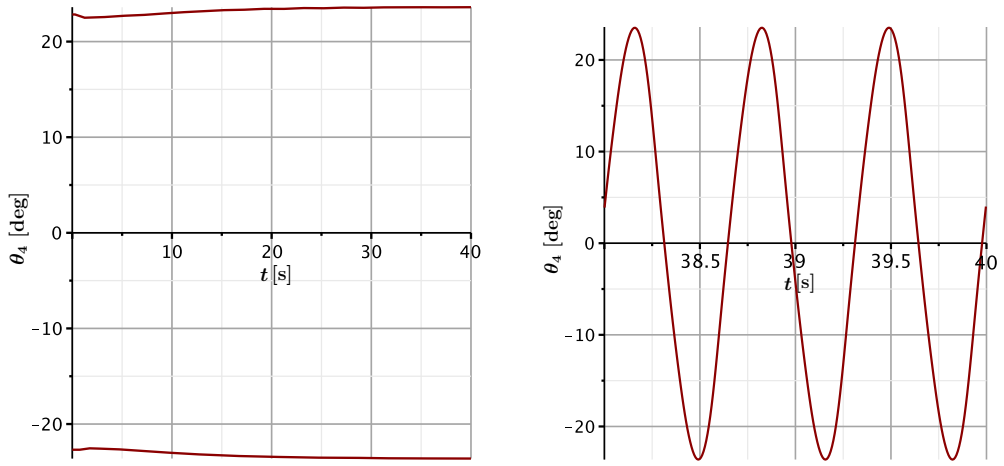

(a) The envelope of oscillation of the caudal fin

(b) The periodic motion of the caudal fin in steady state condition

Figure 7.14: Caudal fin rotation around point F

7.3 Discussion

The simulation reveals the similarities in the dynamic behaviour of both robots in cruising mode since both of them employ similar swimming mechanism in cruising. After nearly 30 seconds, both robots will go through steady state motion. The translational

and angular displacement of the robot and its caudal fin have oscillatory motion which roots in the periodic characteristics of the hydrodynamic forces generated by the robots. However, all types of motion except cruising motion of the fish is oscillating about zero but with an offset in lateral and angular displacements of the robot. For instance, the angular displacement of UC-Ika 2 is oscillating between -1.75 and 2.29. which means that the robot has 0.27 offset.

The offset is due to the difference between the propulsive and resistive forces. The propulsive forces are made by the caudal fin, while the resistive forces are assumed to be generated in the centre of mass. When the robot is not swimming, the centre of mass is not moving too and accordingly the resistive forces are zero. On the other hand, the propulsive forces are assumed to be generated at the caudal fin. It means even if the fish is not swimming, the motion of the caudal fin generates propulsive forces. Accordingly, at the beginning of the motion where the robot is stationary and drag are equal to zero, there is a positive angular motion which remains as an offset in the lateral and angular displacements of the robots.

In addition to the similarities of the robots, the simulation confirms the optimised swimming behaviour of UC-Ika 2 after applying optimisation algorithm described in Chapter 6 in comparison to the dynamic performance of UC-Ika 1 that uses non-optimised constant parameters. This optimised behaviour is verified by optimal swimming factors including Froude efficiency and Strouhal number explained in Chapters 2 and 6.

Considering expressions (6.8) and (6.9), Froude efficiency of both robots are calculated. In cruising mode of UC-Ika 1, $\overline{\dot{x}} = 0.29$ m/s, $\overline{F_{Cx}} = 0.77$ N, $\overline{\dot{y}} = 0.09$ m/s and $\overline{F_{Cy}} = 1.12$ N. Substituting these values into the following expression, the efficiency of UC-Ika 1 is obtained as

$$\eta = \frac{\overline{F_{Cx}}\ \overline{\dot{x}}}{\overline{F_{Cx}}\ \overline{\dot{x}} + \overline{F_{Cy}}\ \overline{\dot{y}}} = \frac{(0.77)\,(0.29)}{(0.77)\,(0.29) + (1.12)\,(0.06)} = 0.70 \tag{7.1}$$

whereas the cruising parameters of UC-Ika 2 are $\overline{\dot{x}} = 0.25$ m/s, $\overline{F_{Cx}} = 0.79$ N, $\overline{\dot{y}} = 0.06$ m/s and $\overline{F_{Cy}} = 0.72$ N which yields the efficiency of 83%.

Besides Froude efficiency, Strouhal number of the robots (see expression (6.10)) also shows the optimality of swimming of UC-Ika 2 in comparison with UC-Ika 1. With a heave of 0.07 m and cruising speed of 0.29 m/s, Strouhal number of UC-Ika 1 is equal to 0.72. Whereas UC-Ika 2 has an optimal Strouhal number of 0.33 which is obtained with the cruising velocity of 0.25 m/s and heave of 0.04 m. As it can be seen, only UC-Ika 2 has optimal Strouhal number since it is between $0.25 - 0.40$ which is an optimal range

for swimming fishes [Anderson et al., 1998].

7.4 Conclusion

In order to analyse the cruising motion of UC-Ika 1 & 2, their dynamic performance is simulated. To do so, the equations of motion of them, (5.20), obtained in Chapter 5 are employed. The constant parameters of each robot, given in Table 7.2 and 7.3, are substituted into the equations. The constant parameters of UC-Ika 1 are experimentally obtained while the constant parameters of UC-Ika 2 is obtained using the optimisation method introduced in Chapter 6. The equations are then solved numerically using Rung-Kutta Fehlberg method.

In terms of UC-Ika 1, the simulation shows the gradual increase of the lateral motion of the tail towards the end of the tail. The robot has the maximum heave of 0.07 m at the end of the caudal fin, shown in Fig. 7.15, provided that the rotation of link 3 is 2.146 times of that of link 1. The model also reveals an average cruising speed of 0.29 m/s where the maximum lateral speed of the robot is equal to 0.15 m/s. The robot is also swinging around its centre of mass, point M, with a maximum of 3.98°. The caudal fin is oscillating around its pivot point F with a maximum of 18.70°, See Fig. 7.15.

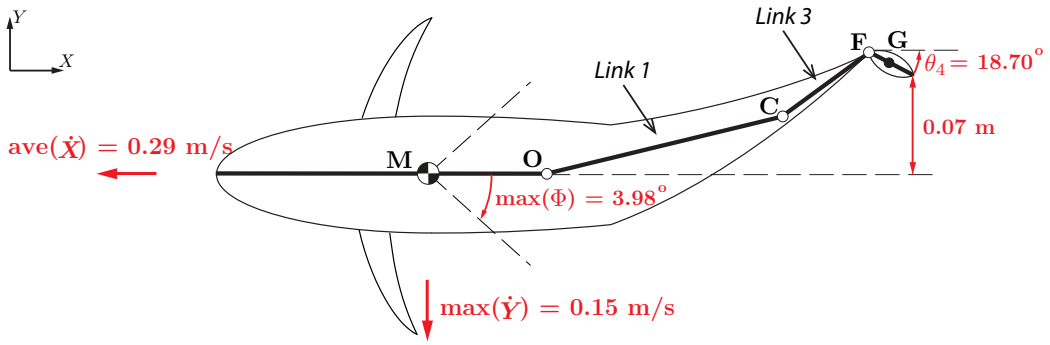

Figure 7.15: Dynamic sketch of UC-Ika 1

In terms of UC-Ika 2, the simulation shows the gradual increase of the lateral motion of the tail towards the end of the tail. The robot has the maximum heave of 0.04 m at the end of the caudal fin, shown in Fig. 7.16, provided that the rotation of link 3 is 2.146 times of that of link 1. The model also reveals an average cruising speed of 0.25 m/s where the maximum lateral speed of the robot is equal to 0.10 m/s. The robot is also swinging around its centre of mass, point M, with a maximum of 2.02°.

The caudal fin is oscillating around its pivot point F with a maximum of 23.60°, See Fig. 7.16.

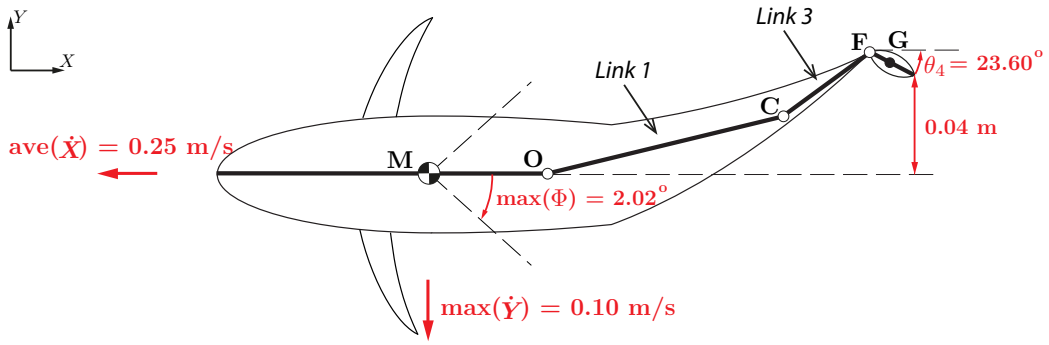

Figure 7.16: Dynamic sketch of UC-Ika 2

The superior performance of UC-Ika 2 in comparison to UC-Ika 1 is also confirmed with the simulation results. Calculating Froude efficiency and Strouhal number shows that UC-Ika 2 with cruising efficiency of 83% and Strouhal number of 0.33 has better swimming performance than UC-Ika 1 with Froude efficiency of 70% and Strouhal number of 0.72 since UC-Ika 2 has higher efficiency and its Strouhal number is within the optimal range of $0.25 - 0.40$.

Chapter 8

Fabrication and Experimental Analysis

One of the main steps of developing biomimetic swimming robots is the fabrication step. In this step, several issues are to be dealt with. Primarily, the fish-mimicking robots have intricate shapes to meet the optimal performance of fishes. This shape cannot be simply made by the conventional machining tools.

Besides, the swimming robots have rigid and flexible parts. The latter must be flexible enough to not demand additional motor torque during bending. Simultaneously, the flexible part has to be stiff enough to stand the pressure of water column.

Moreover, similar to the other underwater robots, the fish robots have waterproofing issues which is more challenging since the electronics and actuation mechanisms inside the body of the robot need to be accessible.

The last issue returns to the underwater communication problem. An underwater robot cannot be remotely controlled without an antenna that is come out of the aquatic environment whereas the antenna affects the hydrodynamic behaviour of the robot under water.

The aforementioned issues are addressed in the fabrication of both UC-Ika 1 & 2. In this chapter, the fabrication process of the robots are described in Sec. 8.1. Moreover, the swimming performance of the robots after their examination is analysed in Sec. 8.2. This chapter is then concluded in Sec. 8.3.

8.1 Fabrication

8.1.1 Fused Deposition Modelling

In order to build the intricate shapes, a rapid prototyping method called Fused Deposition Modelling (FDM) is applied. FDM is a 3D-printing technology directly using the CAD model. Then the design is fabricated layer by layer using two different melted materials as the base and support materials. The base material, Acrylnitril-Butadien-Styrol-Copolymerisat (ABS), is in fact the actual material of the fabrication. After 3D-printing, the support material is resolved and removed from the part in a 70°C hot alkaline bath [Chua et al., 2010].

FDM method is employed for fabrication of complicated rigid parts including the outer surface of the main bodies of both UC-Ika 1 & 2[1]. Figure 8.1 shows the main body of UC-Ika 2 in 3D printer.

(a) The main body of UC-Ika 2 in 3D printing machine

(b) Dissolving support material in alkaline bath (the main body of UC-Ika 1)

Figure 8.1: Applying FDM method for fabrication of the complicated shape of rigid parts of both robots.

[1]The moulds for the flexible parts, explained in Sec. 8.1.2, of both robots are also built with FDM method

8.1.2 Fabrication of Flexible Part

In order to build the flexible parts, Polydimethylsiloxane (PDMS) silicone Sylgard 184 is selected. This silicone is durable, tensile and resistant against water and most solvents [syl, 2013]. The silicone is made up of two components including base and curing agent. These two components need to be combined and poured into a mould. The solidifying of the tail takes approximately 72 hours.

This method of fabrication is applied for fabrication of the tail peduncle of both robots. Figure 8.2 shows casting of the tail peduncle of both robots.

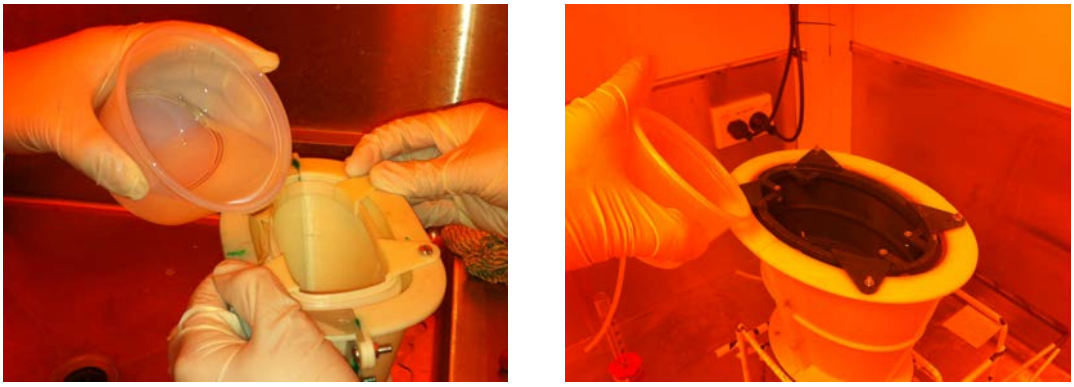

(a) UC-Ika 1 (b) UC-Ika 2

Figure 8.2: Casting of the tail peduncles of both fish robots

Fabrication of the pectoral fins of UC-Ika 2 is slightly different since its ribs (shown in Fig. 8.3) is rigid and PDMS is around it. Accordingly, a mould including the ribs is made with FDM method and then the silicone is poured into the mould which cover the ribs. When the silicone is solidified, the ribs are detached from the mould and left inside the silicone. Note that the main rib is made from aluminium and is not attached to the mould.

8.1.3 Fabrication of the Actuation Mechanisms

The actuation mechanisms of both robots and pectoral fins of first robot are fabricated with commonly known fabrication machines. The materials used in the actuation mechanisms are steel and aluminium.

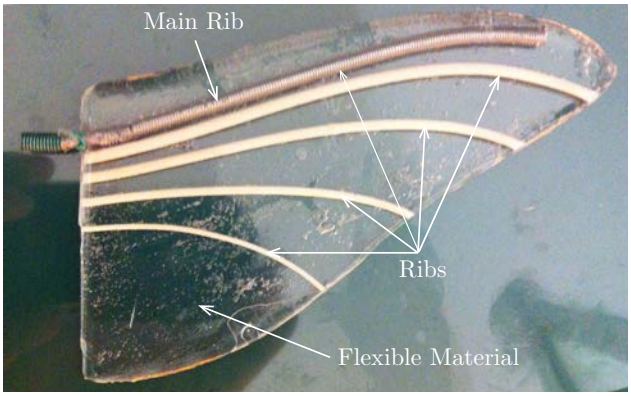

Figure 8.3: The pectoral fin of UC-Ika 2.

8.1.3.1 Cruising Actuation Mechanism

The tail mechanism of both robots have similar kinematic principles; however, the tail mechanism of UC-Ika 2 is optimised. The first tail mechanism shown in Fig. 8.4 is made up of both steel and aluminium while the second tail mechanism is mainly from aluminium to decrease its weight and, thus, its mass moment of inertia[1]. The caudal fin of UC-Ika 1 is made of polumethyl-methacrylat (perspex) sheet while the caudal fin of the second robot is made from ply wood that is filed and polished to have streamlined shape.

8.1.3.2 Manoeuvring Actuation Mechanism

The actuation mechanism of pectoral fins of UC-Ika 2, shown in Fig. 8.5, is fabricated using steel. Instead of aluminium, steel is employed in order to increase the weight of the robot and also decrease the friction when two surfaces of steel are in contact with each other during motion. In fabrication of actuation system one micro-switch is employed for synchronization of the flapping motion of the pectoral fins together since the pectoral fins use two separate motors.

8.1.3.3 Buoyancy Control System

For fabrication of buoyancy control system of UC-Ika 2, a syringe as a cylinder of holding water is employed where its shaft is actuated by a DC motor. The mechanism of buoyancy control system converts the rotational motion of the motor to translational

[1]The tail mechanism with high mass moment of inertia increases the swinging motion of the robot which is not ideal for an efficient cruising.

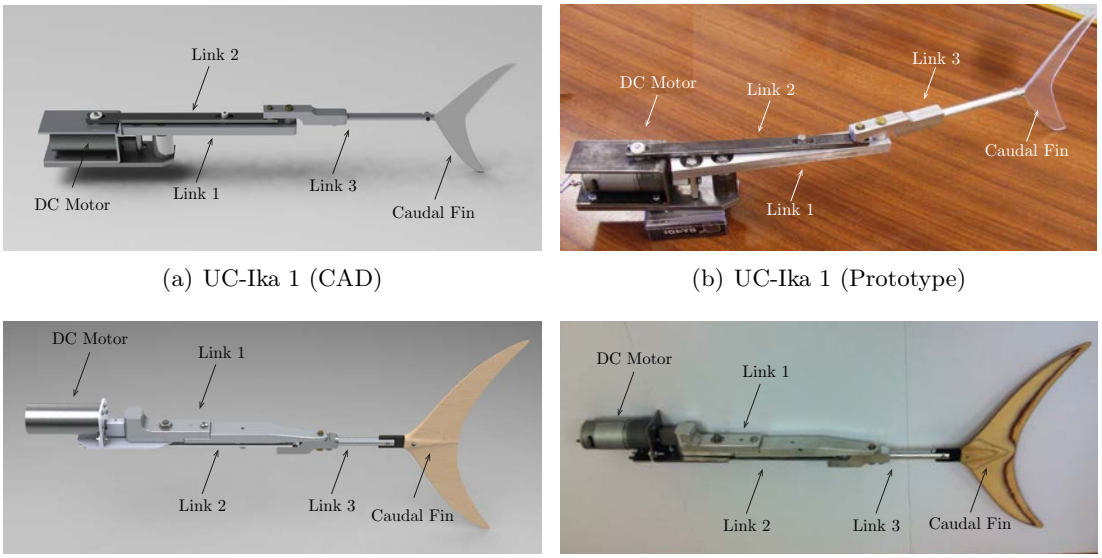

(a) UC-Ika 1 (CAD)

(b) UC-Ika 1 (Prototype)

(c) UC-Ika 2 (CAD)

(d) UC-Ika 2 (Prototype)

Figure 8.4: The tail mechanism of both fish robots

motion of the shaft of syringe. To ensure that the cylinder is filled with or drained from water, two limit switches are used in the path of the piston of the cylinder. Figure 8.6 illustrates the buoyancy control system.

8.1.4 Waterproofing

Besides tight connections of the caudal fin and the tail peduncle, and also the tail peduncle and the main body with a pretension in the tail peduncle, the body is coated with epoxy resin to avoid passing of water through the body over time as it is slightly porous (see Fig. 8.7). Moreover, the caudal fin in UC-Ika 2 which is made from ply wood is coated with polyurethane to ensure its water resistance without degrading its flexibility.

8.1.5 Communication

To solve the communication problem underwater, a microcontroller is employed. For UC-Ika 1, an open loop controller is designed and coded into an Arduino Uno microcontroller to control 12V DC gear head motor of the fish. This controller could communicate with any Bluetooth device like computers and smartphones using a Bluetooth connector. In UC-Ika 2, the microcontroller controls four 12V DC motors and

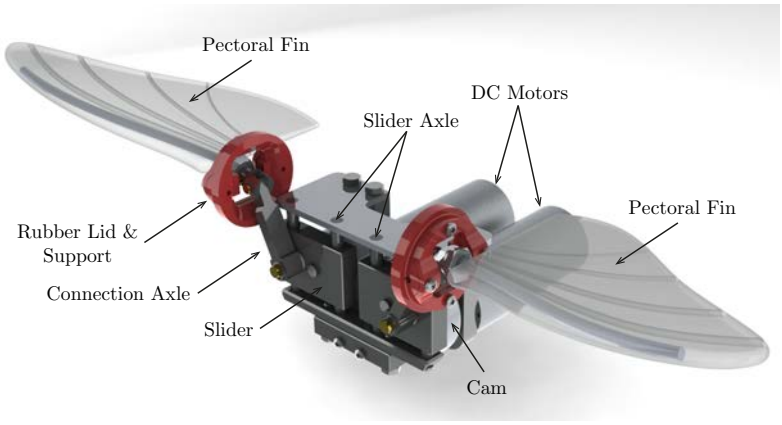

(a) CAD Model

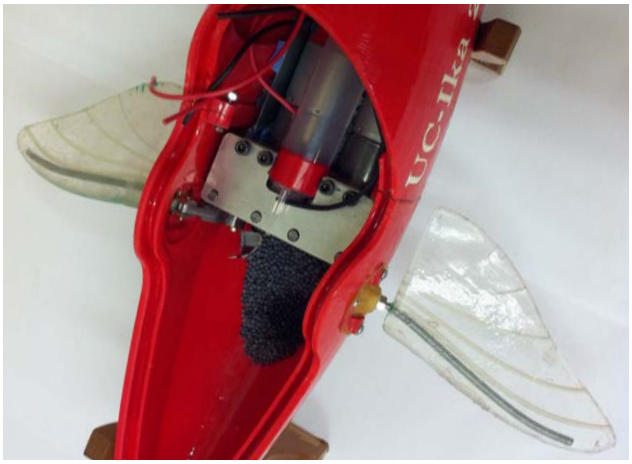

(b) Prototype

Figure 8.5: The pectoral fin actuation mechanism of UC-Ika 2

three limit switches. The codes of both microcontrollers is presented in Appendix A.

8.1.6 Assembly

Besides the actuation mechanisms and electronics parts including batteries, microcontroller, motor shields and Bluetooth device, several pieces of lead and steel as well as lead shots are provided to compensate the difference between the buoyancy and the weight of the robots calculated during the design. The difference is worse in UC-Ika 2 where 2.42 kg is needed to have a neutral buoyant robot. UC-Ika 1 & 2 after complete assembly are shown in Fig. 8.8.

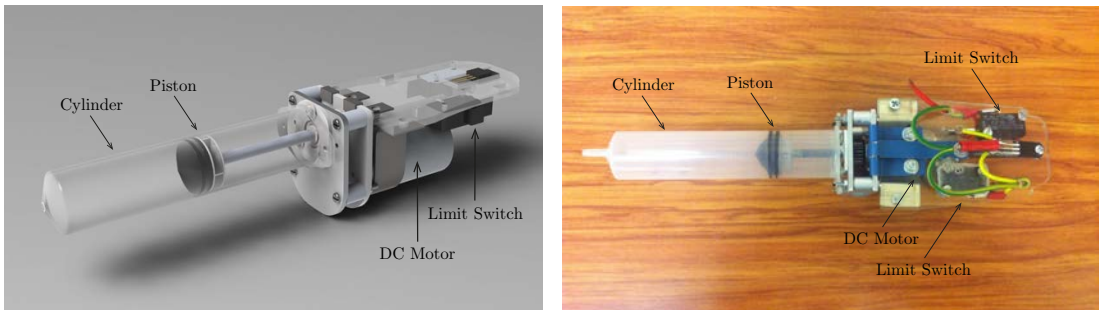

(a) CAD Model (b) Prototype

Figure 8.6: The buoyancy control system of UC-Ika 2

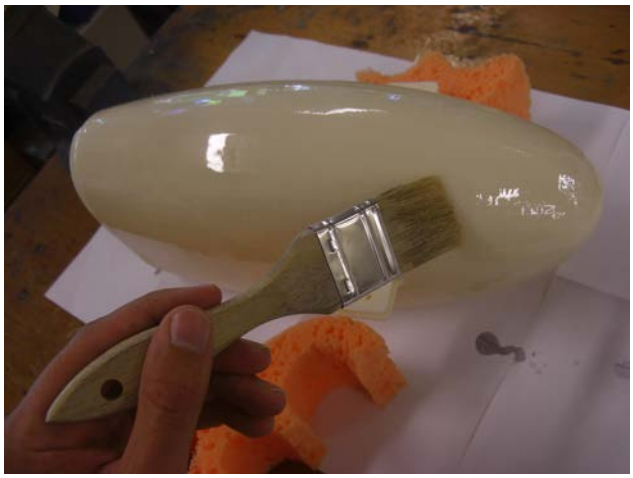

Figure 8.7: Painting of the main body of UC-Ika 1 with epoxy resin.

8.2 Experimental Analysis

8.2.1 Swimming Performance of UC-Ika 1

UC-Ika 1 is a single gaited robot and is only capable of cruising motion with its tail peduncle and caudal fin. When the caudal fin changes its direction at its maximum heave, larger vortices are created which assures a faster performance of the robot. In order to confirm this theory, UC-Ika 1 is tested with two different tail designs: with a fixed joint of the caudal fin shown in Fig. 8.9(a) and a flexible one presented in Fig. 8.9(b). For a fixed joint, the caudal fin has the same orientation of the tail peduncle, while the flexible joint, made by a piece of rubber, causes the caudal fin to change its direction at its maximum heave.

Multiple tests for both aforementioned caudal fin designs are performed in a water

(a) UC-Ika 1

(b) UC-Ika 2

Figure 8.8: The fish robots after assembly.

tank of 4 m length. Table 8.1 shows the result for each test.

The results reveal a cruising speed of 0.21 m/s and 0.29 m/s for UC-Ika 1 with fixed and flexible joints, respectively[1]. Fish speeds are commonly measured and compared

[1]The results obtained from several tests of the robot is completed by the motion analysis of the video of cruising motion of UC-Ika 1.

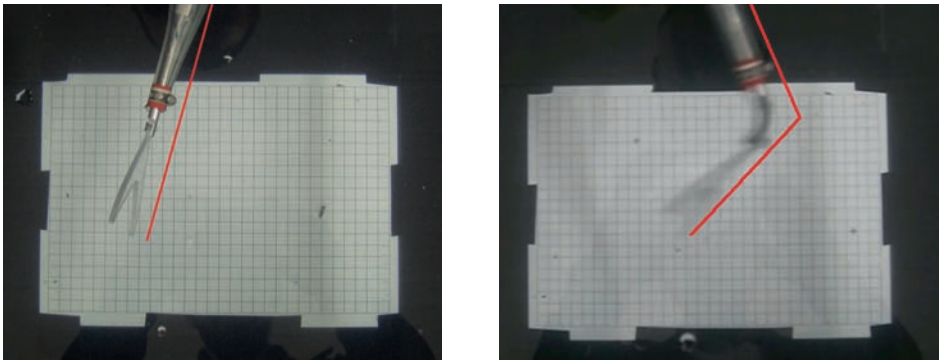

(a) Fixed Joint (b) Flexible Joint

Figure 8.9: Connections of the caudal fin to the tail peduncle

Table 8.1: Time to swim 1.5 meter by the fish robot

Test	**Swimming Time (s)**	
	Fixed Joint	Flexible Joint
1	7.0	4.7
2	6.8	5.5
3	7.4	5.5
4	6.8	5.0
5	7.0	5.2

with respect to their body lengths. Accordingly, the speed of UC-Ika 1 is 0.33 body lengths per second (BL/s) for the fixed joint and 0.44 BL/s for the flexible design.

The optimality of the robot swimming with the flexible joint is also investigated through Strouhal number and Froude efficiency. In order to calculate these two quantities, swimming parameters of UC-Ika 1 are primarily obtained from the experiment. Those parameters are shown in Table 8.2.

It should be noted that $\overline{F_{Cx}}$ and $\overline{F_{Cy}}$ used in Froude efficiency must be obtained when the robot is in cruising. In cruising mode, the average of the propulsive forces are equal to the average of the resistive forces. Accordingly, $\overline{F_{Dx}}$ and $\overline{F_{Dy}}$ are calculated with speed of the robot in cruising mode and replaced $\overline{F_{Cx}}$ and $\overline{F_{Cy}}$[1].

Substituting f, h and $\overline{\dot{x}}$ into (6.10) yields $St = 0.72$. This value of St demonstrates that the vortices produced by the fish robot are not completely ideal. However, Froude efficiency of UC-Ika 1 is approximately high. Substituting the values of $\overline{F_{Cx}}$, $\overline{F_{Cy}}$, $\overline{\dot{x}}$ and $\overline{\dot{y}}$ into (6.8) and (6.9), Froude efficiency of the fish robot is obtained to be equal to

[1]For instance, considering 5.11, $\overline{F_{Cx}} = \overline{F_{Dy}} = (1/2)\ C_{Dx}\,\rho\,S_x\,\overline{\dot{x}}^2 = 0.23N$

Table 8.2: Swimming Parameters of UC-Ika 1

Parameter	Value
Undulation frequency	$f = 1.5$ Hz
Heave	$h = 0.07$ m
Mean forward velocity	$\overline{\dot{x}} = 0.29$ m/s
Mean lateral velocity	$\overline{\dot{y}} = 0.07$ m/s
Mean thrust	$\overline{F_{Cx}} = 0.23$ N
Mean lateral force	$\overline{F_{Cy}} = 0.26$ N

78%.

8.2.2 Swimming Performance of UC-Ika 2

In order to analyse the swimming performance of UC-Ika 2, it is tested in a 5×15 m^2 pool. A motion analysis software is also employed to make the graphs of motion in order to compare with the simulation results. UC-Ika 2 is able to cruise and turn. In cruising mode, only the tail peduncle and the caudal fin are undulating while the pectoral fins are stationary. The graph, shown in Fig. 8.10, reveals that the robot is swimming linearly in time with a slope of 0.246 which is the average cruising speed of UC-Ika 2. This curve matches the simulation results shown in Fig. 7.9 of Chapter 7.

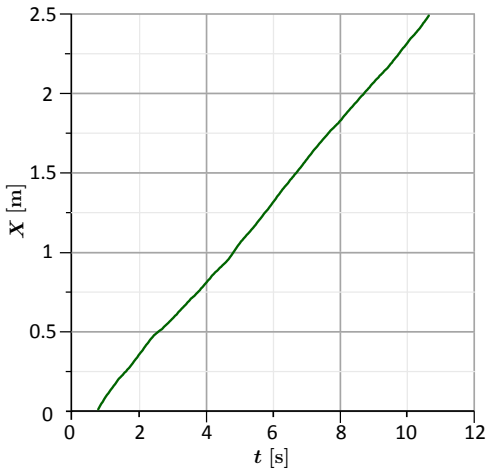

Figure 8.10: Translational motion of UC-Ika 2 along X Axis

Regarding cruising speed of the robot it must be mentioned that the can be speed

analysis of the robot shows that it has periodic motion (see Fig. 8.11) similar to what is shown in Fig. 7.10 obtained from simulation.

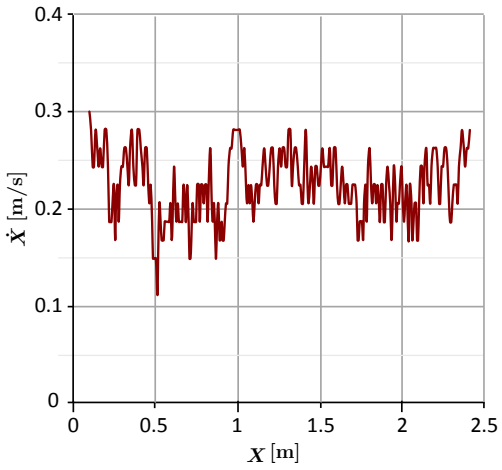

Figure 8.11: Periodic speed of UC-Ika 2 along X Axis

Similar to UC-Ika 1, the swimming parameters of UC-Ika 2 are obtained given in Table 8.3.

Table 8.3: Swimming Parameters of UC-Ika 2

Parameter	**Value**
Undulation frequency	$f = 1.5$ Hz
Heave	$h = 0.04$ m
Mean forward velocity	$\overline{\dot{x}} = 0.25$ m/s
Mean lateral velocity	$\overline{\dot{y}} = 0.04$ m/s
Mean thrust	$\overline{F_{Cx}} = 0.25$ N
Mean lateral force	$\overline{F_{Cy}} = 0.17$ N

Through these results Froude efficiency and Strouhal number of the robot are calculated. UC-Ika 2 has an efficiency of 89% and Strouhal number of 0.37. These values of efficiency and Strouhal number not only validate the mathematical model introduced in Chapter 8, they validate that the fabrication of the robot with the optimised parameters introduced in Chapter 6 has made UC-Ika 2 as an efficient robot in cruising.

Besides cruising, UC-Ika 2 is also able to turn by its flapping pectoral fins similar to the flapping fins of bird-wrasses (see Fig. 4.6) while its tail peduncle and caudal fin

are stationary. The motion analysis of the pectoral fins show the path of the fin in flapping, see Fig. 8.12

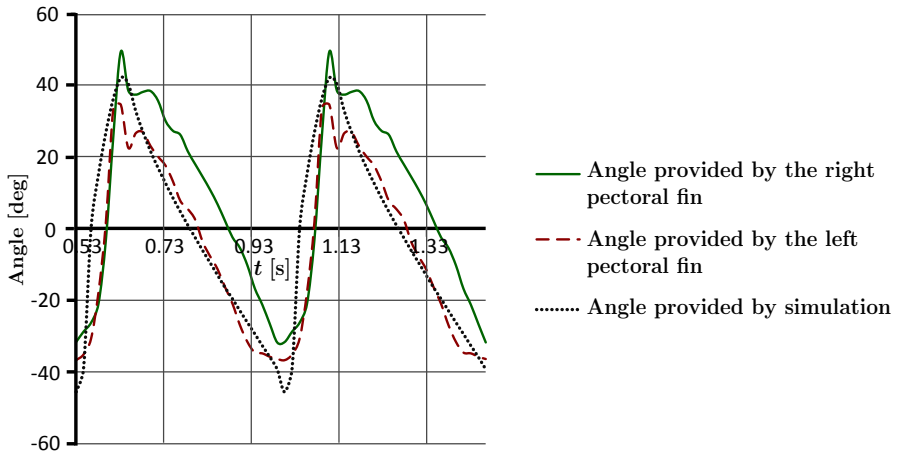

Figure 8.12: The flapping path of the pectoral fins in comparison with the simulation result

The turning motion of the robot in both directions is also tested. In order to turn left, the right pectoral fin of UC-Ika 2 flaps while its left pectoral fin is stationary, and vice versa. The test shows that the robot is able to turn left with a speed of 2.47 deg/s (at the beginning of the motion) and turn right with a speed of 5.24 deg/s. In other words, in swimming to the left, the robot needs to go forward for 2.36 m with its right pectoral fin in order to have the lateral motion 0.97 m in 9 s. Similarly, in swimming to the right, the robot needs to go forward for 0.97 m with its left pectoral fin in order to have the lateral motion 0.59 m in 6 s. The difference between the speed of turning towards left and right directions is due to the different thickness of the left and right fins caused in the fabrication process. The thickness of fins determines their flexibility which plays an essential role in their thrust generation[1].

The mechanism for up-down motion is also tested. The mechanism which consists of a DC motor, a gear box system and a syringe is primarily dry-tested to find out the appropriate gear box ratio and motor voltage. As Fig. 8.13 shows, the speed of filling the syringe depends on two elements: the speed of motor and the ratio of gear box.

During the experiment, the voltage of the motor is set to be 4.0 V. Using this voltage, in a speed of 1000 rpm and gear box ratio of 1.0, the syringe could be filled

[1]This speed is obtained when the caudal fin and the tail peduncle do not have any inclination and are parallel to the axis of the main body. Otherwise, if the tail steers the motion, the speed of turning goes up.

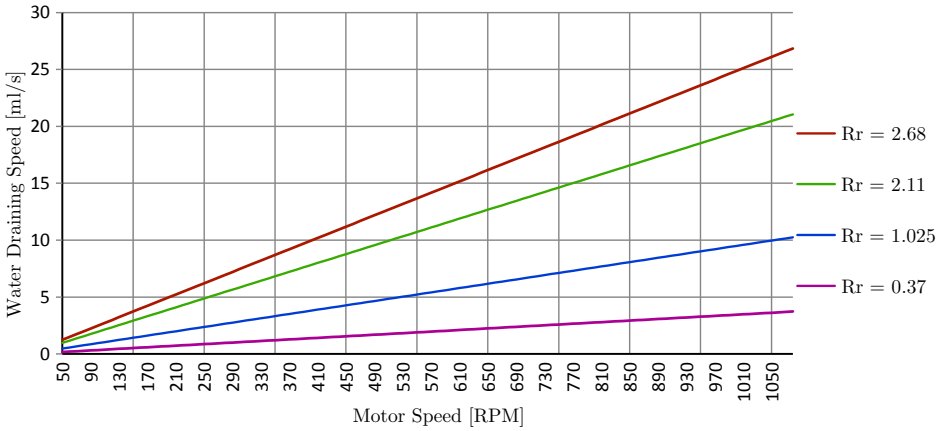

Figure 8.13: The filling speed of syringe with water

with 10 ml/s, see Fig. 8.13. This speed provide sufficient time for robot end-user to control its depth. The mechanism is shown in Fig. 8.14.

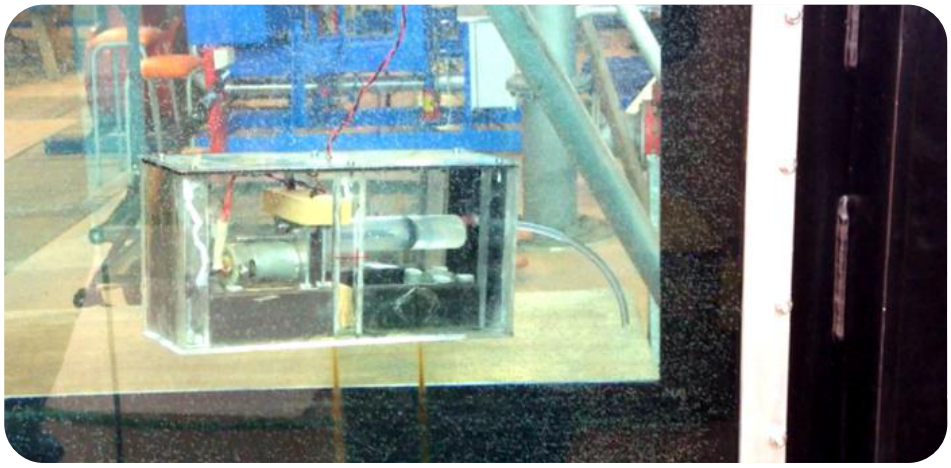

Figure 8.14: The buoyancy control mechanism during the experiment

8.3 Conclusion

The fabrication of biomimetic swimming robots are challenging due to their intricate body shape, flexible parts, waterproofing and communication issues. To address these problems, FDM method as a 3D printing technology is employed for rigid parts of both fish robots. PDMS material is also chosen for fabrication of flexible parts including the tail peduncles and the pectoral fins as PDMS is a durable, tensile and resistant against

water. For waterproofing issue, epoxy resin for coating the main body is employed while the connections of the parts are with a slight pretension to assure that the robot is completely sealed. For communication, a microcontroller for each robot is used to control the motors and the limit switches. By means of any Bluetooth device like smart phones, this microcontroller and, thus, the robot are controlled.

After fabrication and assembly of the robots, their swimming performances are practically tested. UC-Ika 1 & 2 have cruising speed of 0.29 and 0.25 m/s, respectively. Moreover, the experiment validates the optimised swimming performance of UC-Ika 2 with an efficiency of 89% and Strouhal number of 0.37 in comparison to UC-Ika 1 whose efficiency is 78% and its Strouhal number is 0.72. Besides cruising, manoeuvring capability of UC-Ika 2 is tested that shows it could turn in both directions using only the pectoral fins but with different turning speed. In turning left, the robot has a speed of 2.47 deg/s while in the other direction it has a speed of 5.24 deg/s.

Chapter 9

Conclusion

9.1 Summary

This thesis presents a method of developing multiple-gaited fish robots. The accomplishment of this method engages the improvement of all development steps of fish robots including design, mathematical modelling, optimisation and fabrication. As an outcome of the project, two prototypes of fish robots called UC-Ika 1 & 2 are developed.

UC-Ika 2 is designed for two gaits of swimming - cruising and manoeuvring - while it is capable of up-down motion. The cruising motion of the robot must be highly efficient to save energy of swimming. Prior to developing UC-Ika 2, UC-Ika 1 is also designed and fabricated adapted only for cruising gait of motion. The fabrication of this robot is to prove the functionality of the conceptual design for cruising gait of motion of UC-Ika 2. The development procedure of both versions of UC-Ika are shown in Fig. 9.1

In this chapter, the development process of fish robots are summarised (Sec. 9.1); however, the main contributions of this development process is highlighted in Sec. 9.2. In Sec. 9.3, the future tasks to further improve the aforementioned development process of biomimetic swimming robots are explained.

9.1.1 Design

Aquatic swimming species are specialised for a limited number of swimming gait. Their specialities root in the hydrodynamic and biological aspect of their motion. These aspects are taken into account for the design of UC-Ika 1 which is a tuna-mimetic robot and suitable only for cruising gait. From biology point of view, tuna fishes have

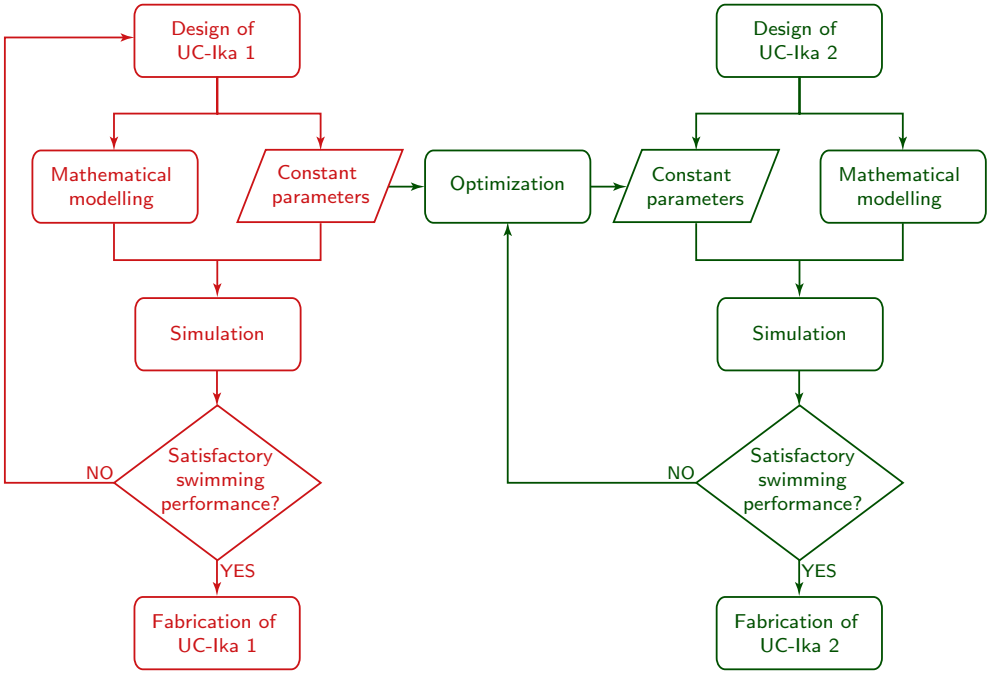

Figure 9.1: The flowchart showing the development process of UC-Ika 1 and 2.

streamlined body shape with narrow tail peduncle and high aspect ratio caudal fin[1]. Tuna fishes swim through the very last part of their tail peduncle and their roughly rigid caudal fin. From hydrodynamics point of view, tuna fishes employ vorticity method. In this method, tuna fishes take their caudal fin through a travelling wave made by the last part of their tail. During each wavelength, the tail peduncle and caudal fin generate two lift forces inclined laterally. The net forces of these two forces propel the fish forward. The CAD design of UC-Ika 1 is shown in Fig. 9.2.

As specialised for cruising gait, UC-Ika 1 is an appropriate robot for long-distance missions. Nevertheless, an underwater robot needs to have multiple gaits of swimming such as cruising, slow swimming and hovering to accomplish marine tasks which are comprised of exploring both long-distance and confined spaces. Accordingly, UC-Ika 2 is designed to have multiple gaits of swimming which submit sufficient cruising and manoeuvrability capabilities.

In order to improve the manoeuvrability skills of UC-Ika 1, UC-Ika 2 is designed to have swimming gaits of bird-wrasse as well as tuna. Bird-wrasses are well-known manoeuvrable fishes. Biologically speaking, bird-wrasses have streamlined body with deep

[1]Large span and short chord

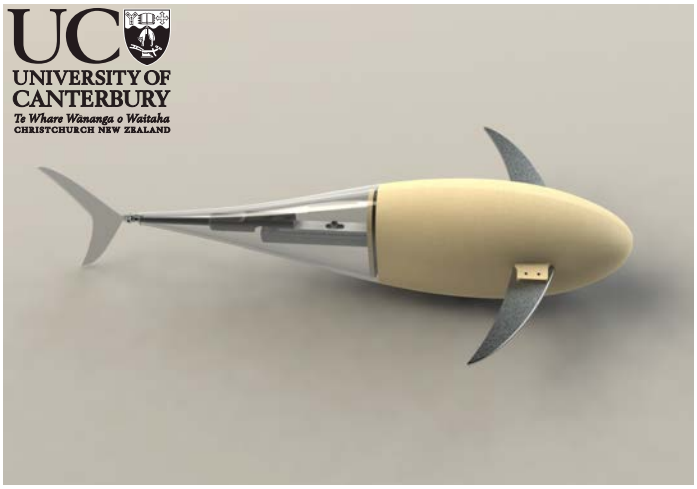

Figure 9.2: CAD Design of UC-Ika 1

tail peduncle and swim through their narrow and flexible pectoral fins. From hydrodynamics perspective, bird-wrasses employ lift-based forces. This method resembles the flapping motion of bird wings in the air. In each flapping cycle, the lift forces produced by pectoral fins of bird-wrasses have two components which are inclined laterally. The lateral components cancel out each other per cycle. The straight components of the lift forces push the fish forward in the water.

Taking biology and hydrodynamics aspects of both tuna and bird-wrasse, UC-Ika 2, shown in Fig. 9.3, has streamlined body shape with narrow tail peduncle similar to tunas but thinner like bird-wrasses. The robot has rather stiff caudal fin with high aspect ratio like a tuna and flexible narrow pectoral fins shape similar to bird-wrasse's pectoral fins. In cruising gait of swimming, the tail peduncle and the caudal fin of UC-Ika 2 are able to undulate and propel the robot forward. For manoeuvrability purposes like slow swimming and turning, the pectoral fins flap and the tail is held straight. For undulatory motion of the tail and the caudal fin, and flapping motion of pectoral fins, the most appropriate actuation systems are designed.

9.1.2 Mathematical Modelling

After mechanical design of the fish robots, the cruising gait of both fish robot is mathematically modelled. Since both robots have similar cruising mechanism, one dynamic model is derived for them. Initially, the tail actuation mechanism is kinematically analysed and the relationship between different links of the tail mechanism is determined.

Then hydrodynamic forces acting on the caudal fin is derived. The model adopts

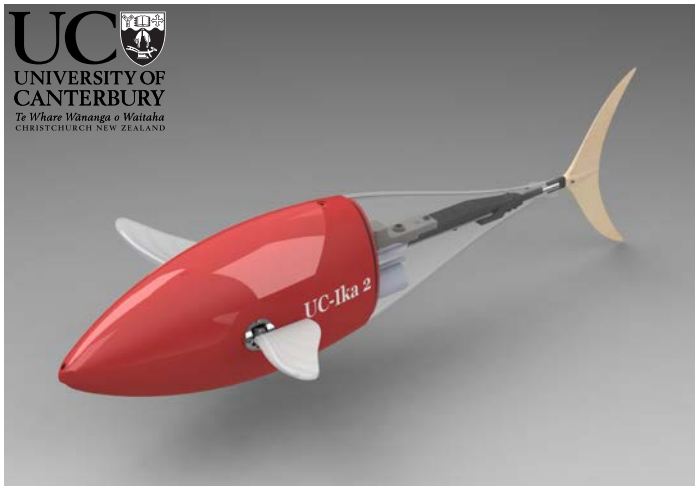

Figure 9.3: CAD Design of UC-Ika 2

and modifies the hydrodynamic force model of Nakashima et al. [2003] with two main differences. Nakashima et al. [2003] assume that the flow around the caudal fin has constant speed while it is variable in fact. The model introduced in this thesis has variable speed. Nakashima et al. [2003] also ignore the lateral speed of the robot for calculation of the flow speed around the caudal fin while the lateral speed of the robot is taken into account in the current model.

Eventually, the dynamic equations of motion of the robots with 4 DOFs are obtained. DOFs of the model are translational displacement X and Y of the centre of mass in X and Y directions, the rotation Φ about the centre of mass of the robots and the rotation θ_4 of the caudal fins.

9.1.3 Optimisation

To simulate the system and analyse its dynamic behaviour, the model must be simulated using the aforementioned dynamic equations of motion. However, the equations contain constant parameters including size and dimensions of the fish robot, amplitude and frequency of undulation of the tail mechanism, and so on. In terms of UC-Ika 1, the constant parameters are experimentally dedicated. Running the simulation with this method does not yield the finest result. Accordingly, UC-Ika 2 makes benefit of an optimisation algorithm called PSO algorithm to determine the most optimal values for constant parameters of the dynamic equations of motion. In this method, all different parts of the robot are optimised simultaneously.

PSO algorithm has two inherent components including particles and fitness function

that are defined for UC-Ika 2. Five particles have been introduced to the system. Each particle has seven dimensions which are constant parameters of the equations of motion[1]. Every particle corresponds to a solution. The solutions are compared by the fitness function.

Fitness function is the criterion of the optimal swimming character of the fish robot. As efficiency in cruising gait is targeted, Froude efficiency, η, is selected as the fitness function. Froude efficiency calculates the swimming efficiency of the fish in cruising mode. Nevertheless, Froude efficiency cannot fully represent the swimming efficiency of a fish since it is derived upon simplified assumptions. To address this problem, PB function is defined which makes benefit of Strouhal number, St. This number is a dimensionless parameter that illustrates the optimal thrust generation of fishes. Indeed, PB function binds the PSO algorithm to employ Froude efficiency as fitness function of the algorithm where the fish swims within the optimal range of Strouhal number. The best value of this number is obtained from experimental observation. PB function is introduced as:

Algorithm 2 Calculate Pbest

function PB($\overline{F_{Cx}}, \bar{\dot{x}}, P_{\text{total}}, f, h$)
  $\eta := \overline{F_{Cx}}\ \bar{\dot{x}}\ (P_{\text{total}})^{-1}$
  $St := 2\, f\, h\, \left(\bar{\dot{x}}\right)^{-1}$
  if $St > 0.35$ **then**
    $k := (80\ (St - 0.325))^{-1}$
  else if $St < 0.30$ **then**
    $k := (80\ (0.325 - St))^{-1}$
  else
    $k := 2$
  end if
  return $k\eta$
end function

9.1.4 Simulation

In order to analyse the cruising motion of UC-Ika 1 & 2, their dynamic performance is simulated. To do so, the equations of motion of them, (5.20), obtained in Chapter 5 are employed. The constant parameters of each robot, given in Table 7.2 and 7.3, are substituted into the equations. The constant parameters of UC-Ika 1 are experimentally

[1]In the mathematical model, there are more than seven unknown parameters; however, those parameters are selected that have crucial role in optimisation of fish robot.

obtained while the constant parameters of UC-Ika 2 is obtained using the optimisation method introduced in Chapter 6. The equations are then solved numerically using Rung-Kutta Fehlberg method.

In terms of UC-Ika 1, the simulation shows the gradual increase of the lateral motion of the tail towards the end of the tail. The robot has the maximum heave of 0.07 m at the end of the caudal fin, shown in Fig. 9.4, provided that the rotation of link 3 is 2.146 times of that of link 1. The model also reveals an average cruising speed of 0.29 m/s where the maximum lateral speed of the robot is equal to 0.15 m/s. the robot is also swinging around its centre of mass, point M, with a maximum of 3.98°. The caudal fin is oscillating around its pivot point F with a maximum of 18.70°, See Fig. 9.4.

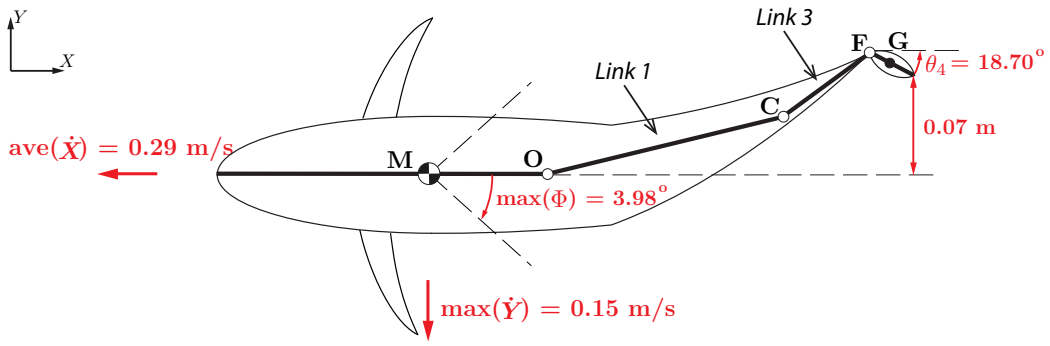

Figure 9.4: Dynamic sketch of UC-Ika 1

In terms of UC-Ika 2, the simulation shows the gradual increase of the lateral motion of the tail towards the end of the tail. The robot has the maximum heave of 0.04 m at end of the caudal fin, shown in Fig. 9.5, provided that the rotation of link 3 is 2.146 times of that of link 1. The model also reveals an average cruising speed of 0.25 m/s where the maximum lateral speed of the robot is equal to 0.10 m/s. the robot is also swinging around its centre of mass, point M, with a maximum of 2.02°. The caudal fin is oscillating around its pivot point F with a maximum of 23.60°, See Fig. 9.5.

The superior performance of UC-Ika 2 in comparison to UC-Ika 1 is also confirmed with the simulation results. Calculating Froude efficiency and Strouhal number shows that UC-Ika 2 with cruising efficiency of 83% and Strouhal number of 0.33 has better swimming performance than UC-Ika 1 with Froude efficiency of 70% and Strouhal number of 0.72 since UC-Ika 2 has higher efficiency and its Strouhal number is within the optimal range of $0.25 - 0.40$.

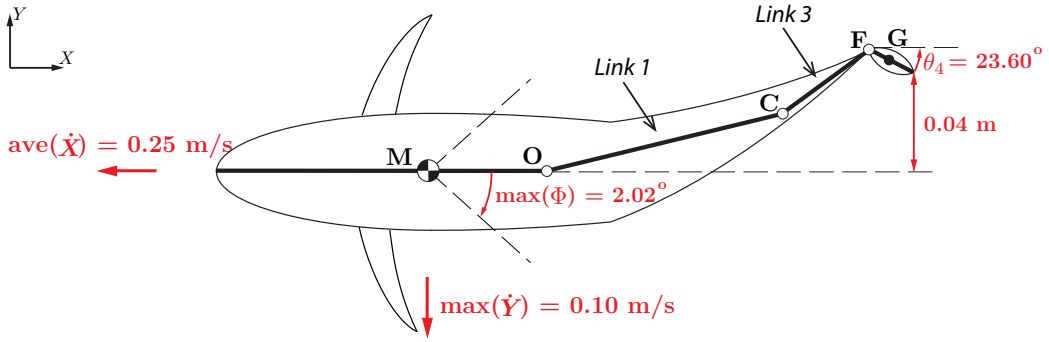

Figure 9.5: Dynamic sketch of UC-Ika 2

9.1.5 Fabrication

The fabrication of biomimetic swimming robots are challenging due to their intricate body shape, flexible parts, waterproofing and communication issues. To address these problems, FDM method as a 3D printing technology is employed for rigid parts of both fish robots. PDMS material is also chosen for fabrication of flexible parts including the tail peduncles and the pectoral fins as PDMS is a durable, tensile and resistant against water. For waterproofing issue, epoxy resin for coating the main body is employed while the connections of the parts are with a slight pretension to assure that the robot is completely sealed. For communication, a microcontroller for each robot is used to control the motors and the limit switches. By means of any Blutooth device like smart phones, this microcontroller and, thus, the robot are controlled. UC-Ika 1 & 2 are shown in Fig. 9.6.

After fabrication and assembly of the robots, their swimming performance are practically tested. UC-Ika 1 & 2 have cruising speed of 0.29 and 0.25 m/s, respectively. Moreover, the experiment validates the optimised swimming performance of UC-Ika 2 with an efficiency of 89% and Strouhal number of 0.37 in comparison to UC-Ika 1 whose efficiency is 78% and its Strouhal number is 0.72. Besides cruising, manoeuvring capability of UC-Ika 2 is tested that shows it could turn in both directions using only the pectoral fins but with different turning speed. In turning left, the robot has a speed of 2.47 deg/s while in the other direction it has a speed of 5.24 deg/s.

9.2 Contributions

Every single step of the development of the aforementioned fish robots is inevitably completed using novel ideas and contributions to the field of biomimetic robots that

(a) UC-Ika 1

(b) UC-Ika 2

Figure 9.6: The fabricated tail mechanism of both fish robots

are summarized in the previous sections. Nevertheless, five main contributions are pointed out in this section.

Initially, a process is defined for developing biomimetic swimming robots. The process is designed and applied to optimise the final prototype in each step. Not only that, the process allows improvements and modifications of the model infinitely before

fabrication.

The second main contribution takes place in the design process where the swimming characteristics of multiple gaits cannot be combined in a single robot. Accordingly, the gaits are thoroughly investigated from both hydrodynamics and biology points of view. Following that the compatibility problems of the gaits in each design element of UC-Ika 2 are addressed.

The next contribution is the optimal generation of undulatory motion of the tail part using a series of linkages actuated with only one DC motor and a silicone-based tail peduncle. In order to mimic the undulation of tuna tail, several methods could be employed such as making artificial muscles or most often using a series of links that are actuated with several motors. In UC-Ika 1 & 2, the cruising mechanism has three main links that the first one is actuated actively by motor whereas the others are passively actuated. In order to generate the undulatory wave, the kinematics of link system is simulated, analysed and modified according to real undulation of tuna. The Strouhal number calculated during simulation and experiment confirms the optimality of the mechanism.

Mathematical modelling of the swimming robots is a great challenge during the development process. The existing models are often incomplete due to their assumptions. These model could be employed either with a controller or are modified based on the real swimming behavior of the system. In the case of UC-Ika 1 & 2, neither of the methods is appropriate since the model is going to be employed for the design process before fabrication and experiment of the robot. Accordingly, a comprehensive model with 4 DOFs is presented that addresses assumptions made by others such as the constant speed of the flow. The mathematical model of UC-Ika 1 & 2 is based the variable speed of flow.

The last but not the least contribution of the process is the application of PSO algorithm for optimising the cruising motion of the robot using a novel fitness function. Using the mathematical model, two important elements of PSO algorithm including particles and fitness function are defined. To assure that the fitness function yields the most optimised robot, both analytical results and experimental observation are considered for the definition of the fitness function. The function is defined based on Froude efficiency and Strouhal number.

9.3 Future Works

In order to further improve the development process of fish robots similar to UC-Ika 2, several works could be performed which are considered in this section.

9.3.1 Modelling Tail Peduncle and Pectoral Fins

The primary improvement returns to the mathematical model of the robot. Previously, the cruising gait of the robot is modelled with the assumption that the propulsion forces are mainly produced by the caudal fin whereas in practice the motion of the tail peduncle has an important effect on the motion of tuna-mimetic robot by more than 10%. By considering the effects of the tail peduncle on both resistive and propulsive forces, the mathematical model could represent the dynamic behaviour of the fish robots more accurately.

Besides the cruising gait, the robot is highly capable of manoeuvring due to the flapping motion of its pectoral fins. In order to investigate and enhance the manoeuvring performance of the robot, a separate model must be presented. This model considers the swimming motion of the robot based on hydrodynamic forces generated by the pectoral fins and has different states including forward swimming motion using both pectoral fins, turning at its position using one flapping pectoral fin at its position, and turning of the robot using two pectoral fins with different frequencies of flapping.

9.3.2 Fabrication of Test Rigs For Force Measurement

Once the model for both cruising and manoeuvring gaits of swimming are presented, they need to be validated. The swimming motion of fish robot is through the propulsive forces generated by their body or fins. The effects of these forces on the propulsion must be measured experimentally. Having fabricated robotic fish, the kinematical behaviour of the system could be validated. Nevertheless, the model is consisted from both kinematics and dynamics of the robotic fish. Accordingly, appropriate test rigs must be designed and constructed for measuring the hydrodynamic forces experimentally.

Since UC-Ika 2 has two gaits of swimming, it also needs two types of test rigs. The first one must be able to measure thrust, lateral and swinging forces made by the last part of the tail peduncle and the caudal fin of swimming robots under water since the tuna-mimetic robots generate propulsive forces by these aforementioned parts of the body. The second test rig must be designed to experimentally measure the propulsive forces that are produced by the pectoral fins. This test rig requires the capability of

detecting the forces produced by each pectoral fin individually in both up- and down-strokes.

The test rigs allow calculation of the swimming efficiency of the fish robot for both cruising and manoeuvring performances since the efficiency depends on the forward and lateral components of both velocities and forces of the swimming robot.

9.3.3 Improving Design of Pectoral Fins

The last main improvement is changing the design and fabrication of pectoral fins. In nature, the pectoral fins have 4-DOFs including flapping, feathering, lead-lag motion and abduction (or adduction). These 4 types of motion for pectoral fins allow the fish to have different types of motion. For instance, lead-lag motion provides the fast-start motion for the fish. However, the pectoral fins of UC-Ika 2 are able to have flapping and roughly feathering motion. By designing a new actuation mechanism for the robot capable of having all four types of motion, the robot will show more adaptability to its environment and higher swimming efficiency.

A Microcontroller Code of UC-Ika 1

```
#include <TimerOne.h>

//*********************************************************************************
//              ROBOT FISH MOTOR CONTROL AND SENSOR DATA ACQUISTION
//              PROJECT LEADER: SAYYED FARIDEDDIN MASOOMI
//              ORIGINALLY WRITTEN BY AXEL HAUNHOLTER, DOMINIC MERZ, MERVIN CHANDRAPAL
//              ALL COMMUNICATION IS DONE SERIALLY THROUGH A BLUETOOTH DONGLE
//*********************************************************************************

//*****************************INITIALIZE ALL CONSTANTS*******************************
const int E1 = 6;              // Initialisation of  the motor
const int M1 = 7;
const int analogInPin = 0;     // current sensorconnected to analog pin 0
const int optoswitch = 2;      // the number of the pushbutton pin
const int ledPin =  13;        // the number of the LED pin
int incomingByte;              // A variable to read incoming serial data into
int Flag = 0;                  // Used to dedounce the optoswitch
int count = 0;                 // Used to store the optoswitch counts
int RPM = 0;                   // Motor RPM as caluclated from optoswitch

//****************************PERIPHERAL INITIALIZATION*******************************
```

```
void setup()
{
  Serial.begin(9600);              //Open a connection to the Bluetooth Mate
  pinMode(M1, OUTPUT);             // Define output for Motor
  pinMode(ledPin, OUTPUT);         // Initialize the LED pin as an output:
  pinMode(optoswitch, INPUT);      //Initialize the pushbutton pin as an input
  digitalWrite(optoswitch, HIGH);  //turn on pullup resistors
  Timer1.initialize(5000000);      // initialize timer1, and set a 5 second period
  Timer1.attachInterrupt(T1ISR);   // attaches T1ISR() as a timer overflow interrupt
                                   // service routine
}

//****************************INTERRUPT SERVICE ROUTINE*********************************
void T1ISR()
{
  RPM = 60/5 * count;       //RPM calculation since ISR is taken every 5 seconds
  count = 0;                //Reset the counter
}

//**********************MAIN FUNCTION OF THE MICROCONTROLLER*****************************

void loop()
{

//********************Current sensor-Check ANIn Pin for sensor************************
  int sensorValue;
  float outputValue,voltage,current,offset;

  sensorValue = analogRead(analogInPin);    // read the analog in value:
  voltage = (float)sensorValue*5020/1024;   //sensor voltage in milivolts-Supposed to be
  5000mV
  offset = (float)voltage - 2500;           // Introduce the offset at 0 at 2500mV
```

```
  current= (float) offset/66;               //Sensor output: 1A = 66mV
  Serial.print("Current(A): ");
  Serial.println(current,4);

//*********************RPM sensor-Check DigitalIn Pin for sensor************************
  int OptoState = 0;                          // variable for reading the pushbutton status
  OptoState = digitalRead(optoswitch);        // read the state of the pushbutton value

  if (OptoState == HIGH && Flag ==1)          // check if the pushbutton is pressed. If it
  is, the buttonState is HIGH.
    {
      Flag = 0;                               // Reset the debounce flag
      count++;
                                              //digitalWrite(ledPin, HIGH);  // turn LED on
    }
  else if (OptoState == LOW && Flag == 0)
    {
      Flag = 1;                               //Set the debounce flag
    }
  else
    {
                                             // Do nothing
    }

    Serial.print("RPM: \t");
    Serial.println(RPM);

//*************************Motor Speed Control*****************************************
  if (Serial.available() > 0)

     {                                  //Look for data coming in from Bluetooth Mate
        char cmd = Serial.read();       // Read the character
```

```
digitalWrite(M1,HIGH);          // PWM motor on
Serial.println(cmd);        // Echo the character back

if(cmd =='1')

  {   //Increase the speed step by step till the maximum and switch off
     int value = 0;
     for(value = 0 ; value <= 255; value+=50)
     {
       Serial.print("Speed: \t");
       Serial.println(value);
       analogWrite(E1, value); //PWM Speed Control
       delay(4000);  //Time between increases
     }
  }

else if (cmd =='0')

  { //If the character 0 was pressured on the keyboard
    int value = 0;
    analogWrite(E1, value);  // The engine is turned off
    //digitalWrite(ledPin, LOW);
    Serial.println("Speed: 0");  // Echo as feed back
    Serial.println("Commants: S=Slow\tM=Medium\tF=Fast\t1=Step mode\t0=Out");
    //Commands
  }

else if (cmd =='M')
  { //Case M is pressed on the keyboard
    int value = 150;
    analogWrite(E1, value);
    Serial.println("Speed is medium 150");
```

```
        }

    else if (cmd ==’S’)
        { //Case S is pressed on the keyboard
          int value = 100;
          analogWrite(E1, value);
          Serial.println("Speed is slow 100");
        }

    else if (cmd ==’F’)
        { //Case F is pressed on the keyboard
          int value = 250;
          analogWrite(E1, value);
          Serial.println("Speed is fast 250");
        }
    }

  delay(20);
}
```

B Microcontroller Code of UC-Ika 2

```
#include <avr/sleep.h>
#include <avr/power.h>

//*****************************************************************************
//              ROBOT FISH MOTOR CONTROL
//              PROJECT LEADER: SAYYED FARIDEDDIN MASOOMI
//              ORIGINALLY WRITTEN BY CONNOR EATWELL
//              ALL COMMUNICATION IS DONE SERIALLY THROUGH A BLUETOOTH DONGLE
//*****************************************************************************

int left_pec_PWM = 11;            // Initialisation of the motors
int left_pec_dir = 13;            //Note that all motors will have to be attached
                                  //to the 3,11,12 and 13 pins as required by the
int right_pec_PWM = 3;            //L298P Motor Shield, but that has been changed
int right_pec_dir = 12;           //by alternate wiring. Note the pecs have been switched
due
                                  //space requirements inside the fish
int tail_PWM = 5;
int tail_dir = 7;

int bouyancy_PWM = 10;
```

```
int bouyancy_dir = 8;

int NSYNC = 4;                  // Will return true if the pectoral fins are in synch with
each other

int incomingByte;               // A variable to read incoming serial data into

int pin2 = 2;                  // number of interrupting pin


void pin2Interrupt(void)       //Brings microcontroller back from sleep
{
  detachInterrupt(0);
}

void enterSleep(void)
{
  attachInterrupt(0, pin2Interrupt, LOW); // Set pin2 as an interrupt and attach
  handler
  delay(100);                           //necessary to prevent internal error
  set_sleep_mode(SLEEP_MODE_PWR_DOWN);  //chosen sleepmode (5 available)
  sleep_enable();
  sleep_mode();                         // The program will continue from here
  sleep_disable();                      // First thing to do is disable sleep
  Serial.write(0x1B);                   //Escape
  Serial.write('0;0f');                 //[ 'Bracket'
                                        // Code to place the cursor to prevent
                                        floating
                                        // Translation from ASCII characters
  Serial.println("Awake");
  delay(1000);
}
```

```
void straightAhead(void)
{
  int left_pec_running = (pulseIn(left_pec_PWM, HIGH) != 0);
  int right_pec_running = (pulseIn(right_pec_PWM, HIGH) != 0);

  if (left_pec_running && right_pec_running) {   // If both pectoral fins are running
  and they're not in sync, stop the faster one until they are in sync
    while (digitalRead(NSYNC) == 0) {             //I know while loops are bad practice
    but it needed to be done
      analogWrite(right_pec_PWM, 0);
      delay(10);
    }
    analogWrite(right_pec_PWM, 200);
  }
}

void setup()
{
  Serial.begin(115200);               //Open a connection to the Bluetooth Mate
  pinMode(left_pec_dir, OUTPUT);    // Definition as output
  pinMode(right_pec_dir, OUTPUT);
  pinMode(tail_dir, OUTPUT);
  pinMode(bouyancy_dir, OUTPUT);
  pinMode(pin2, INPUT);            // setup pin direction
  pinMode(NSYNC, INPUT);
}

void loop() {                            //Main function of the microcontroller

  straightAhead();
```

```
if (Serial.available() > 0) {            //Look for data coming in from Bluetooth Mate

  char cmd = Serial.read();              // Read the character

  digitalWrite(left_pec_dir,HIGH);       // This sets the motor direction, NEEDS TO BE
  SET TO FIND OUT WHICH
  digitalWrite(right_pec_dir,HIGH);      //WAY EACH MOTOR GOES. HIGH MEANS BACKWARDS.
  digitalWrite(tail_dir,HIGH);
  digitalWrite(bouyancy_dir,HIGH);
  digitalWrite(NSYNC, HIGH);             // Turns on pull up resistor for fin
  synchronization

  Serial.println(cmd);                   // Echo the character back

  if(cmd ==’a’) {
    int value = 200;
    analogWrite(left_pec_PWM, value);    //Perform a left turn by using left pectoral
    fin by itself
    Serial.println("Turning Left");
    delay(5000);                         // Turn for 5 seconds
    analogWrite(left_pec_PWM, 0);        //Stop turning left

  } else if (cmd == ’b’) {
    int value = 200;
    analogWrite(right_pec_PWM, value);   //Perform a right turn by using right pectoral
    fin by itself
    Serial.println("Turning Right");
    delay(5000);                         //Do this for 5 seconds
    analogWrite(right_pec_PWM, 0);       //Stop

  } else if (cmd == ’c’) {               // Use both pectoral fins for slow cruise
     int value = 200;
```

```
    analogWrite(left_pec_PWM, value);
    analogWrite(right_pec_PWM, value);
    straightAhead();

} else if (cmd == 'd') {                //d and e are slow adjustment commands for
the pectoral fins
  analogWrite(left_pec_PWM, 30);

} else if (cmd =='e') {
  analogWrite(right_pec_PWM, 30);

} else if (cmd =='k') {                // k is to adjust tail
  analogWrite(tail_PWM, 30);

} else if (cmd =='x') {                //Use X as a command to stop turning
    int value = 0;
    analogWrite(left_pec_PWM, value); //Motors to each pec fin are turned off
    analogWrite(right_pec_PWM, value);
    Serial.println("Straight Ahead");

} else if (cmd =='0') {                //Use 0 as a command to stop everything
    int value = 0;
    analogWrite(left_pec_PWM, value); // Turn off all motors
    analogWrite(right_pec_PWM, value);
    analogWrite(tail_PWM, value);
    analogWrite(bouyancy_PWM, value);

    digitalWrite(bouyancy_dir, HIGH); //Reset direction of bouyancy control as
    well, just in case

    Serial.println("Speed: 0");      // Echo as feed back
```

```
} else if (cmd ==’u’) {             //Increase Bouyancy, wait 3s, then decrease
bouyancy
   int value = 255;
   analogWrite(bouyancy_PWM, value);
   Serial.println("Going Up!");
   delay(3000);
   digitalWrite(bouyancy_dir,LOW);
   Serial.println("Going Down!");
   delay(3000);
   analogWrite(bouyancy_PWM, 0);
   digitalWrite(bouyancy_dir, HIGH);

} else if (cmd ==’j’) {             //Stop messing with the bouyancy
   int value = 0;
   analogWrite(bouyancy_PWM, value);
   Serial.println("Floating at a constant level");

} else if (cmd ==’1’) {             //Slowest Movement Forward
   int value = 100;
   analogWrite(tail_PWM, value);
   Serial.println("Slowly Forwards");

} else if (cmd ==’2’) {             //Picking up speed, second slowest
   int value = 150;
   analogWrite(tail_PWM, value);
   Serial.println("Semi-slowly Forwards");

} else if (cmd ==’3’) {             //Nearly top speed
   int value = 200;
   analogWrite(tail_PWM, value);
   Serial.println("Semi-quickly Forwards");
```

```
 } else if (cmd ==’4’) {              //Top tail speed
    int value = 255;
    analogWrite(tail_PWM, value);
    Serial.println("Quickly Forwards");

 } else if (cmd ==’g’) {              //go nuts
    int value = 255;
    analogWrite(left_pec_PWM, value); // Turn on all movement motors to full
    analogWrite(right_pec_PWM, value);
    straightAhead();
    analogWrite(tail_PWM, value);
    Serial.println("Going Nuts");

} else if (cmd == ’p’) {            // Turns on Bouyancy motor in pulses for adjustments
to the bouyancy of the fish
   analogWrite(bouyancy_PWM, 0);     //turns off motor for accuracy
   delay(50);                        //Delays to make sure motor is, in fact, off
   digitalWrite(bouyancy_dir, HIGH); //Change direction of motor (just in case it has
   been changed before)
   analogWrite(bouyancy_PWM, 255);
   delay(500);
   analogWrite(bouyancy_PWM, 0);

} else if (cmd == ’m’) {             //Slowly turns on bouyancy motor in other direction
   analogWrite(bouyancy_PWM, 0);     //turns off motor for accuracy
   delay(50);                        //Delays to make sure motor is, in fact, off
   digitalWrite(bouyancy_dir, LOW);  //Change direction of motor
   analogWrite(bouyancy_PWM, 255);
   delay(500);
   analogWrite(bouyancy_PWM, 0);

} else if (cmd == ’y’) {                   //Cruise, turn left, then turn right
```

```
    Serial.println("Forward, left, right");
    int value = 150;             //Have initially chosen a mid-range value, to see
    how it goes
    delay(1000);
    analogWrite(tail_PWM, value);             //Go straight for 5 seconds
    delay(6000);
    analogWrite(left_pec_PWM, 200);         //Turn Left for 4 seconds
    delay(6000);
    analogWrite(right_pec_PWM, 200);
    straightAhead();                           //Just to sync fins a little bit, has
    greater chance of the fins not being completely wonky
    analogWrite(left_pec_PWM, 0);             //Turn the motor off and give it a half
    second delay before...
    delay(500);
    analogWrite(right_pec_PWM, 200);        //...making the fish turn right for 4
    seconds
    delay(4000);
    analogWrite(left_pec_PWM, 200);
    straightAhead();                            //Synching as above
    analogWrite(left_pec_PWM, 0);
    analogWrite(right_pec_PWM, 0);            //When it's all done, turn off relevant
    parts
    analogWrite(tail_PWM, 0);

} else if (cmd == 'i') {
  Serial.println("Forward, Up, Down");      //Go forward mid pace...
  int value = 150;
  delay(1000);
  digitalWrite(bouyancy_dir, HIGH);          //Make sure bouyancy is in right
  direction
  analogWrite(tail_PWM, value);
  delay(4000);
```

```
  analogWrite(bouyancy_PWM, 255);             //Start rising
  delay(1500);
  analogWrite(bouyancy_PWM, 0);              //Stop rising
  delay(500);
  digitalWrite(bouyancy_dir, LOW);
  analogWrite(bouyancy_PWM, 255);             //Start sinking
  delay(1500);
  analogWrite(bouyancy_PWM, 0);             //Stop again
  digitalWrite(bouyancy_dir, HIGH);
  analogWrite(tail_PWM, 0);

} else if(cmd == 'f') {
   int maxVal = 255;
   delay(1000);
   digitalWrite(bouyancy_dir, HIGH);
   analogWrite(tail_PWM, maxVal);
   analogWrite(left_pec_PWM, maxVal);        // Caudal fin on full, full left turn
   analogWrite(bouyancy_PWM, maxVal);        // Rise...
   delay(4000);
   analogWrite(right_pec_PWM, maxVal);       // Start turning right...
   straightAhead();                          // Synch fins...
   analogWrite(left_pec_PWM, 0);             // Turn off left pec...
   digitalWrite(bouyancy_dir, LOW);          // Start sinking...
   analogWrite(bouyancy_PWM, maxVal);
   delay(4000);
   analogWrite(right_pec_PWM, 0);            // Turn off everything and reset BCS
   direction
   analogWrite(bouyancy_PWM, 0);
   digitalWrite(bouyancy_dir, HIGH);
   analogWrite(tail_PWM, 0);

}else if(cmd =='q') {                        // Sleep mode, says it all
```

```
    Serial.println("Entering Sleep Mode");
    delay(200);
    enterSleep();
   }
  }
  delay(100);
}
```

C Assembly Drawing of UC-Ika 1

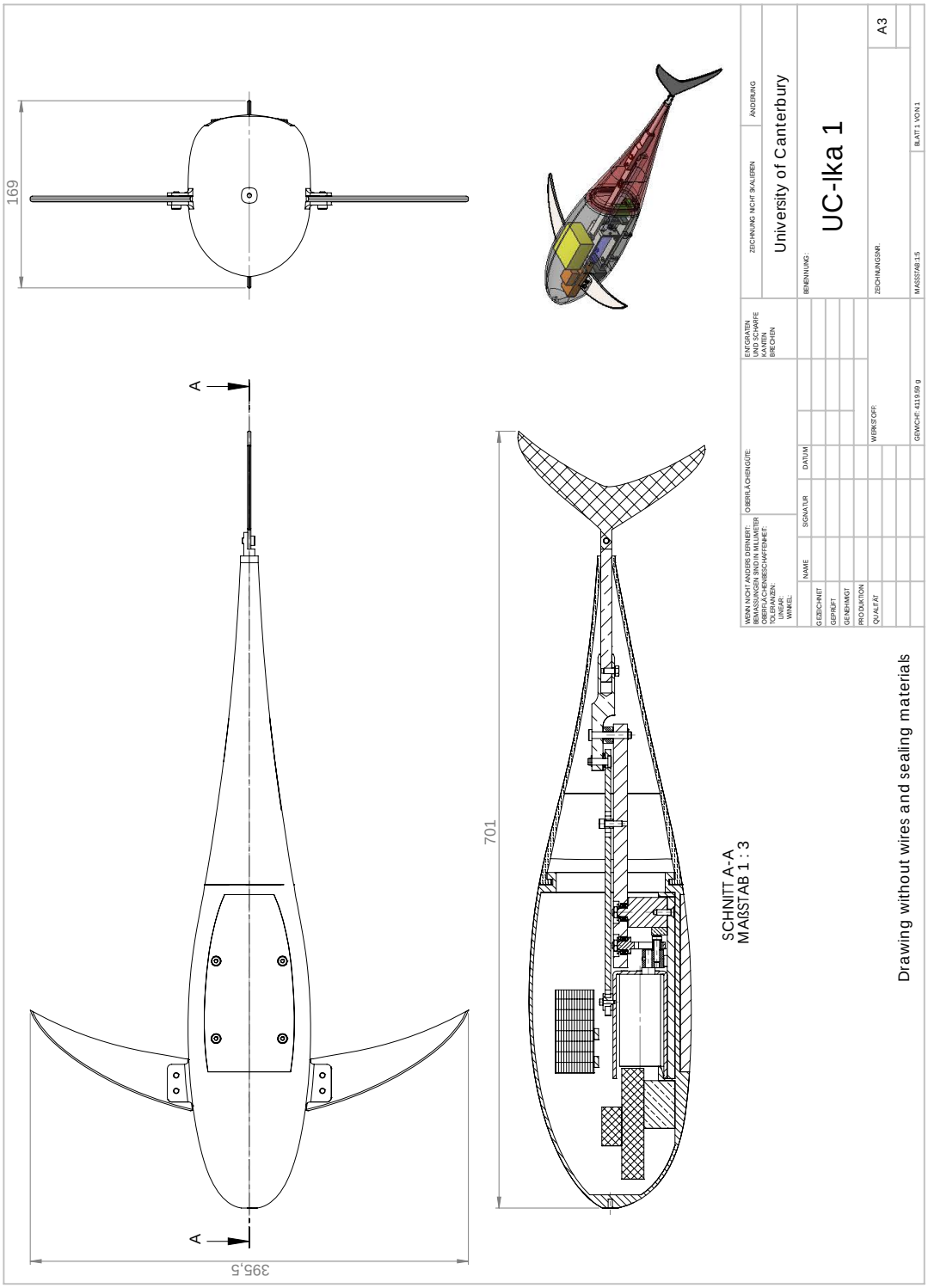
169
395,5
701
A
A
SCHNITT A-A
MAßSTAB 1 : 3
University of Canterbury
UC-Ika 1
A3
Drawing without wires and sealing materials

References

Robotic fish spc-03, bua - casia, china. URL http://www.robotic-fish.net/index.php?lang=en&id=robots#top. 50

Aqua ray. Brochure, October 2013. URL http://www.festo.com/rep/en_corp/assets/pdf/Aqua_ray_en.pdf. 1, 2

Autonomous underwater vehicles (auvs) the hugin family. Brochure, 2013. URL http://www.atmarine.fi/ckfinder/userfiles/files/HUGIN_Family_brochure_r2_lr%281%29.pdf. 1, 2

Merlin wr200. Brochure, 2013. URL http://www.ikm.no/filearchive/193dc306-8669-4bc7-a276-274d7eee4401.pdf. 1, 2

Quepos, costa rica offshore fishing, October 2013. URL http://www.queposfishadventure.com/Tuna.html. 9

Bird wrasse (gomphosus varius), October 2013a. URL http://www.liveaquaria.com/product/prod_display.cfm?c=15+1379+297&pcatid=297. 7

The bird wrasse, October 2013b. URL http://mauicharters.com/wordpress/?p=351. 9

Airacuda. Brochure, October 2013. URL http://www.festo.com/rep/en_corp/assets/pdf/Airacuda_en.pdf(AccessSeptember2013). 50

Sylgard 184 silicone elastomer. Brochure, April 2013. URL http://ncnc.engineering.ucdavis.edu/pages/equipment/Sylgard_184_data_sheet.pdf. 12, 123

Ajith Abraham, He Guo, and Hongbo Liu. Swarm intelligence: Foundations, perspectives and applications. In Nadia Nedjah and LuizadeMacedo Mourelle, editors, *Swarm Intelligent Systems*, volume 26 of *Studies in Computational Intelligence*, pages 3–25. Springer Berlin Heidelberg, 2006.

ISBN 978-3-540-33868-0. doi: 10.1007/978-3-540-33869-7_1. URL http://dx.doi.org/10.1007/978-3-540-33869-7_1. 97, 99

Yazan Aldehayyat, Richard Dahan, Iman Fayyad, Jean Martin, Matthew Perkins, and Rachel Sharples. Ocra-xi: An autonomous underwater vehicle. *OCRA AUV Team*, 2009. URL http://web.mit.edu/orca/www/. 1

R Alexander. Dynamics of dinosaurs and other extinct giants, 1989. 15

R.M.N. Alexander. *Principles of animal locomotion*. Princeton University Press, 2002. xiii, xv, 9, 26, 27, 28, 33, 44, 69, 75

John D Altringham and DAVID J Ellerby. Fish swimming: patterns in muscle function. *Journal of Experimental Biology*, 202(23):3397–3403, 1999. 19

V. y Alvarado. *Design of biomimetic compliant devices for locomotion in liquid environments*, volume 68. 2007. 46, 63

J.M. Anderson and N.K. Chhabra. Maneuvering and stability performance of a robotic tuna. *Integrative and Comparative Biology*, 42(1):118–126, 2002. 2, 7, 48, 62, 67, 95

JM Anderson, K. Streitlien, DS Barrett, and MS Triantafyllou. Oscillating foils of high propulsive efficiency. *Journal of Fluid Mechanics*, 360(1):41–72, 1998. 111, 116, 119

M. Anton, Zheng Chen, M. Kruusmaa, and Xiaobo Tan. Analytical and computational modeling of robotic fish propelled by soft actuation material-based active joints. In *Intelligent Robots and Systems, 2009. IROS 2009. IEEE/RSJ International Conference on*, pages 2126–2131, 2009. doi: 10.1109/IROS.2009.5354189. 83

J. Ayers, C. Wilbur, and C. Olcott. Lamprey robots. 2000. 44, 62

P.R. Bandyopadhyay. Trends in biorobotic autonomous undersea vehicles. *Oceanic Engineering, IEEE Journal of*, 30(1):109 – 139, jan. 2005. ISSN 0364-9059. doi: 10.1109/JOE.2005.843748. 1

D. Barrett, M. Grosenbaugh, and M. Triantafyllou. The optimal control of a flexible hull robotic undersea vehicle propelled by an oscillating foil. In *Autonomous Underwater Vehicle Technology, 1996. AUV '96., Proceedings of the 1996 Symposium on*, pages 1–9, 1996. doi: 10.1109/AUV.1996.532833. 83

George Keith Batchelor. *An Introduction to Fluid Dynamics*. London [England] : Cambridge University Press, 1967. 91

D.N. Beal. *Propulsion through wake synchronization using a flapping foil*. PhD thesis, Massachusetts Institute of Technology, 2003. 48

Damir Beciri. Fish robots search for pollution in the waters, May 2009. URL http://www.robaid.com/bionics/fish-robots-search-for-pollution-in-the-waters.htm. 3, 49

A.A. Biewener. *Animal locomotion*. Oxford University Press, USA, 2003. xi, xiii, xiv, xv, 24, 25, 27, 29, 35, 74, 75

David Bingham, Tony Drake, Andrew Hill, and Roger Lott. The application of autonomous underwater vehicle (auv) technology in the oil industry - vision and experiences. In *FIG XXII International Congress*, Washington D.C., USA, April 2002. 1

F. Boyer, D. Chablat, P. Lemoine, and P. Wenger. The eel-like robot. *Arxiv preprint arXiv:0908.4464*, 2009. 44, 63

Youngsu Cha, Matteo Verotti, Horace Walcott, Sean D Peterson, and Maurizio Porfiri. Energy harvesting from the tail beating of a carangiform swimmer using ionic polymer–metal composites. *Bioinspiration & biomimetics*, 8(3):036003, 2013. 62

Won-Shik Chu, Kyung-Tae Lee, Sung-Hyuk Song, Min-Woo Han, Jang-Yeob Lee, Hyung-Soo Kim, Min-Soo Kim, Yong-Jai Park, Kyu-Jin Cho, and Sung-Hoon Ahn. Review of biomimetic underwater robots using smart actuators. *International Journal of Precision Engineering and Manufacturing*, 13(7):1281–1292, 2012. 62, 63

Chee Kai Chua, Kah Fai Leong, and C Chu Sing Lim. *Rapid prototyping: principles and applications*. World Scientific Publishing Company, 2010. 12, 122

J.E. Colgate and K.M. Lynch. Mechanics and control of swimming: a review. *Oceanic Engineering, IEEE Journal of*, 29(3):660 – 673, july 2004. ISSN 0364-9059. doi: 10.1109/JOE.2004.833208. 46, 51

Oscar M. Curet, Neelesh A. Patankar, George V. Lauder, and Malcolm A. MacIver. Aquatic manoeuvering with counter-propagating waves: a novel locomotive strategy. *Journal of The*

Royal Society Interface, 8(60):1041–1050, 2011a. doi: 10.1098/rsif.2010.0493. URL http://rsif.royalsocietypublishing.org/content/8/60/1041.abstract. 59

Oscar M Curet, Neelesh A Patankar, George V Lauder, and Malcolm A MacIver. Mechanical properties of a bio-inspired robotic knifefish with an undulatory propulsor. *Bioinspiration & Biomimetics*, 6 (2):026004, 2011b. URL http://stacks.iop.org/1748-3190/6/i=2/a=026004. 59

G. Dogangil, E. Ozcicek, and A. Kuzucu. Design, construction, and control of a robotic dolphin. In *IEEE International Conference on Robotics and Biomimetics (ROBIO)*, pages 51 –56, 0-0 2005. doi: 10.1109/ROBIO.2005.246400. 50, 62

Paolo Domenici and R Blake. The kinematics and performance of fish fast-start swimming. *Journal of Experimental Biology*, 200(8):1165–1178, 1997. 18

rjan Ekeberg. A combined neuronal and mechanical model of fish swimming. *Biological Cybernetics*, 69(5-6):363–374, 1993. ISSN 0340-1200. doi: 10.1007/BF01185408. URL http://dx.doi.org/10.1007/BF01185408. 84

M. Epstein, J.E. Colgate, and M.A. MacIver. Generating thrust with a biologically-inspired robotic ribbon fin. In *IEEE/RSJ International Conference on Intelligent Robots and Systems*, pages 2412–2417. IEEE, 2006. 7, 59, 60, 62, 96

Christopher J Esposito, James L Tangorra, Brooke E Flammang, and George V Lauder. A robotic fish caudal fin: effects of stiffness and motor program on locomotor performance. *The Journal of experimental biology*, 215(1):56–67, 2012. xiv, 52, 53

Benjamin Fankhauser and Auke Jan Ijspeert. Boxybot ii, the fish robot: Fin design, programmation, simulation and testing. *EPFL-Semester Project*, 2010. 3, 57, 67

BE Flammang and GV Lauder. Caudal fin shape modulation and control during acceleration, braking and backing maneuvers in bluegill sunfish, lepomis macrochirus. *Journal of Experimental Biology*, 212(2):277–286, 2009. 52

Brooke E Flammang and George V Lauder. Speed-dependent intrinsic caudal fin muscle recruitment during steady swimming in bluegill sunfish, lepomis macrochirus. *Journal of Experimental Biology*, 211(4):587–598, 2008. 52

Jun Gao, Shusheng Bi, Yicun Xu, and Cong Liu. Development and design of a robotic manta ray featuring flexible pectoral fins. In *IEEE International Conference on Robotics and Biomimetics (ROBIO)*, pages 519 –523, dec. 2007. doi: 10.1109/ROBIO.2007.4522216. 54, 55

Jun Gao, Shusheng Bi, Ji Li, and Cong Liu. Design and experiments of robot fish propelled by pectoral fins. In *IEEE International Conference on Robotics and Biomimetics (ROBIO)*, pages 445 –450, dec. 2009. doi: 10.1109/ROBIO.2009.5420688. 7, 54, 55, 95

G. Griffiths and I. Edwards. Auvs: designing and operating next generation vehicles. *Elsevier Oceanography Series*, 69:229–236, 2003. 1

K.A. Harper, M.D. Berkemeier, and S. Grace. Modeling the dynamics of spring-driven oscillating-foil propulsion. *IEEE Journal of Oceanic Engineering*, 23(3):285 –296, jul 1998. ISSN 0364-9059. doi: 10.1109/48.701206. 83

Rania Hassan, Babak Cohanim, Olivier De Weck, and Gerhard Venter. A comparison of particle swarm optimization and the genetic algorithm. In *Proceedings of the 1st AIAA multidisciplinary design optimization specialist conference*, 2005. 97

Seok Heo, Tedy Wiguna, Hoon Cheol Park, and Nam Seo Goo. Effect of an artificial caudal fin on the performance of a biomimetic fish robot propelled by piezoelectric actuators. *Journal of Bionic Engineering*, 4(3):151 – 158, 2007. ISSN 1672-6529. doi: http://dx.doi.org/10.1016/S1672-6529(07)60027-4. URL http://www.sciencedirect.com/science/article/pii/S1672652907600274. 62

Huosheng Hu, Jindong Liu, I. Dukes, and G. Francis. Design of 3d swim patterns for autonomous robotic fish. In *IEEE/RSJ International Conference on Intelligent Robots and Systems*, pages 2406 –2411, oct. 2006. doi: 10.1109/IROS.2006.281680. 1

Huosheng Hu, John Oyekan, and Dongbing Gu. A school of robotic fish for pollution detection in port. *Biologically Inspired Robotics (Y. Liu and D. Sun, eds.)*, pages 85–104, 2012. 1

T. Hu, L. Shen, L. Lin, and H. Xu. Biological inspirations, kinematics modeling, mechanism design and experiments on an undulating robotic fin inspired by gymnarchus niloticus. *Mechanism and machine theory*, 44(3):633–645, 2009. 58, 60, 62

Alexander Inzartsev and Alexander Pavin. Auv application for inspection of underwater communications. *Alexander V. Inzartsev. Vienna: In-Tech Publishers*, pages 215–234, 2009. 1

REFERENCES

M.V. Jakuba. Design and fabrication of a flexible hull for a bio-mimetic swimming apparatus, 2000. 48

C Jordi, S Michel, and E Fink. Fish-like propulsion of an airship with planar membrane dielectric elastomer actuators. *Bioinspiration and biomimetics*, 5(2):026007, 2010. 62

Voratas Kachitvichyanukul. Comparison of three evolutionary algorithms: Ga, pso, and de. *Industrial Engineering and Management Systems*, 11(3):215–223, September 2012. 97

N. Kato. Control performance in the horizontal plane of a fish robot with mechanical pectoral fins. *IEEE Journal of Oceanic Engineering*, 25(1):121 –129, jan 2000. ISSN 0364-9059. doi: 10.1109/48.820744. 56

N. Kato, B.W. Wicaksono, and Y. Suzuki. Development of biology-inspired autonomous underwater vehicle bass iii with high maneuverability. In *Proceedings of the International Symposium on Underwater Technology*, pages 84–89. IEEE, 2000. 7, 56, 96

Naomi Kato. Fish fin motion. URL `http://www.naoe.eng.osaka-u.ac.jp/~kato/fin9.html`. xiv, 57

Naomi Kato, Hao Liu, and Hirohisa Morikawa. Biology-inspired precision maneuvering of underwater vehicles (part 2). In *International Offshore and Polar Engineering Conference*, pages 178–185, May 2003. 56

Naomi Kato, Yoshito Ando, Toshihide Shigetomi, and Tomohisa Katayama. Biology-inspired precision maneuvering of underwater vehicles (part 4). *International Journal of Offshore and Polar Engineering*, 16(3):195–201, September 2006. 56

Eunjung Kim and Youngil Youm. Design and dynamic analysis of fish robot: Potuna. In *Robotics and Automation, 2004. Proceedings. ICRA '04. 2004 IEEE International Conference on*, volume 5, pages 4887–4892 Vol.5, 2004. doi: 10.1109/ROBOT.2004.1302492. 48, 67

HyoungSeok Kim, ByungRyong Lee, and RakJin Kim. A study on the motion mechanism of articulated fish robot. In *Mechatronics and Automation, 2007. ICMA 2007. International Conference on*, pages 485 –490, aug. 2007. doi: 10.1109/ICMA.2007.4303591. 50

P. Kodati, J. Hinkle, A. Winn, and Xinyan Deng. Microautonomous robotic ostraciiform (marco): Hydrodynamics, design, and fabrication. *IEEE Transactions on Robotics*, 24(1):105 –117, feb. 2008. ISSN 1552-3098. doi: 10.1109/TRO.2008.915446. xiv, 7, 51, 52, 62, 67, 95

Daisy Lachat, A Crespi, and AJ Ijspeert. Boxybot, the fish robot design and realization. *EPFL-Semester Project*, 27, 2005. xiv, 2, 3, 56, 57, 96

Hamed Lashkari, Aghil Yousefi-Koma, Peyman Karimi Eskandary, Donya Mohammadshahi, and Alireza Kashaninia. Development of a fish-like propulsive mechanism. In *Proceedings of the 3rd WSEAS international conference on Engineering mechanics, structures, engineering geology*, pages 389–395. World Scientific and Engineering Academy and Society (WSEAS), 2010. 48, 67

S. Lee, J. Park, and C. Han. Optimal control of a mackerel-mimicking robot for energy efficient trajectory tracking. *Journal of Bionic Engineering*, 4(4):209–215, 2007. 49

J. Liang, T. Wang, and L. Wen. Development of a two-joint robotic fish for real-world exploration. *Journal of Field Robotics*, 28(1):70–79, 2011. 7, 49, 62, 96

MJ Lighthill. Note on the swimming of slender fish. *J. Fluid Mech*, 9(2):305–317, 1960. 6, 71, 83, 91, 102

MJ Lighthill. Aquatic animal propulsion of high hydromechanical efficiency. *Journal of Fluid Mechanics*, 44(02):265–301, 1970. 6, 83

MJ Lighthill. Large-amplitude elongated-body theory of fish locomotion. *Proceedings of the Royal Society of London. Series B. Biological Sciences*, 179(1055):125–138, 1971. 83

PF Linden and JS Turner. optimalvortex rings and aquatic propulsion mechanisms. *Proceedings of the Royal Society of London. Series B: Biological Sciences*, 271(1539):647–653, 2004. xiv, 31, 70

C.C. Lindsey. Form, function, and locomotory habits in fish. In W.S. Hoar and D.J. Randall, editors, *Locomotion*, volume 7 of *Fish Physiology*, pages 1 – 100. Academic Press, 1979. doi: http://dx.doi.org/10.1016/S1546-5098(08)60163-6. URL http://www.sciencedirect.com/science/article/pii/S1546509808601636. 9, 18, 37, 44, 45, 46, 47, 51, 53, 56, 58, 59, 68, 72, 73, 75

Hao Liu, R Wassersug, and Keiji Kawachi. A computational fluid dynamics study of tadpole swimming. *Journal of Experimental Biology*, 199(6):1245–1260, 1996. 83

J. Liu and H. Hu. A 3d simulator for autonomous robotic fish. *International Journal of Automation and Computing*, 1(1):42–50, 2004. 2, 48

J. Liu, I. Dukes, R. Knight, and H. Hu. Development of fish-like swimming behaviours for an autonomous robotic fish. *Proceedings of the Control*, 4, 2004. 49, 84

REFERENCES

J. Liu, I. Dukes, and H. Hu. Novel mechatronics design for a robotic fish. In *IEEE/RSJ International Conference on Intelligent Robots and Systems, 2005. (IROS 2005).*, pages 807–812. IEEE, 2005. 49, 62, 87

Jindong Liu. Welcome! essex robotic fish, August 2006. URL http://dces.essex.ac.uk/staff/hhu/jliua/index.htm#Profile. 49

Jindong Liu. Mt1 image gallery, January 2008. URL http://dces.essex.ac.uk/staff/hhu/jliua/images/gallery/MT1/P1010049.JPG. 49

Y. Liu, W. Chen, and J. Liu. Research on the swing of the body of two-joint robot fish. *Journal of Bionic Engineering*, 5(2):159–165, 2008. 6, 84, 91

K. H. Low, Jie Yang, A.P. Pattathil, and Yonghua Zhang. Initial prototype design and investigation of an undulating body by sma. In *Automation Science and Engineering, 2006. CASE '06. IEEE International Conference on*, pages 472–477, 2006. doi: 10.1109/COASE.2006.326927. 62

KH Low. Modelling and parametric study of modular undulating fin rays for fish robots. *Mechanism and Machine Theory*, 44(3):615–632, 2009. 2, 59, 61

K.H. Low and A. Willy. Development and initial investigation of ntu robotic fish with modular flexible fins. In *IEEE International Conference on Mechatronics and Automation*, volume 2, pages 958 – 963 Vol. 2, july-1 aug. 2005. doi: 10.1109/ICMA.2005.1626681. xiv, 7, 54, 59, 62, 96

K.H. Low and Junzhi Yu. Development of modular and reconfigurable biomimetic robotic fish with undulating fin. In *Robotics and Biomimetics, 2007. ROBIO 2007. IEEE International Conference on*, pages 274 –279, dec. 2007. doi: 10.1109/ROBIO.2007.4522173. 59

K.H. Low, S. Prabu, Jie Yang, Shiwu Zhang, and Yonghua Zhang. Design and initial testing of a single-motor-driven spatial pectoral fin mechanism. In *International Conference on Mechatronics and Automation (ICMA)*, pages 503 –508, aug. 2007. doi: 10.1109/ICMA.2007.4303594. 56

M.A. MacIver, E. Fontaine, and J.W. Burdick. Designing future underwater vehicles: principles and mechanisms of the weakly electric fish. *Oceanic Engineering, IEEE Journal of*, 29(3):651 – 659, july 2004. ISSN 0364-9059. doi: 10.1109/JOE.2004.833210. 59

Stefano Marras and Maurizio Porfiri. Fish and robots swimming together: attraction towards the robot demands biomimetic locomotion. *Journal of The Royal Society Interface*, 9(73):1856–1868, 2012. 1

R. Mason and J. Burdick. Construction and modelling of a carangiform robotic fish. *Experimental Robotics VI*, pages 235–242, 2000. 50

Richard J. Mason. *Fluid locomotion and trajectory planning for shape-changing robots*. PhD thesis, California Institute of Technology, 2003. URL http://resolver.caltech.edu/CaltechETD:etd-05292003-160843. 10, 84

S. F. Masoomi, S. Gutschmidt, X.Q. Chen, and M. Sellier. *Engineering Creative Design in Robotics and Mechatronics*, chapter Novel Swimming Mechanism for a Robotis Fish, pages 41–58. IGI Global, Hershey, PA, USA, 2013. doi: 10.4018/978-1-4666-4225-6. URL http://services.igi-global.com/resolvedoi/resolve.aspx?doi=10.4018/978-1-4666-4225-6. 2

C. Mavroidis, C. Pfeiffer, and M. Mosley. 5.1 conventional actuators, shape memory alloys, and electrorheological fluids. *Automation, miniature robotics, and sensors for nondestructive testing and evaluation*, 4:189, 2000. 63

E. Mbemmo, Zheng Chen, S. Shatara, and Xiaobo Tan. Modeling of biomimetic robotic fish propelled by an ionic polymer-metal composite actuator. In *Robotics and Automation, 2008. ICRA 2008. IEEE International Conference on*, pages 689–694, 2008. doi: 10.1109/ROBOT.2008.4543285. 62

K.A. McIsaac and J.P. Ostrowski. Experiments in closed-loop control for an underwater eel-like robot. In *Robotics and Automation, 2002. Proceedings. ICRA '02. IEEE International Conference on*, volume 1, pages 750 – 755 vol.1, 2002. doi: 10.1109/ROBOT.2002.1013448. 84

K.A. McIsaac and J.P. Ostrowski. Motion planning for anguilliform locomotion. *Robotics and Automation, IEEE Transactions on*, 19(4):637 – 652, aug. 2003. ISSN 1042-296X. doi: 10.1109/TRA.2003.814495. 44, 84

Donya Mohammadshahi, Aghil Yousefi-Koma, Shahnaz Bahmanyar, Hesam Maleki, WB Mikhael, AA Caballero, N Abatzoglou, MN Tabrizi, R Leandre, MI Garcia-Planas, et al. Design, fabrication and hydrodynamic analysis of a biomimetic robot fish. In *WSEAS International Conference. Proceedings. Mathematics and Computers in Science and Engineering*, number 10. World Scientific and Engineering Academy and Society, 2008. 50

K.A. Morgansen. Geometric methods for modeling and control of a free-swimming carangiform fish robot. *Proc. 13th Unmanned Untethered Submersible Technology*, 2003. 49, 84

REFERENCES

K.A. Morgansen, B.I. Triplett, and D.J. Klein. Geometric methods for modeling and control of free-swimming fin-actuated underwater vehicles. *IEEE Transactions on Robotics*, 23(6):1184 –1199, dec. 2007. ISSN 1552-3098. doi: 10.1109/LED.2007.911625. 1, 3, 6, 7, 49, 50, 62, 84, 96

M. Nakashima and K. Ono. Development of a two-joint dolphin robot. *Neurotechnology for biomimetic robots*, page 309, 2002. 50

M. Nakashima, N. Ohgishi, and K. Ono. A study on the propulsive mechanism of a double jointed fish robot utilizing self-excitation control. *JSME International Journal Series C*, 46(3):982–990, 2003. 85, 91, 138

M. Nakashima, Y. Takahashi, T. Tsubaki, and K. Ono. Three-dimensional maneuverability of the dolphin robot (roll control and loop-the-loop motion). *Bio-mechanisms of Swimming and Flying*, pages 79–92, 2004. 50

Phi Luan Nguyen, Van Phu Do, and Byung Ryong Lee. Dynamic modeling of a non-uniform flexible tail for a robotic fish. *Journal of Bionic Engineering*, 10(2):201 – 209, 2013. ISSN 1672-6529. doi: http://dx.doi.org/10.1016/S1672-6529(13)60216-4. URL http://www.sciencedirect.com/science/article/pii/S1672652913602164. 84

QS Nguyen, S Heo, HC Park, and D Byun. Performance evaluation of an improved fish robot actuated by piezoceramic actuators. *Smart Materials and Structures*, 19(3):035030, 2010. 62

J. Palmisano, R. Ramamurti, K.-J. Lu, J. Cohen, W. Sandberg, and B. Ratna. Design of a biomimetic controlled-curvature robotic pectoral fin. In *Robotics and Automation, 2007 IEEE International Conference on*, pages 966–973, 2007. doi: 10.1109/ROBOT.2007.363110. 58

G Polverino, N Abaid, V Kopman, S Macrì, and M Porfiri. Zebrafish response to robotic fish: preference experiments on isolated individuals and small shoals. *Bioinspiration & Biomimetics*, 7(3):036019, 2012. 1

S. Saimek and P.Y. Li. Motion planning and control of a swimming machine. *The International Journal of Robotics Research*, 23(1):27–53, 2004. 50

Taavi Salume. Design of a compliant underwater propulsion mechanism by investigating and mimicking the body a rainbow trout (oncorhynchus mykiss). Master's thesis, Tallinn University if Technology, 2010. 45, 62, 63, 96

M. Sfakiotakis, D.M. Lane, and J.B.C. Davies. Review of fish swimming modes for aquatic locomotion. *IEEE Journal of Oceanic Engineering*, 24(2):237 –252, apr 1999. ISSN 0364-9059. doi: 10.1109/48.757275. xiii, xiv, xv, 16, 17, 20, 28, 29, 44, 46, 47, 52, 54, 61, 68, 69, 70, 78, 102

Liwei Shi, Shuxiang Guo, and K. Asaka. A novel multifunctional underwater microrobot. In *Robotics and Biomimetics (ROBIO), 2010 IEEE International Conference on*, pages 873–878, 2010. doi: 10.1109/ROBIO.2010.5723441. 63

Y. Shi and R.C. Eberhart. Empirical study of particle swarm optimization. In *Proceedings of the 1999 Congress on Evolutionary Computation, 1999 (CEC 99)*, volume 3, pages 3 vol. (xxxvii+2348), 1999. doi: 10.1109/CEC.1999.785511. 98

Nagahiko Shinjo. *Investigations into the use of shape memory alloy for biomimetic propulsion of underwater vehicles*. PhD thesis, Florida Institute of Technology, 2005. 62

M. Siahmansouri, A. Ghanbari, and M.M.S. Fakhrabadi. Design, implementation and control of a fish robot with undulating fins. *International Journal of Advanced Robotic Systems*, 8(5):61–69, 2011. xiv, 59, 61

Patar Ebenezer Sitorus, Yul Yunazwin Nazaruddin, Edi Leksono, and Agus Budiyono. Design and implementation of paired pectoral fins locomotion of labriform fish applied to a fish robot. *Journal of Bionic Engineering*, 6(1):37 – 45, 2009. ISSN 1672-6529. doi: http://dx.doi.org/10.1016/S1672-6529(08)60100-6. URL http://www.sciencedirect.com/science/article/pii/S1672652908601006. 57

Afzal Suleman and Curran Crawford. Design and testing of a biomimetic tuna using shape memory alloy induced propulsion. *Computers & Structures*, 86(35):491 – 499, 2008. ISSN 0045-7949. doi: http://dx.doi.org/10.1016/j.compstruc.2007.02.007. URL http://www.sciencedirect.com/science/article/pii/S0045794907000740. ¡ce:title¿Smart Structures¡/ce:title¿. 62

Graham K. Taylor, Robert L. Nudds, and Adrian L. R. Thomas. Flying and swimming animals cruise at a strouhal number tuned for high power efficiency. *Nature*, 425(6959):707–711, 2003. doi: http://www.nature.com/nature/journal/v425/n6959/suppinfo/nature02000_S1.html. 30

GS Triantafyllou, MS Triantafyllou, and MA Grosenbaugh. Optimal thrust development in oscillating foils with application to fish propulsion. *Journal of Fluids and Structures*, 7(2):205–224, 1993. 30, 71, 103

REFERENCES

M. Triantafyllou, J.M. Kumph, et al. Maneuvering of a robotic pike. Master's thesis, Massachusetts Institute of Technology, 2000. 7, 48, 62, 95

M.S. Triantafyllou and G.S. Triantafyllou. An efficient swimming machine. *Scientific american*, 272 (3):64–71, 1995. 1, 48, 62, 63

J.J. Videler. *Fish swimming*, volume 10. Springer, 1993. xi, xiii, xiv, xv, 5, 23, 30, 36, 38, 39, 69, 72, 76

Steven Vogel. *Life in moving fluids: the physical biology of flow*, chapter The thrust of flying and swimming, pages 262–289. Princeton University Press, 1994. 34

Jianxun Wang and Xiaobo Tan. A dynamic model for tail-actuated robotic fish with drag coefficient adaptation. *Mechatronics*, 23(6):659 – 668, 2013. ISSN 0957-4158. doi: http://dx.doi.org/10.1016/j.mechatronics.2013.07.005. URL http://www.sciencedirect.com/science/article/pii/S095741581300127X. 6, 84

Tianmiao Wang, Jianhong Liang, Gongxin Shen, and Guangkun Tan. Stabilization based design and experimental research of a fish robot. In *Intelligent Robots and Systems, 2005. (IROS 2005). 2005 IEEE/RSJ International Conference on*, pages 954 – 959, aug. 2005. doi: 10.1109/IROS.2005.1545281. 49

Paul W. Webb. *Mechanics and Physiology of Animal Swimming*, chapter The biology of fish swimming, pages 45–62. Cambridge University Press, 1994. 5, 15, 16, 18, 19, 20, 21, 23, 38, 68, 73, 102

Paul W. Webb and Cynthia L. Gerstner. *Biomechanics in Animal Behaviours*, chapter Fish swimming behaviour: predictions from physical principles, pages 59–78. BIOS Scientific, 2000. 16

CD Williams. Auv systems research at the nrc-iot: an update. In *Underwater Technology, 2004. UT'04. 2004 International Symposium on*, pages 59–73. IEEE, 2004. 1

A. Willy and K.H. Low. Development and initial experiment of modular undulating fin for untethered biorobotic auvs. In *IEEE International Conference on Robotics and Biomimetics (ROBIO)*, pages 45 –50, 0-0 2005. doi: 10.1109/ROBIO.2005.246399. 54

T. Wu. Swimming of a waving plate. *Journal of Fluid Mechanics*, 10(03):321–344, 1961. 6, 83, 91

Jian-Xin Xu and Xue-Lei Niu. Analytical control design for a biomimetic robotic fish. In *IEEE International Symposium on Industrial Electronics (ISIE)*, pages 864 –869, june 2011a. doi: 10.1109/ISIE.2011.5984272. 84

Jian-Xin Xu and Xue-Lei Niu. Gait generation and sliding mode control design for anguilliform biomimetic robotic fish. In *IECON 2011 - 37th Annual Conference on IEEE Industrial Electronics Society*, pages 3947 –3952, nov. 2011b. doi: 10.1109/IECON.2011.6119954. 84

Qin Yan, Zhen Han, Shi wu Zhang, and Jie Yang. Parametric research of experiments on a carangiform robotic fish. *Journal of Bionic Engineering*, 5(2):95 – 101, 2008. ISSN 1672-6529. doi: http://dx.doi.org/10.1016/S1672-6529(08)60012-8. URL http://www.sciencedirect.com/science/article/pii/S1672652908600128. 6, 84

Hui Yu, Anwen Shen, and Liang Peng. A new autonomous underwater robotic fish designed for water quality monitoring. In *Modelling, Identification Control (ICMIC), 2012 Proceedings of International Conference on*, pages 561–566, 2012. 1

J. Yu, Y. Hu, R. Fan, L. Wang, and J. Huo. Mechanical design and motion control of a biomimetic robotic dolphin. *Advanced Robotics, 21*, 3(4):499–513, 2007a. 50, 63

Junzhi Yu and Long Wang. Parameter optimization of simplified propulsive model for biomimetic robot fish. In *IEEE International Conference on Robotics and Automation (ICRA 2005)*, pages 3306 – 3311, april 2005. doi: 10.1109/ROBOT.2005.1570620. 1, 71, 84

Junzhi Yu, Min Tan, Shuo Wang, and Erkui Chen. Development of a biomimetic robotic fish and its control algorithm. *IEEE Transactions on Systems, Man, and Cybernetics, Part B: Cybernetics*, 34 (4):1798 –1810, aug. 2004. ISSN 1083-4419. doi: 10.1109/TSMCB.2004.831151. 1, 6, 84

Junzhi Yu, Lizhong Liu, and Long Wang. Dynamic modeling of robotic fish using schiehien's method. In *Robotics and Biomimetics, 2006. ROBIO '06. IEEE International Conference on*, pages 457–462, 2006. doi: 10.1109/ROBIO.2006.340235. 6, 84

Junzhi Yu, Yonghui Hu, Jiyan Huo, and Long Wang. An adjustable scotch yoke mechanism for robotic dolphin. In *IEEE International Conference on Robotics and Biomimetics, 2007 (ROBIO 2007).*, pages 513 –518, dec. 2007b. doi: 10.1109/ROBIO.2007.4522215. xiv, 7, 50, 51, 87, 95

REFERENCES

Xinjie Yu and Mitsuo Gen. Introduction. In *Introduction to Evolutionary Algorithms*, volume 0 of *Decision Engineering*, pages 3–10. Springer London, 2010a. ISBN 978-1-84996-128-8. doi: 10.1007/978-1-84996-129-5_1. URL http://dx.doi.org/10.1007/978-1-84996-129-5_1. 97

Xinjie Yu and Mitsuo Gen. Swarm intelligence. In *Introduction to Evolutionary Algorithms*, volume 0 of *Decision Engineering*, pages 327–354. Springer London, 2010b. ISBN 978-1-84996-128-8. doi: 10.1007/978-1-84996-129-5_8. URL http://dx.doi.org/10.1007/978-1-84996-129-5_8. 97

Yong-Hua Zhang, Jian-Hui He, Jie Yang, Shi-Wu Zhang, and KinHuat Low. A computational fluid dynamics (cfd) analysis of an undulatory mechanical fin driven by shape memory alloy. *International Journal of Automation and Computing*, 3(4):374–381, 2006. ISSN 1476-8186. doi: 10.1007/s11633-006-0374-4. URL http://dx.doi.org/10.1007/s11633-006-0374-4. 83

Chao Zhou, Min Tan, Zhiqiang Cao, Shuo Wang, D. Creighton, Nong Gu, and S. Nahavandi. Kinematic modeling of a bio-inspired robotic fish. In *Robotics and Automation, 2008. ICRA 2008. IEEE International Conference on*, pages 695–699, 2008. doi: 10.1109/ROBOT.2008.4543286. 6, 84